

Electronic Supplementary Information

Full-color Emission of Fluorinated Benzothiadiazole-based D-A-D Fluorophores and Bioimaging Application

Si-Hong Chen^a, Xi-Ying Cao^a, Peng-Tao Hu^a, Kai Jiang^{b,}, Yong-Tong Liang^a, Bing-Jia Xu^{a,*},
Zhong-Hao Li^a, and Zhao-Yang Wang^{a,b,*}*

^a *School of Chemistry, South China Normal University; Key Laboratory of Theoretical Chemistry of Environment,
Ministry of Education; Guangzhou Key Laboratory of Analytical Chemistry for Biomedicine; GDMPA Key
Laboratory for Process Control and Quality Evaluation of Chiral Pharmaceuticals, Guangzhou 510006, China*

^b *Key Laboratory of Functional Molecular Engineering of Guangdong Province, South China University of Technology,
Guangzhou 510640, China*

E-mail: wangzy@scnu.edu.cn; Fax: (+86) 20-39310187; Tel.: (+86) 20-39310258

E-mail: 201910104301@mail.scut.edu.cn

E-mail: bingjiaxu@m.scnu.edu.cn

Contents

1. Chemicals and apparatus	3
2. Synthesis and characterization (Schemes S1-S3)	4
3. Analytical methods	10
4. ¹ H, ¹³ C, ¹⁹ F NMR and HRMS spectra of synthesized compounds (Figs. S1-S62)	11
5. Single crystal data of compounds 3e , 3f , 3m and 3p (Tables S1-S4, Fig. S63)	42
6. Thermogravimetric analyses of compounds 3a-3p (Fig. S64)	46
7. Fluorescent lifetime of compounds 3a-3p (Table S5)	47
8. Fluorescence spectra of compounds 3a-3p in different states (Figs. S65-S67)	48
9. Fluorescence spectra of compounds 3a-3p in various solvents (Figs. S68-S75, Tables S6 and S7) ..	50
10. Fluorescent behaviors of 3a-3p in solution and aggregation states (Figs. S76-S91)	55
11. AIE behavior of compounds 3k and 3m (Figs. S92-S94)	63
12. Photostability of compounds 3a-3p (Fig. S95)	65
13. Computational results of compounds 3a-3p (Tables S8-S23)	66
14. Supplementary material reference	104

1. Chemicals and apparatus

The melting point (m.p.) was determined using INESA WRS-1B digital melting point apparatus without correction. The ^1H , ^{13}C and ^{19}F NMR spectra were measured with a Bruker DRX-600 spectrometer using TMS as an internal standard. High-resolution mass spectra (HRMS) were obtained with a LCMS-IT-TOF mass spectrometer. Single crystal X-ray analysis was obtained using Bruker APEX2 Smart CCD.

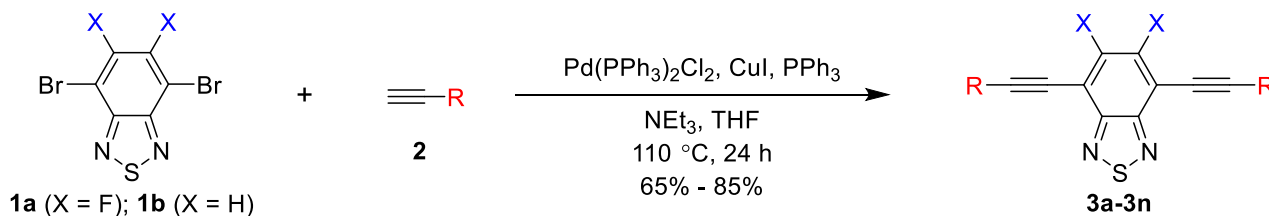
Thermogravimetric analyses (TGA) were measured by a PerkinElmer TGA-8000 thermogravimetric analyzer at a heating rate of 10 °C/min from 50 °C to 800 °C under an air atmosphere. The UV-*vis* spectra were measured by using a Shimadzu UV-2700 ultraviolet absorption detector at room temperature. The fluorescence spectra were recorded with a Hitachi F-4600 spectrophotometer. Absolute PL quantum yields (Φ_{F}) were measured by Edinburgh FLS 980 fluorescence spectrometer with a calibrated integrating sphere. The fluorescence lifetime was measured by using an Edinburgh FLS 980 fluorescence spectrometer. The dynamic light scattering (DLS) experiments were performed on a Malvern Zetasizer Nano ZS90. Cell viability was tested by a Thermo Multiskan MK3 microplate reader. Fluorescence imaging of cells was obtained by Leica TCS SP8 confocal laser scanning microscope.

Reactions were monitored by using thin-layer chromatography (TLC) and visualized with UV light at 254 or 365 nm. All reagents and solvents were purchased from commercial sources (Energy Chemical or Guangzhou chemical reagent factory) and used without further purification, and all chemicals used in this work were of analytical grade purity and used as received. For the real water samples, tap water was collected from the laboratory.

2. Synthesis and characterization

2.1. Synthesis of compounds 3a-3n

As **Scheme S1**, compounds **3a-3n** were synthesized by a modification of the literature procedure.¹ A Schlenk tube with a magnetic stir bar was charged with compound **1** (0.2 mmol, 0.0659 g), CuI (0.02 mmol, 0.0038 g), Pd(PPh₃)₂Cl₂ (0.02 mmol, 0.0140 g), PPh₃ (0.02 mmol, 0.0052 g), and trimethylsilyl acetylene (0.42 mmol, 0.0413 g) in the mixture of 2 mL dry triethylamine and 2 mL dry THF. Then, the mixed reactants were stirred at 110 °C for 24 h under N₂ atmosphere. After the reaction was complete, the obtained mixture was cooled to room temperature and quenched by using the saturated NH₄Cl aqueous solution, and then was extracted with dichloromethane (3×15 mL). The organic solvent was evaporated by decompression. The residue was subjected to silica gel column chromatography with the mixture of petroleum ether (PE) and dichloromethane (DCM) as the ration of PE/DCM = 8/1 to afford pure compound **3a**.



Scheme S1. Synthesis of compounds **3a-3n**.

Similarly, other compounds **3b-3n** were synthesized in the same way. Among them, for the compounds **3b-3e** and **3g-3j**, the eluent was a mixture of PE/DCM (1/6). For the compounds **3f** and **3k**, the eluent was a mixture of PE/DCM (1/4). For the compounds **3l-3n**, the eluent was a mixture of PE/DCM (1/3).

All target compounds were well characterized (**3b-3m** were first reported).

5,6-Difluoro-4,7-bis(trimethylsilylethynyl)benzo[*c*][1,2,5]thiadiazole (3a), white solid (0.0513 g), 70 % yield (71 %² or 93%³ yield); m.p. = 105.8 - 107.1 °C; ¹H NMR (CDCl₃, 600 MHz): δ = 0.35 (s, 18H) ppm; ¹³C NMR (CDCl₃, 150 MHz): δ = 0.2, 92.6, 104.6 (dd, *J*₁ = 13.1 Hz, *J*₂ = 5.1 Hz), 111.6, 150.7 (dd, *J*₁ = 3.3 Hz, *J*₂ = 2.3 Hz), 155.6 (dd, *J*₁ = 263.6 Hz, *J*₂ = 19.4 Hz) ppm; ¹⁹F NMR (CDCl₃, 564 MHz): δ = -123.7 ppm; HRMS, *m/z* (%): Calcd for C₁₆H₁₉F₂N₂SSi₂⁺ ([M+H]⁺): 365.0770 (100), Found: 365.0776 (100).

5,6-Difluoro-4,7-di(hex-1-yn-1-yl)benzo[*c*][1,2,5]thiadiazole (3b), white solid (0.0492 g), 74 % yield; m.p. = 89.2 - 90.3 °C; ¹H NMR (CDCl₃, 600 MHz): δ = 0.98 (t, *J* = 7.2 Hz, 6H), 1.52-1.59 (m, 4H), 1.68-1.73 (m, 4H), 2.64 (t, *J* = 7.2 Hz, 4H) ppm; ¹³C NMR (CDCl₃, 150 MHz): δ = 13.6, 19.9, 22.0, 30.4, 69.6, 104.0 (dd, *J*₁ = 13.4 Hz, *J*₂ = 4.8 Hz), 105.6, 150.7 (dd, *J*₁ = 3.6 Hz, *J*₂ = 2.4 Hz), 154.8 (dd, *J*₁ = 260.4 Hz, *J*₂ = 19.4 Hz) ppm; ¹⁹F NMR (CDCl₃, 564 MHz): δ = -125.8 ppm; HRMS, *m/z* (%): Calcd for C₁₈H₁₉F₂N₂S⁺ ([M+H]⁺): 333.1232 (100), Found: 333.1226 (100).

5,6-Difluoro-4,7-bis(thiophen-2-ylethynyl)benzo[*c*][1,2,5]thiadiazole (3c), orange solid (0.0502 g), 65 % yield; m.p. > 300.0 °C (carbonization, decomposition temperature is lower than melting point); ¹H NMR (CDCl₃, 600 MHz): δ = 7.09-7.10 (m, 2H), 7.45 (d, *J* = 6.0 Hz, 2H), 7.51 (d, *J* = 4.2 Hz, 2H) ppm; ¹³C NMR (CDCl₃, 150 MHz): δ = 82.0, 96.8, 103.9 (dd, *J*₁ = 13.2 Hz, *J*₂ = 5.9 Hz), 121.7, 127.5, 129.6, 134.1, 150.1 (dd, *J*₁ = 4.8 Hz, *J*₂ = 2.4 Hz), 154.0 (dd, *J*₁ = 262.4 Hz, *J*₂ = 19.8 Hz) ppm; ¹⁹F NMR (CDCl₃, 564 MHz): δ = -124.2 ppm; HRMS, *m/z* (%): Calcd for C₁₈H₇F₂N₂S₃⁺ ([M+H]⁺): 384.9734 (100), Found: 394.9727 (100).

5,6-Difluoro-4,7-bis(phenylethynyl)benzo[*c*][1,2,5]thiadiazole (3d), yellow solid (0.0567 g), 76 % yield; m.p. = 202.4 - 203.8 °C; ¹H NMR (CDCl₃, 600 MHz): δ = 7.38-7.43 (m, 6H), 7.66-7.69 (m, 4H) ppm; ¹³C NMR (CDCl₃, 150 MHz): δ = 78.1, 103.5, 104.1 (dd, *J*₁ = 13.1 Hz, *J*₂ = 5.1 Hz), 121.9, 128.5, 129.7, 132.1, 150.3 (dd, *J*₁ = 3.0 Hz, *J*₂ = 2.4 Hz), 154.3 (dd, *J*₁ = 262.5 Hz, *J*₂ = 18.9 Hz) ppm; ¹⁹F NMR (CDCl₃, 564 MHz): δ = -124.4 ppm; HRMS, *m/z* (%): Calcd for C₂₂H₁₁F₂N₂S⁺ ([M+H]⁺): 373.0606 (100), Found: 373.0601 (100).

5,6-Difluoro-4,7-bis(*p*-tolylethynyl)benzo[*c*][1,2,5]thiadiazole (3e), yellow solid (0.0630 g), 79 % yield; m.p. = 228.3 - 229.8 °C; ¹H NMR (CDCl₃, 600 MHz): δ = 2.41 (s, 6H), 7.22 (d, *J* = 7.8 Hz, 4H), 7.59 (d, *J* = 8.4 Hz, 4H) ppm; ¹³C NMR (CDCl₃, 150 MHz): δ = 21.7, 77.7, 103.8, 104.1 (dd, *J*₁ = 13.4 Hz, *J*₂ = 5.3 Hz), 118.9, 129.3, 132.1, 140.1, 150.4 (dd, *J*₁ = 3.5 Hz, *J*₂ = 3.2 Hz), 154.4 (dd, *J*₁ =

262.2 Hz, $J_2 = 19.4$ Hz) ppm; ^{19}F NMR (CDCl_3 , 564 MHz): $\delta = -124.8$ ppm; HRMS, m/z (%): Calcd for $\text{C}_{24}\text{H}_{14}\text{F}_2\text{N}_2\text{S}^-$ ($[\text{M}+\text{H}]^+$): 400.0851 (100), Found: 400.5853 (100).

5,6-Difluoro-4,7-bis(4-methoxyphenylethynyl)benzo[*c*][1,2,5]thiadiazole (3f), yellow solid (0.0685 g), 79 % yield; m.p. = 224.7 - 226.5 °C; ^1H NMR (CDCl_3 , 600 MHz): $\delta = 3.86$ (s, 6H), 6.94 (d, $J = 8.4$ Hz, 4H), 7.64 (d, $J = 9.0$ Hz, 4H) ppm; ^{13}C NMR (CDCl_3 , 150 MHz): $\delta = 55.4$, 103.8, 104.1 (dd, $J_1 = 12.9$ Hz, $J_2 = 4.8$ Hz), 114.0, 114.2, 133.8, 150.4 (dd, $J_1 = 3.3$ Hz, $J_2 = 2.4$ Hz), 154.1 (dd, $J_1 = 261.3$ Hz, $J_2 = 19.2$ Hz), 160.8, ppm; ^{19}F NMR (CDCl_3 , 564 MHz): $\delta = -125.2$ ppm; HRMS, m/z (%): Calcd for $\text{C}_{24}\text{H}_{15}\text{F}_2\text{N}_2\text{O}_2\text{S}^+$ ($[\text{M}+\text{H}]^+$): 433.0817 (100), Found: 443.0809 (100).

4,7-Bis(4-chlorophenylethynyl)-5,6-difluorobenzo[*c*][1,2,5]thiadiazole (3g), yellow solid (0.0645 g), 73 % yield; m.p. = 225.3 - 226.3 °C; ^1H NMR (CDCl_3 , 600 MHz): $\delta = 7.40$ (d, $J = 9.0$ Hz, 4H), 7.63 (d, $J = 8.4$ Hz, 4H) ppm; ^{13}C NMR (CDCl_3 , 150 MHz): $\delta = 79.0$, 102.3, 104.0 (dd, $J_1 = 12.5$ Hz, $J_2 = 5.6$ Hz), 120.3, 129.0, 133.4, 136.0, 152.2 (dd, $J_1 = 3.0$ Hz, $J_2 = 2.4$ Hz), 154.4 (dd, $J_1 = 262.5$ Hz, $J_2 = 19.5$ Hz), ppm; ^{19}F NMR (CDCl_3 , 564 MHz): $\delta = -124.0$ ppm; HRMS, m/z (%): Calcd for $\text{C}_{22}\text{H}_8\text{Cl}_2\text{F}_2\text{N}_2\text{S}^-$: 439.9759 (100), 441.9729 (64%), Found: 439.9763 (100), 441.9731 (64%).

5,6-Difluoro-4,7-bis(naphthalen-1-ylethynyl)benzo[*c*][1,2,5]thiadiazole (3h), yellow solid (0.0686 g), 73 % yield; m.p. = 197.1 - 198.6 °C; ^1H NMR (CDCl_3 , 600 MHz): $\delta = 7.53$ -7.55 (m, 2H), 7.59-7.62 (m, 2H), 7.70-7.73 (m, 2H), 7.92 (d, $J = 8.4$ Hz, 2H), 7.96 (d, $J = 7.8$ Hz, 2H), 7.97 (d, $J = 7.8$ Hz, 2H), 8.67 (d, $J = 8.4$ Hz, 2H) ppm; ^{13}C NMR (CDCl_3 , 150 MHz): $\delta = 78.8$, 106.6 (dd, $J_1 = 18.6$ Hz, $J_2 = 5.4$ Hz), 109.5, 125.3, 126.2, 126.8, 127.6, 128.5, 130.4, 131.5, 133.2, 133.3, 143.3 (dd, $J_1 = 4.2$ Hz, $J_2 = 3.5$ Hz), 153.0 (dd, $J_1 = 260.1$ Hz, $J_2 = 20.6$ Hz) ppm; ^{19}F NMR (CDCl_3 , 564 MHz): $\delta = -124.5$ ppm; HRMS, m/z (%): Calcd for $\text{C}_{30}\text{H}_{15}\text{F}_2\text{N}_2\text{S}^+$ ($[\text{M}+\text{H}]^+$): 473.0919 (100), Found: 473.0912 (100).

4,7-Bis([1,1'-biphenyl]-4-ylethynyl)-5,6-difluorobenzo[*c*][1,2,5]thiadiazole (3i), yellow solid (0.0794 g), 76 % yield; m.p. = 254.2 - 255.8 °C; ^1H NMR (CDCl_3 , 600 MHz): $\delta = 7.38$ -7.41 (m, 2H), 7.47-7.49 (m, 4H), 7.64 (d, $J = 7.8$ Hz, 4H), 7.67 (d, $J = 8.4$ Hz, 4H), 7.78 (d, $J = 8.4$ Hz, 4H) ppm; ^{13}C NMR (CDCl_3 , 150 MHz): $\delta = 78.9$, 103.6, 103.9 (dd, $J_1 = 17.1$ Hz, $J_2 = 5.6$ Hz), 120.7, 127.1, 127.2, 128.0, 129.0, 132.7, 140.1, 142.5, 150.4 (dd, $J_1 = 3.9$ Hz, $J_2 = 2.7$ Hz), 156.2 (dd, $J_1 = 254.6$ Hz, $J_2 = 19.5$ Hz) ppm; ^{19}F NMR (CDCl_3 , 564 MHz): $\delta = -124.4$ ppm; HRMS, m/z (%): Calcd for $\text{C}_{34}\text{H}_{19}\text{F}_2\text{N}_2\text{S}^+$ ($[\text{M}+\text{H}]^+$): 525.1232 (100), Found: 525.1222 (100).

4,7-Bis(4-(9H-carbazol-9-yl)phenylethynyl)-5,6-difluorobenzo[*c*][1,2,5]thiadiazole (3j), yellow

solid (0.1159 g), 82 % yield; m.p. > 300.0 °C; ¹H NMR (CDCl₃, 600 MHz): δ = 7.32-7.34 (m, 4H), 7.44 (d, *J* = 8.4 Hz, 4H), 7.46-7.50 (m, 4H), 7.68 (d, *J* = 8.4 Hz, 4H), 7.96 (d, *J* = 8.4 Hz, 4H), 8.16 (d, *J* = 7.8 Hz, 4H) ppm; ¹³C NMR (CDCl₃, 150 MHz): δ = 79.0, 102.9, 103.2 (dd, *J*₁ = 17.8 Hz, *J*₂ = 4.2 Hz), 109.8, 120.5, 120.6, 123.8, 126.2, 126.9, 133.8, 139.0, 140.4, 150.8 (dd, *J*₁ = 4.4 Hz, *J*₂ = 4.2 Hz), 155.6 (dd, *J*₁ = 273.5 Hz, *J*₂ = 20.7 Hz) ppm; ¹⁹F NMR (CDCl₃, 564 MHz): δ = -124.0 ppm; HRMS, *m/z* (%): Calcd for C₄₆H₂₅F₂N₄S⁺ ([M+H]⁺): 703.1763 (100), Found: 703.1759 (100).

4,4'-((5,6-Difluorobenzo[*c*][1,2,5]thiadiazole-4,7-diyl)bis(ethyne-2,1-diyl))bis(*N,N*-diphenylamine) (3k), red solid (0.1139 g), 81 % yield; m.p. = 255.2 - 256.1 °C; ¹H NMR (CDCl₃, 600 MHz): δ = 7.02 (d, *J* = 8.4 Hz, 4H), 7.08-7.11 (m, 4H), 7.14 (d, *J* = 7.2 Hz, 8H), 7.28-7.31 (m, 8H), 7.50 (d, *J* = 9.0 Hz, 4H) ppm; ¹³C NMR (CDCl₃, 150 MHz): δ = 77.9, 103.9 (dd, *J*₁ = 13.1 Hz, *J*₂ = 4.7 Hz), 104.3, 124.1, 121.5, 124.1, 125.4, 129.5, 133.2, 146.9, 149.1, 150.4 (dd, *J*₁ = 3.2 Hz, *J*₂ = 2.4 Hz), 154.0 (dd, *J*₁ = 261.2 Hz, *J*₂ = 19.4 Hz) ppm; ¹⁹F NMR (CDCl₃, 564 MHz): δ = -126.0 ppm; HRMS, *m/z* (%): Calcd for C₄₆H₂₉F₂N₄S⁺ ([M+H]⁺): 707.2076 (100), Found: 707.2072 (100).

4,4'-((5,6-Difluorobenzo[*c*][1,2,5]thiadiazole-4,7-diyl)bis(ethyne-2,1-diyl))bis(*N,N*-bis(4-methoxyphenyl)aniline) (3l), dark red solid (0.1354 g), 82 % yield; m.p. = 197.9 - 199.6 °C; ¹H NMR (CDCl₃, 600 MHz): δ = 3.81 (s, 12H), 6.86 (d, *J* = 9.0 Hz, 4H), 6.87 (d, *J* = 9.0 Hz, 8H), 7.10 (d, *J* = 9.0 Hz, 8H), 7.45 (d, *J* = 9.0 Hz, 4H) ppm; ¹³C NMR (CDCl₃, 150 MHz): δ = 55.5, 77.6, 103.9 (dd, *J*₁ = 13.1 Hz, *J*₂ = 5.4 Hz), 104.8, 112.1, 114.9, 118.5, 127.4, 133.1, 139.8, 149.9, 150.4 (dd, *J*₁ = 3.3 Hz, *J*₂ = 3.3 Hz), 153.9 (dd, *J*₁ = 260.4 Hz, *J*₂ = 19.5 Hz), 156.7 ppm; ¹⁹F NMR (CDCl₃, 564 MHz): δ = -125.9 ppm; HRMS, *m/z* (%): Calcd for C₅₀H₃₇F₂N₄O₄S⁺ ([M+H]⁺): 827.2498 (100), Found: 827.2494 (100).

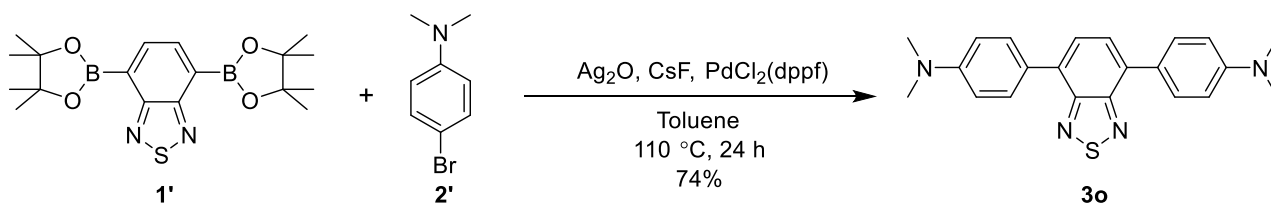
4,4'-((5,6-Difluorobenzo[*c*][1,2,5]thiadiazole-4,7-diyl)bis(ethyne-2,1-diyl))bis(*N,N*-dimethylaniline) (3m), red solid (0.0780 g), 85 % yield; m.p. > 300.0 °C (carbonization); ¹H NMR (CDCl₃, 600 MHz): δ = 3.05 (s, 12H), 7.02 (d, *J* = 9.0 Hz, 4H), 7.50 (d, *J* = 7.8 Hz, 4H) ppm; ¹³C NMR (CDCl₃, 150 MHz): δ = 40.1, 105.5, 103.9 (dd, *J*₁ = 19.5 Hz, *J*₂ = 5.6 Hz), 108.5, 111.7, 128.3, 133.5, 150.5 (dd, *J*₁ = 3.2 Hz, *J*₂ = 2.4 Hz), 150.9, 153.5 (dd, *J*₁ = 259.5 Hz, *J*₂ = 19.4 Hz) ppm; ¹⁹F NMR (CDCl₃, 564 MHz): δ = -126.3 ppm; HRMS, *m/z* (%): Calcd for C₂₆H₂₁F₂N₄S⁺ ([M+H]⁺): 459.1450 (100), Found: 459.1440 (100).

4,4'-(Benzo[*c*][1,2,5]thiadiazole-4,7-diyl)bis(ethyne-2,1-diyl)bis(*N,N*-dimethylaniline) (3n), dark red solid (0.0657 g), 78 % yield (45 % yield⁴); m.p. > 300 °C (carbonization); ¹H NMR (CDCl₃,

600 MHz): $\delta = 3.02$ (s, 12H), 6.69 (d, $J = 9.0$ Hz, 4H), 7.54 (d, $J = 9.0$ Hz, 4H), 7.70 (s, 2H) ppm; ^{13}C NMR (CDCl_3 , 150 MHz): $\delta = 40.2, 84.2, 99.2, 109.2, 111.7, 117.0, 131.7, 133.3, 150.5, 154.5$ ppm; HRMS, m/z (%): Calcd for $\text{C}_{26}\text{H}_{23}\text{N}_4\text{S}^+$ ($[\text{M}+\text{H}]^+$): 423.1638 (100), Found: 423.1632 (100).

2.2. Synthesis of compound 3o

As **Scheme S2**, compound **3o** was synthesized by a modification of the literature procedure.⁵ A Schlenk tube with a magnetic stir bar was charged with compound **1'** (0.2 mmol, 0.0776 g), Ag_2O (0.6 mmol, 0.1361 g), CsF (0.6 mmol, 0.0911 g), $\text{PdCl}_2(\text{dppf})$ (0.01 mmol, 0.0072 g), and compound **2'** (0.6 mmol, 0.1615 g) in 3 mL toluene. Then, the mixture was stirred for 24 h at 110 °C. After the reaction was complete, the obtained mixture was cooled to room temperature and extracted with dichloromethane (3×15 mL). The organic solvent was evaporated by decompression. Finally, the residue was subjected to silica gel column chromatography (PE/DCM = 6/1) to afford pure compound **3o**.



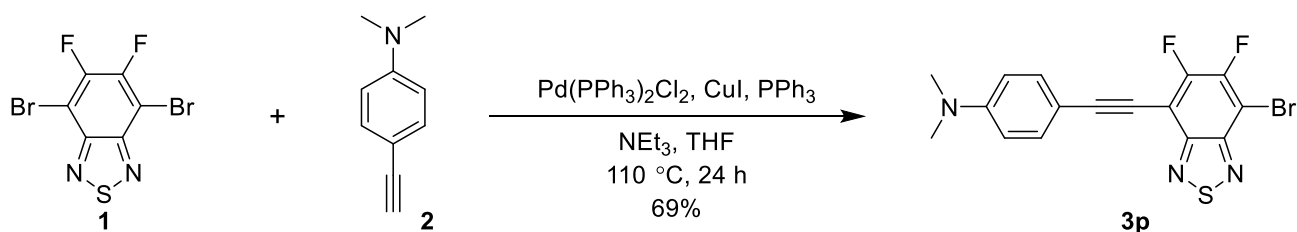
Scheme S2. Synthesis of compound **3o**.

4,4'-(Benzo[*c*][1,2,5]thiadiazole-4,7-diyl)bis(*N,N*-dimethylaniline) (3o), red solid (0.0554 g), 74 % yield (85 % yield⁶); m.p. = 209.6 - 211.4 °C; ^1H NMR (CDCl_3 , 600 MHz): $\delta = 3.04$ (s, 12H), 6.89 (d, $J = 8.4$ Hz, 4H), 7.68 (s, 2H), 7.91 (d, $J = 8.4$ Hz, 4H) ppm; ^{13}C NMR (CDCl_3 , 150 MHz): $\delta = 40.5, 112.4, 125.7, 126.6, 129.9, 132.0, 154.4, 154.5$ ppm; HRMS, m/z (%): Calcd for $\text{C}_{22}\text{H}_{23}\text{N}_4\text{S}^+$ ($[\text{M}+\text{H}]^+$): 375.1638 (100), Found: 375.1641 (100).

2.3. Synthesis of compound 3p

As **Scheme S3**, compound **3p** was synthesized by a modification of the literature procedure.¹ A Schlenk tube with a magnetic stir bar was charged with compound **1** (0.2 mmol, 0.0659 g), CuI (0.02

mmol, 0.0038 g), Pd(PPh₃)₂Cl₂ (0.02 mmol, 0.0140 g), PPh₃ (0.02 mmol, 0.0052 g), and trimethylsilyl acetylene (0.22 mmol, 0.0206 g) in the mixture of 2 mL dry triethylamine and 2 mL dry THF. Then, the mixed reactants were stirred at 110 °C for 24 h under N₂ atmosphere. After the reaction was complete, the obtained mixture was cooled to room temperature and quenched by using the saturated NH₄Cl aqueous solution, and then was extracted with dichloromethane (3×15 mL). The organic solvent was evaporated by decompression. The residue was subjected to silica gel column chromatography (PE/DCM = 6/1) to afford pure compound **3p**.



Scheme S3. Synthesis of compound **3p**.

The control compound **3p** was first reported and well characterized.

4-((7-Bromo-5,6-difluorobenzo[c][1,2,5]thiadiazol-4-yl)ethynyl)-N,N-dimethylaniline (3p), orange solid (0.0543 g), 69 % yield; m.p. = 167.6-168.9 °C; ¹H NMR (CDCl₃, 600 MHz): δ = 3.04 (s, 6H), 6.69 (d, *J* = 9.0 Hz, 2H), 7.56 (d, *J* = 9.0 Hz, 2H) ppm; ¹³C NMR (CDCl₃, 150 MHz): δ = 40.1, 76.4 (d, *J* = 4.8 Hz), 98.4 (dd, *J*₁ = 21.8 Hz, *J*₂ = 1.7 Hz), 104.7 (dd, *J*₁ = 15.6 Hz, *J*₂ = 2.9 Hz), 105.6 (d, *J* = 5.9 Hz), 108.1, 111.6, 133.5, 149.5 (d, *J* = 5.4 Hz), 149.8 (d, *J* = 6.2 Hz), 151.0, 152.1 (dd, *J*₁ = 255.6 Hz, *J*₂ = 19.1 Hz), 153.4 (dd, *J*₁ = 261.8 Hz, *J*₂ = 18.6 Hz) ppm; ¹⁹F NMR (CDCl₃, 564 MHz): δ = -124.4 (d, *J* = 19.7 Hz), -120.7 (d, *J* = 20.3 Hz) ppm; HRMS, *m/z* (%): Calcd for C₁₆H₁₁BrF₂N₃S⁺ ([M+H]⁺): 393.9820 (100), 395.9799 (97), Found: 393.9812 (100), 395.9790 (97).

3. Analytical methods

General procedure for optical spectral measurements. The stock solutions of compounds **3a-3p** (10^{-3} M) were prepared in THF. Then, the 10^{-5} M aqueous solutions of compounds **3a-3p** were prepared for the measurement of both UV-*vis* absorption and fluorescence spectra at room temperature. Both the excitation and emission slit widths were set at 5 nm during the fluorescence experiments.

Method of theoretical calculations. As the reported method,⁷ all theoretical calculations were performed using Gaussian 09 serials software. The ground-state structures were obtained by B3LYP density functional method with basis set 6-31G (d,p) level. The HOMO and LUMO distributions were visualized using Gaussview 6.0 software.

Preparing films. Firstly, 1 mg of compound **3a** and 1.5 mL of dichloromethane were added into a 3 mL clear glass bottle. After **3a** was fully dissolved, 100 mg of poly(methylmethacrylate) (PMMA)⁸ was added. After standing the mixed solution still for 3 h, PMMA was completely dissolved. Then, using a glass glue tip dropper to pipette an appropriate amount of solution into the quartz round mold, and letting it dry naturally made the preparation of the **3a**-coated thinfilm completed. Similarly, **3b-3p** films were prepared using the same method.

Cell viability. According to the literature,⁹ to evaluate the biocompatibility of dye **3m**, the cell viability of 4T1 mouse breast cancer cells stained by **3m** with different concentrations was tested. Cells were seeded in 96-well plates at a density of 5×10^3 cells/well and cultured in standard medium for 12 h. The cells were then incubated with various concentrations of **3m** (10, 30, 60, 80 and 100 $\mu\text{g/mL}$) in the dark for 48 h. Then, MTT solution (100 μL , 0.5 mg/mL) was added into each well and incubated for 4 h. Next, DMSO (100 μL , 15 min) was added into each well to dissolve the purple formazan crystals. The absorbance of MTT at 490 nm was measured by the microplate reader.

Cell imaging¹⁰. The 4T1 cells were cultured in 1640 medium containing 10% fetal bovine serum (FBS) and 1% penicillin streptomycin (100 $\mu\text{g/mL}$) in a 5% CO_2 humidified incubator at 37°C. The 4T1 cells (5×10^3 cells/well) were cultured 12 h and then stained with the **3m** solution (DMSO, 50 and 100 $\mu\text{g/mL}$). After the cells continue to be incubated in the medium for 12 h, cell imaging is performed using confocal laser scanning microscopy ($\lambda_{\text{ex}} = 405$ nm, $\lambda_{\text{em}} = 620\text{-}670$ nm, scale bars = 25 μm).

4. ^1H , ^{13}C , ^{19}F NMR and HRMS spectra of compounds 3a-3p

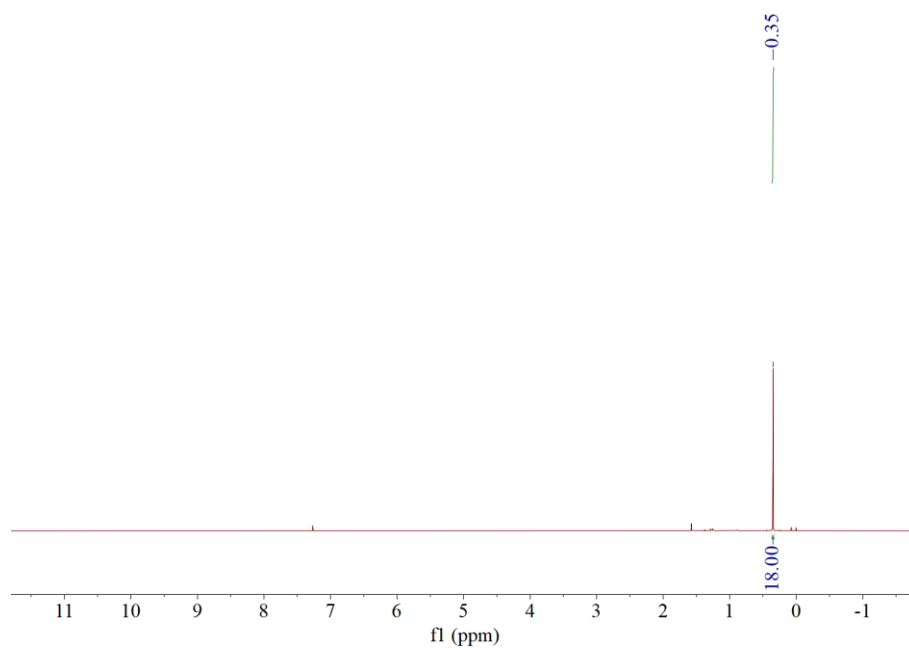


Fig. S1. ^1H NMR spectrum of compound 3a.

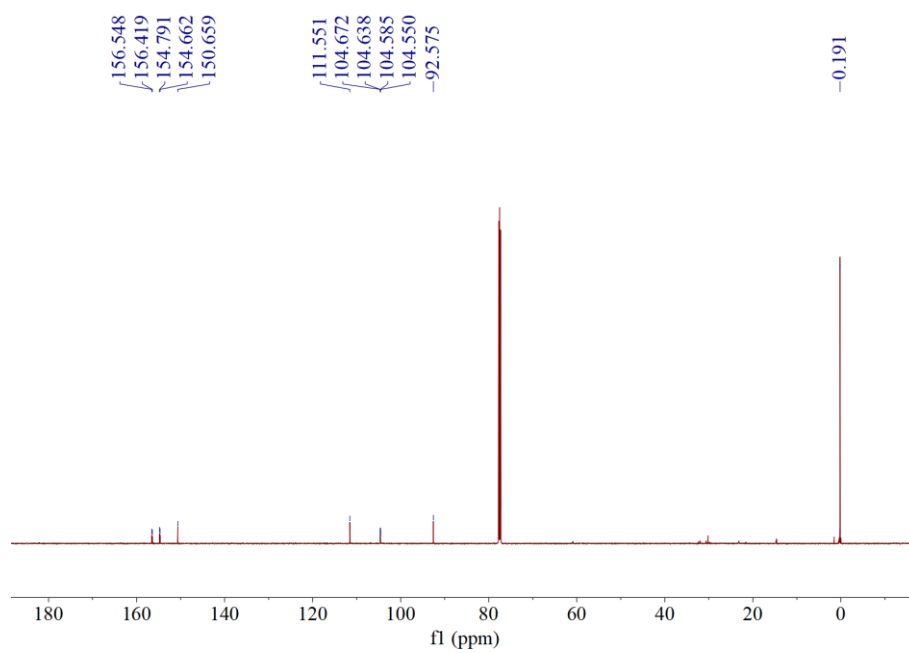


Fig. S2. ^{13}C NMR spectrum of compound 3a.

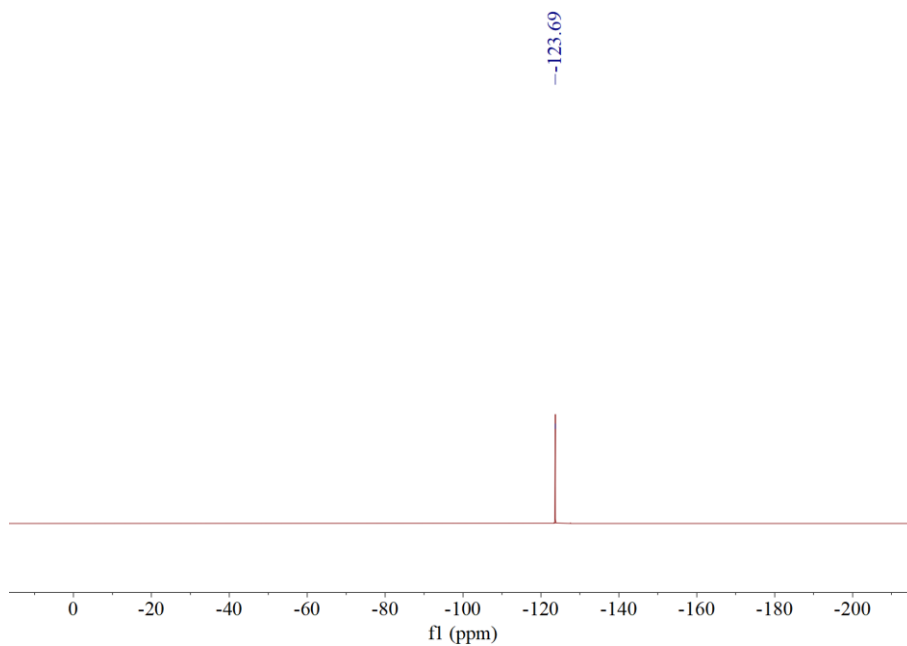


Fig. S3. ^{19}F NMR spectrum of compound **3a**.

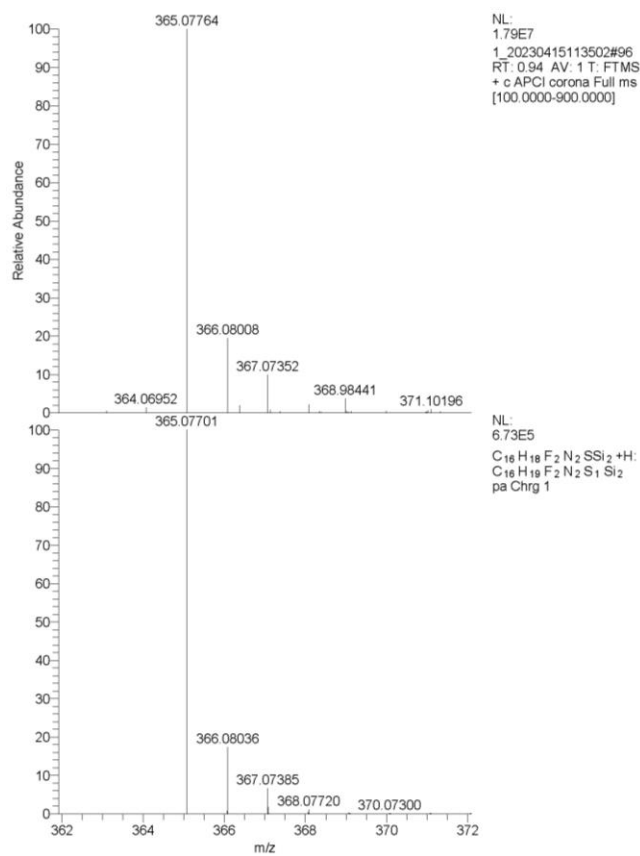


Fig. S4. HRMS spectrum of compound **3a**.

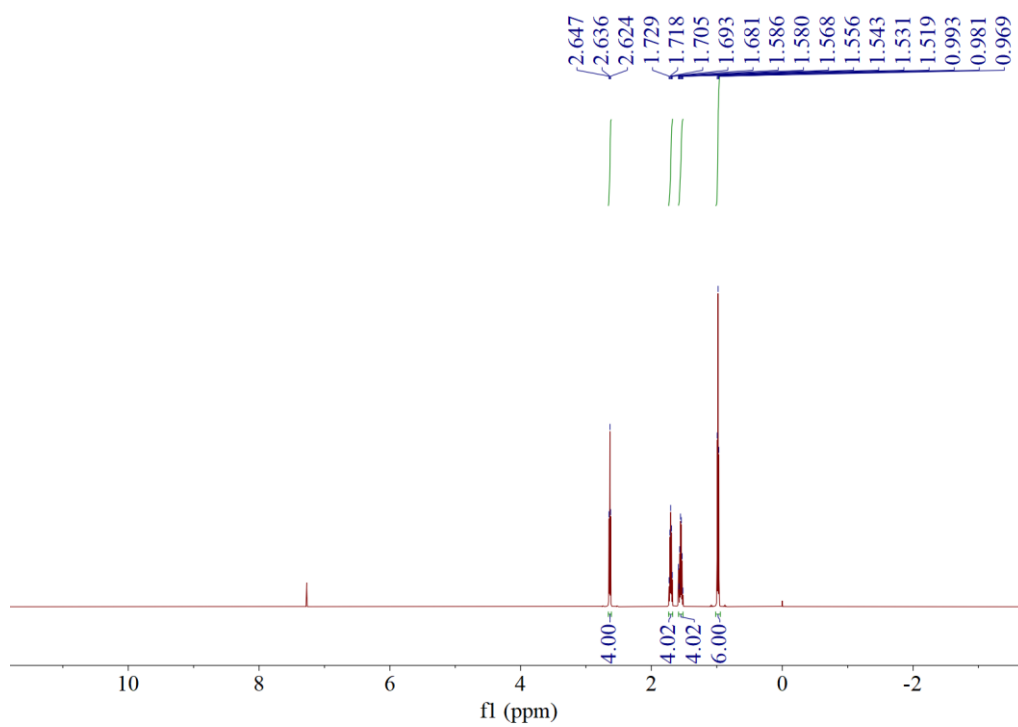


Fig. S5. ^1H NMR spectrum of compound **3b**.

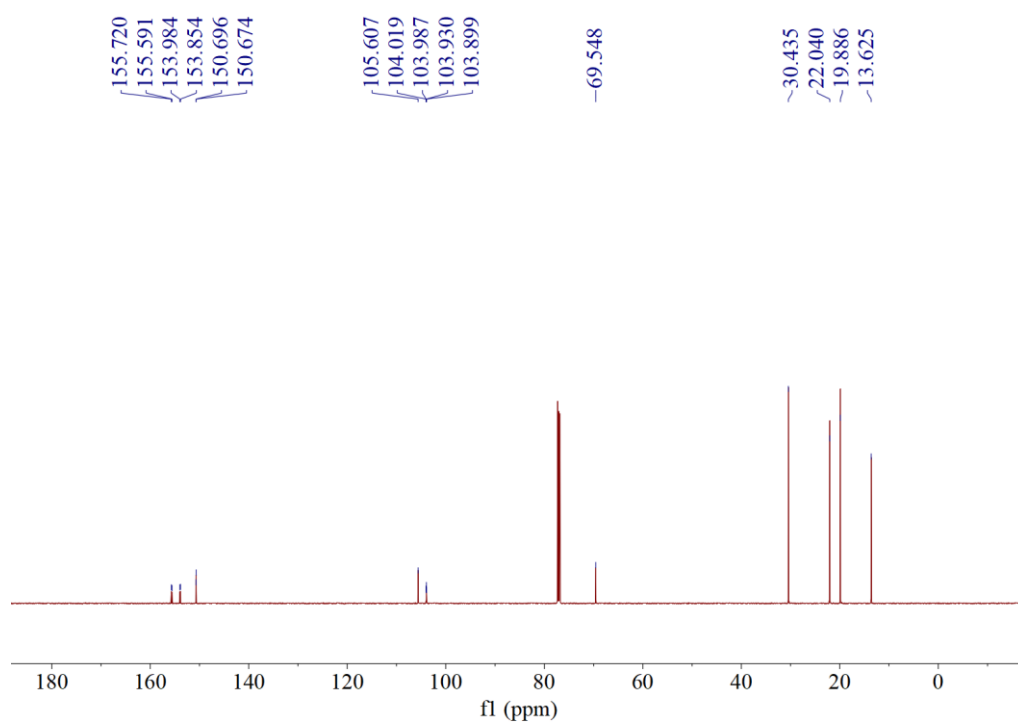


Fig. S6. ^{13}C NMR spectrum of compound **3b**.

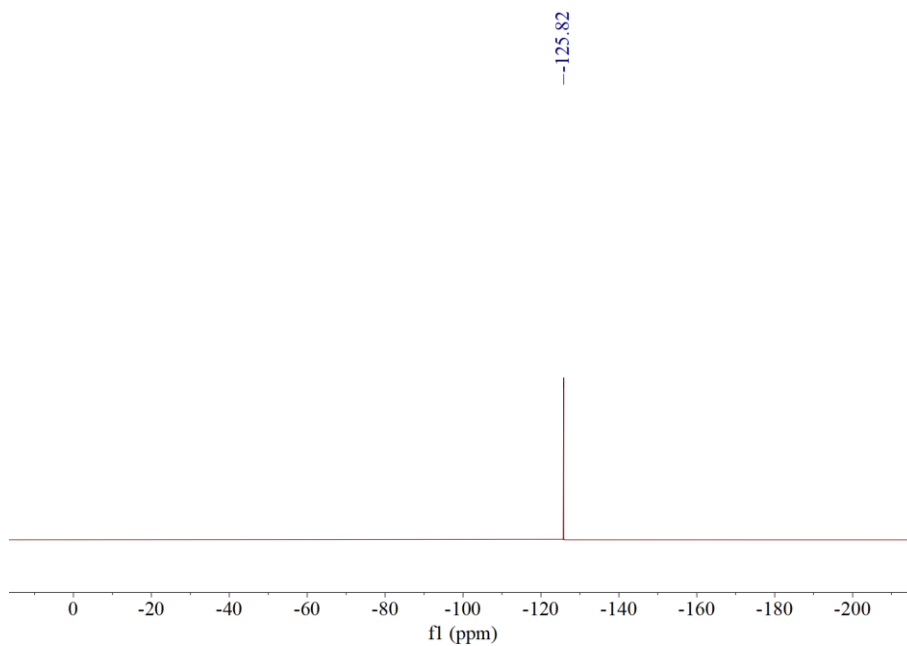


Fig. S7. ^{19}F NMR spectrum of compound **3b**.

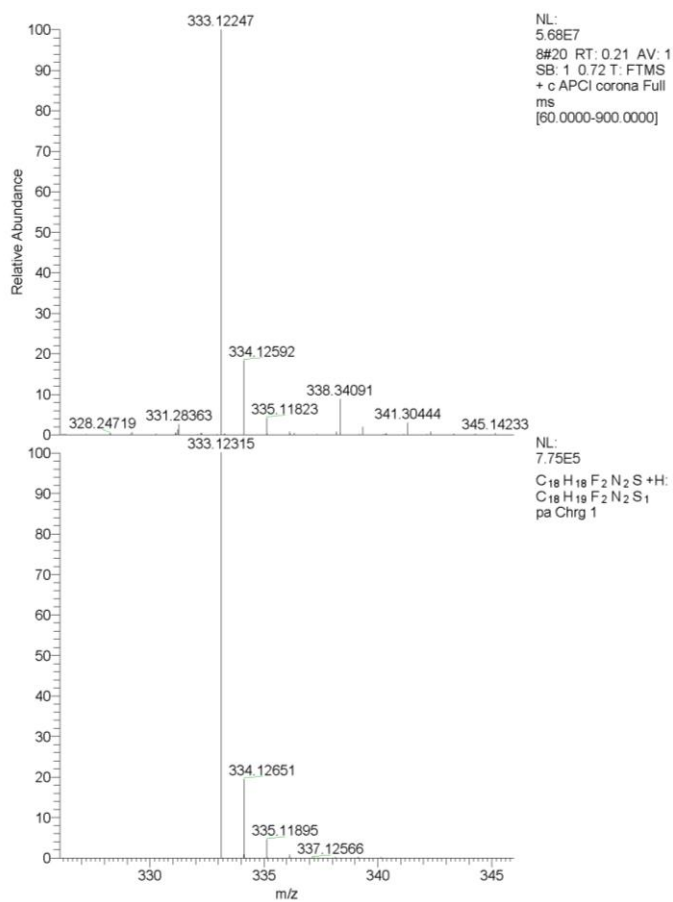


Fig. S8. HRMS spectrum of compound **3b**.

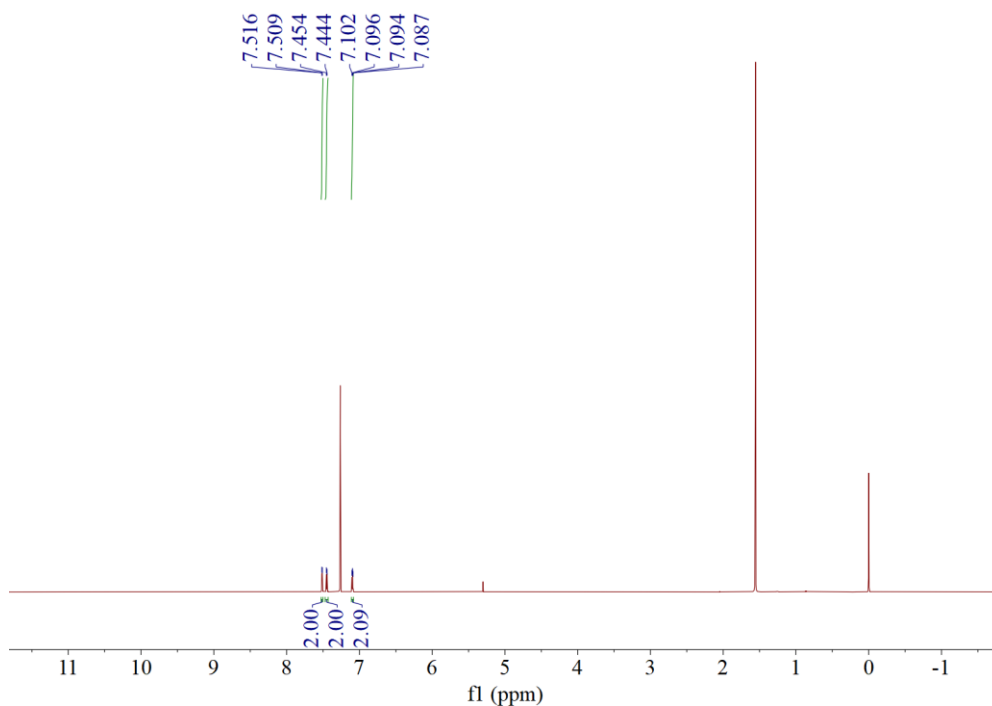


Fig. S9. ^1H NMR spectrum of compound **3c**.

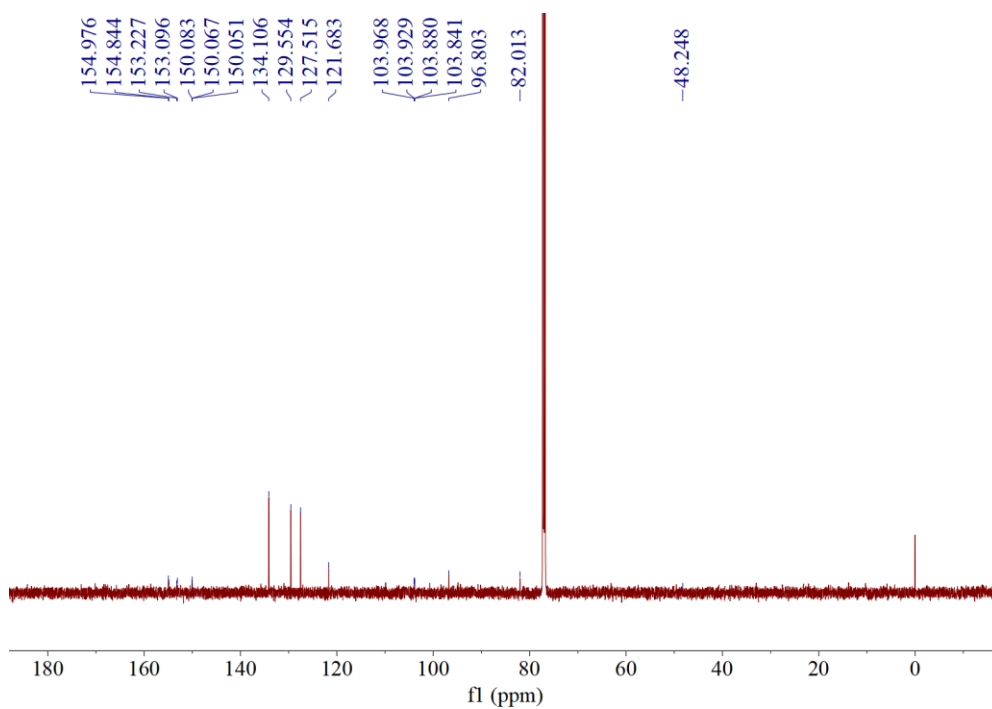


Fig. S10. ^{13}C NMR spectrum of compound **3c**.

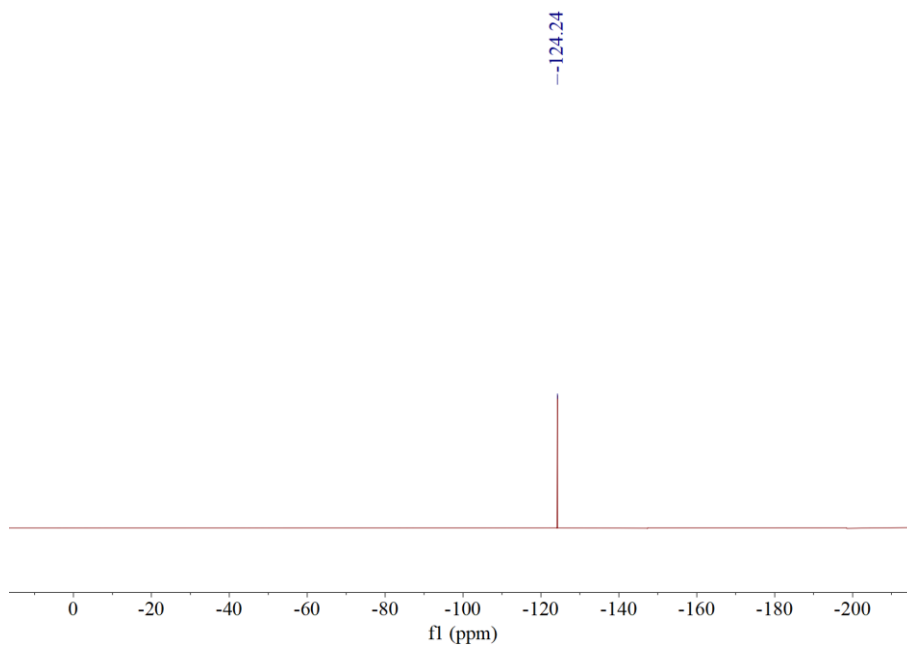


Fig. S11. ^{19}F NMR spectrum of compound **3c**.

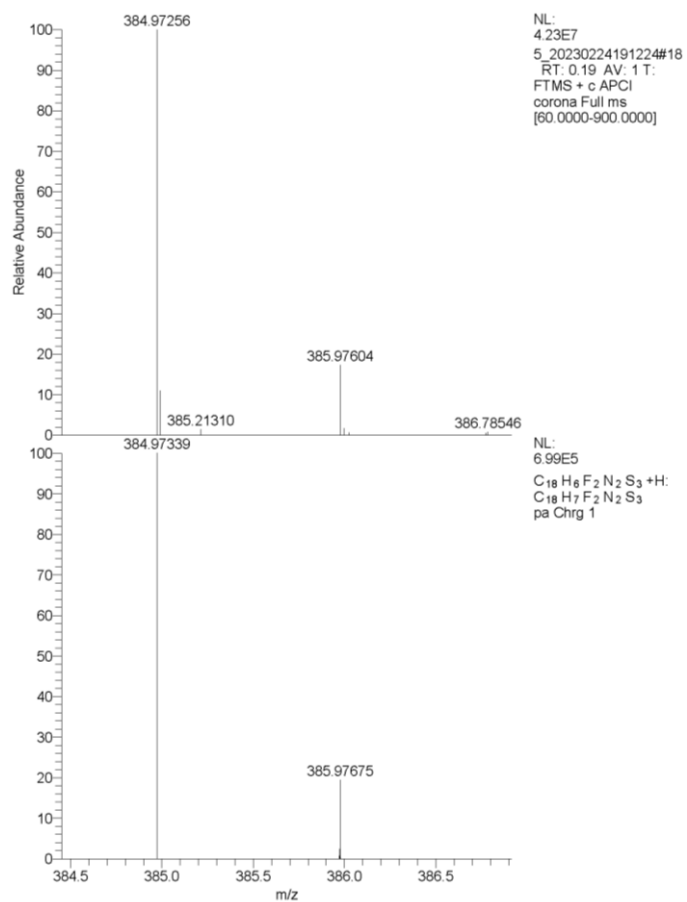


Fig. S12. HRMS spectrum of compound **3c**.

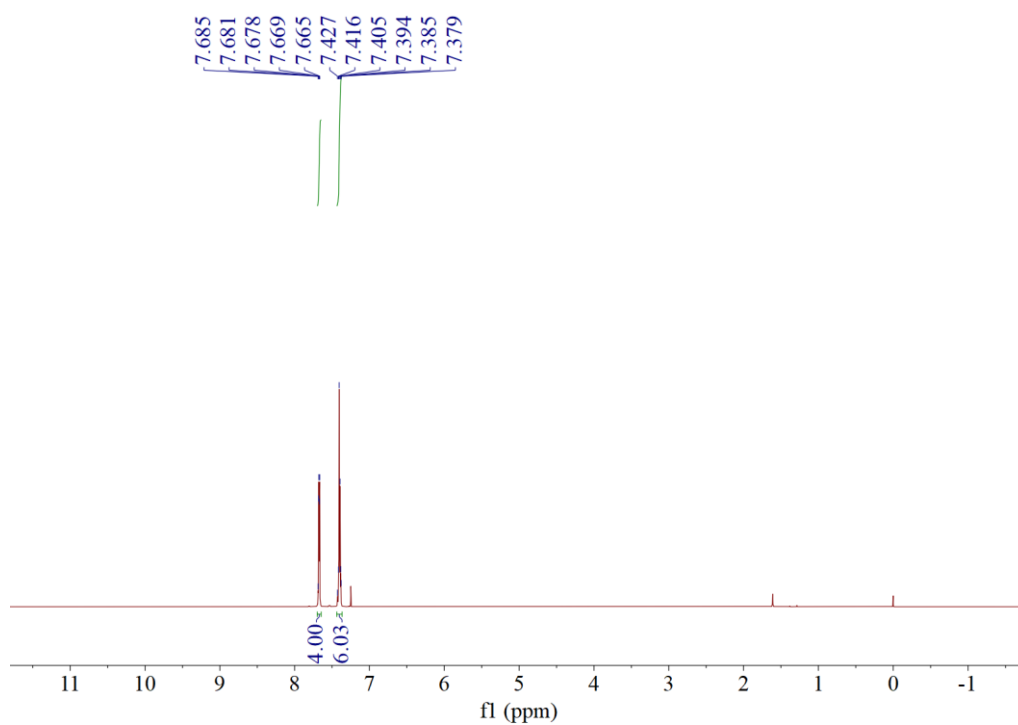


Fig. S13. ^1H NMR spectrum of compound **3d**.

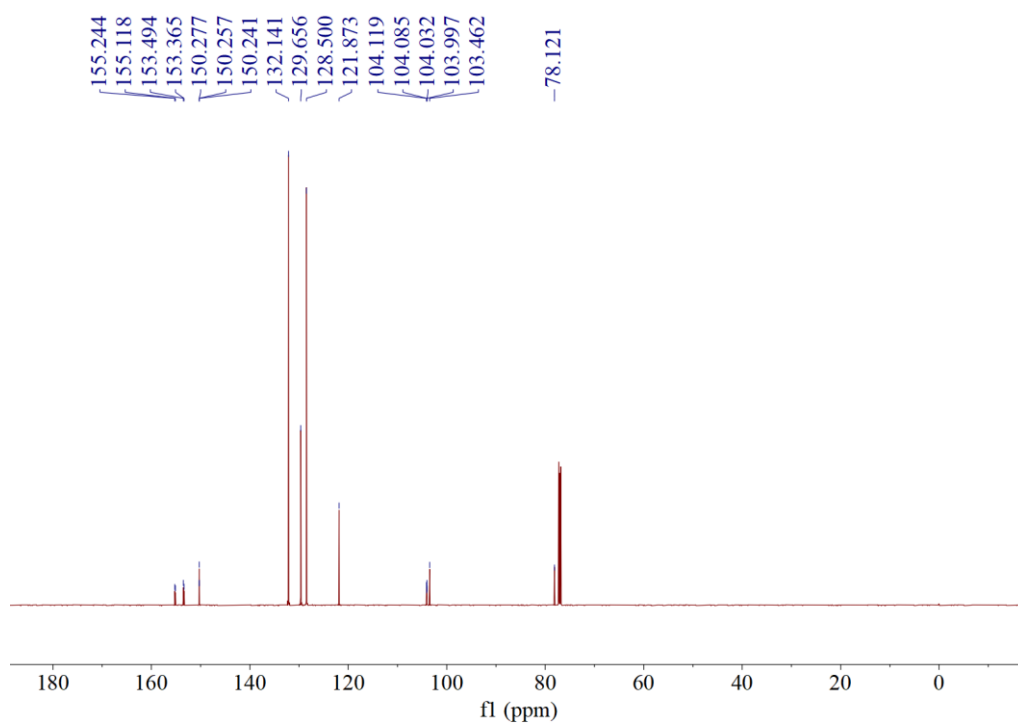


Fig. S14. ^{13}C NMR spectrum of compound **3d**.

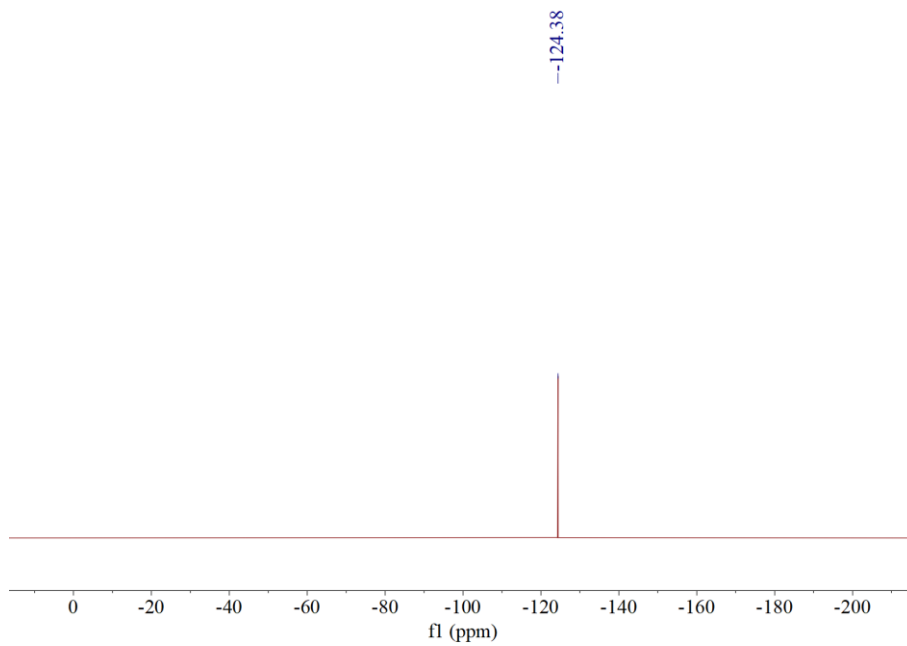


Fig. S15. ^{19}F NMR spectrum of compound **3d**.

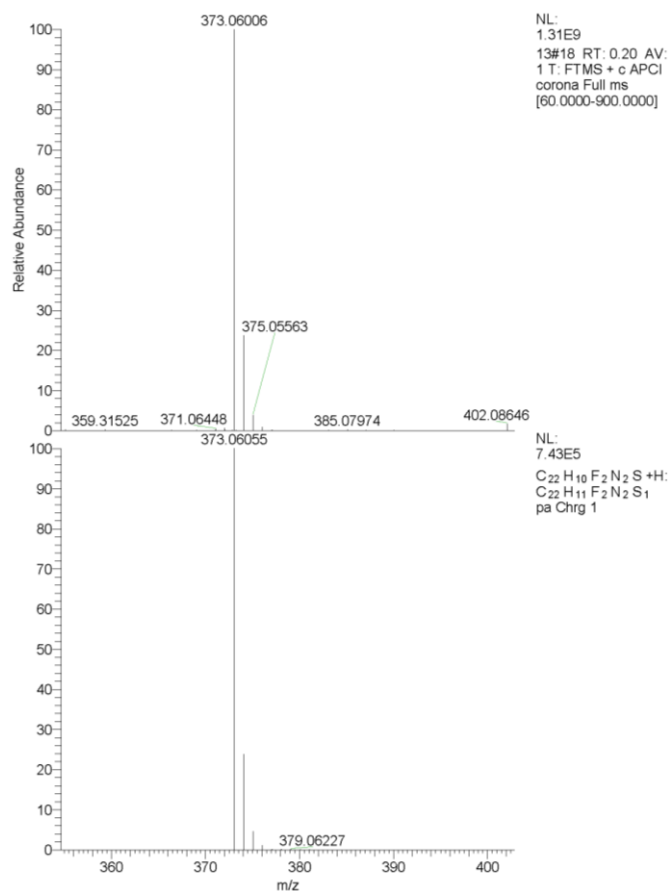


Fig. S16. HRMS spectrum of compound **3d**.

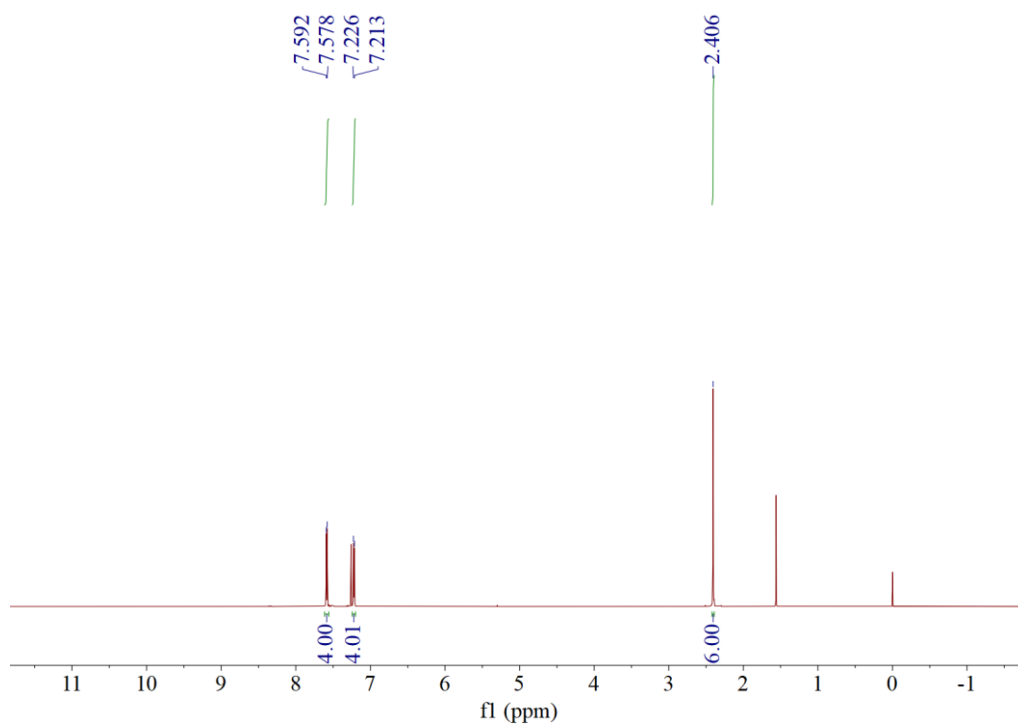


Fig. S17. ^1H NMR spectrum of compound **3e**.

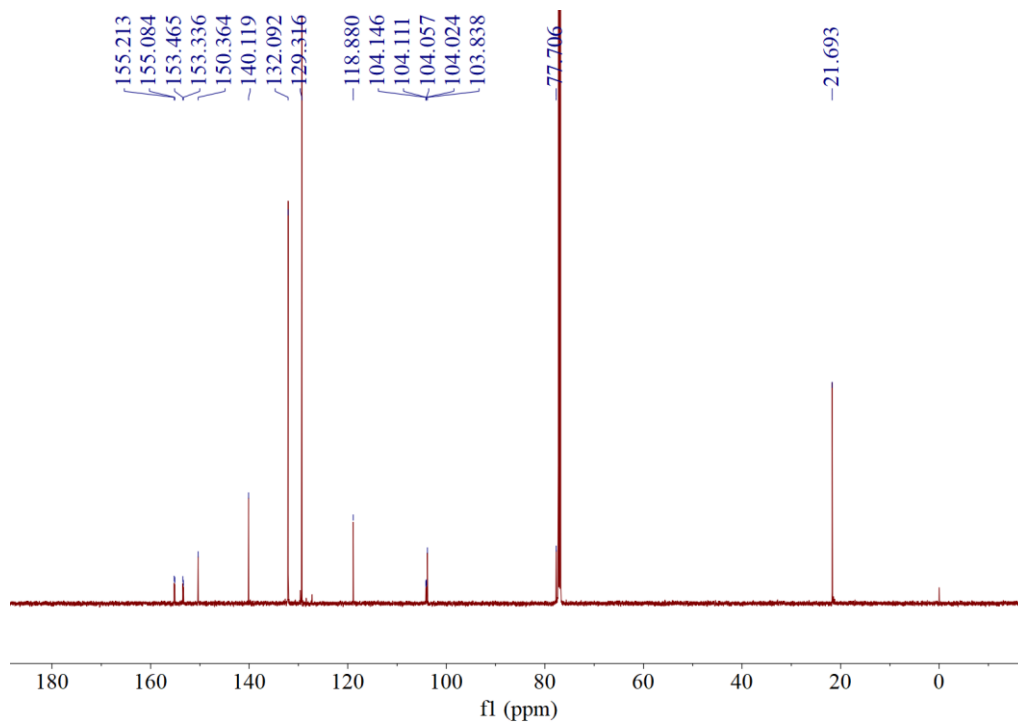


Fig. S18. ^{13}C NMR spectrum of compound **3e**.

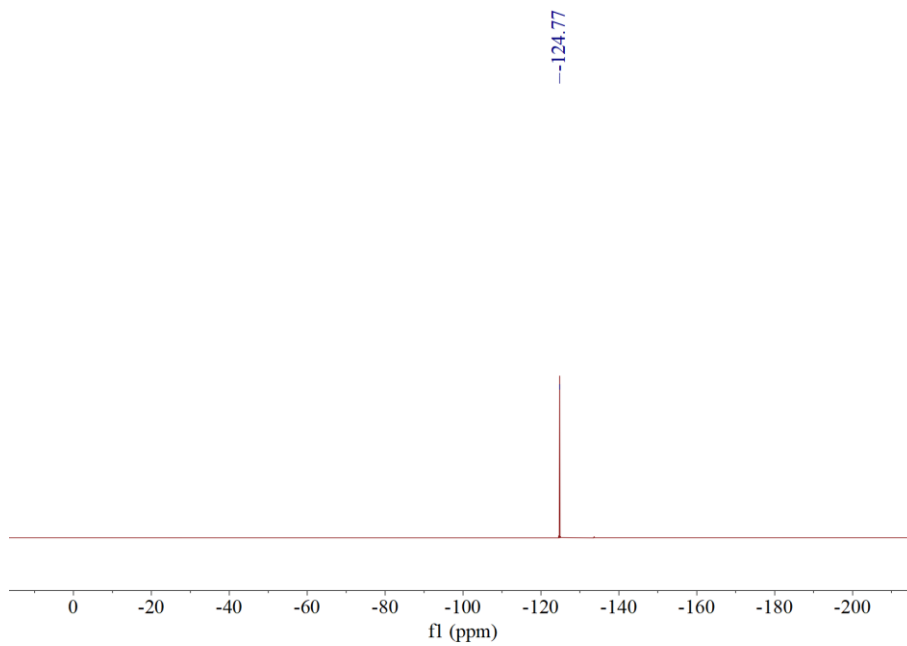


Fig. S19. ^{19}F NMR spectrum of compound **3e**.

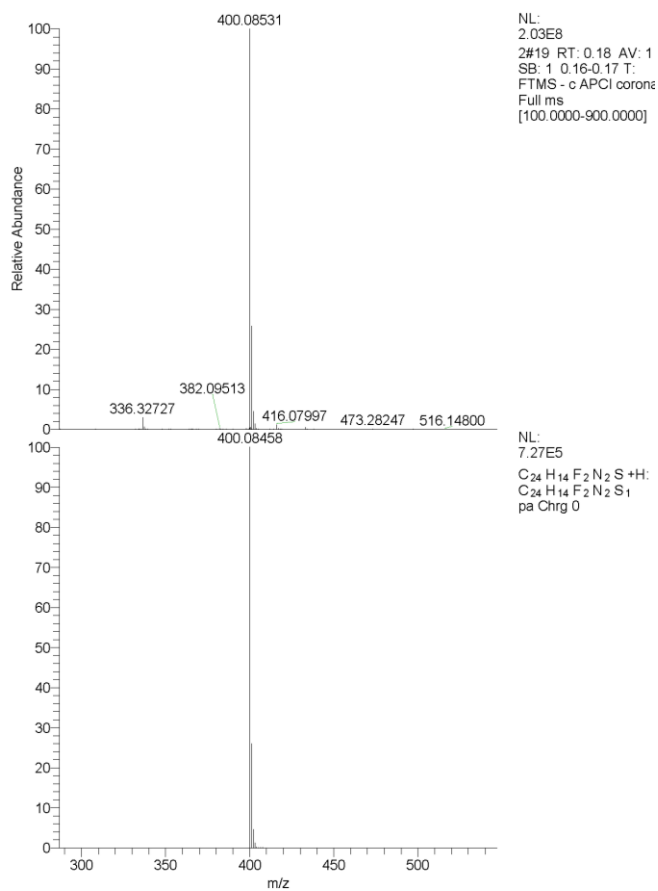


Fig. S20. HRMS spectrum of compound **3e**.

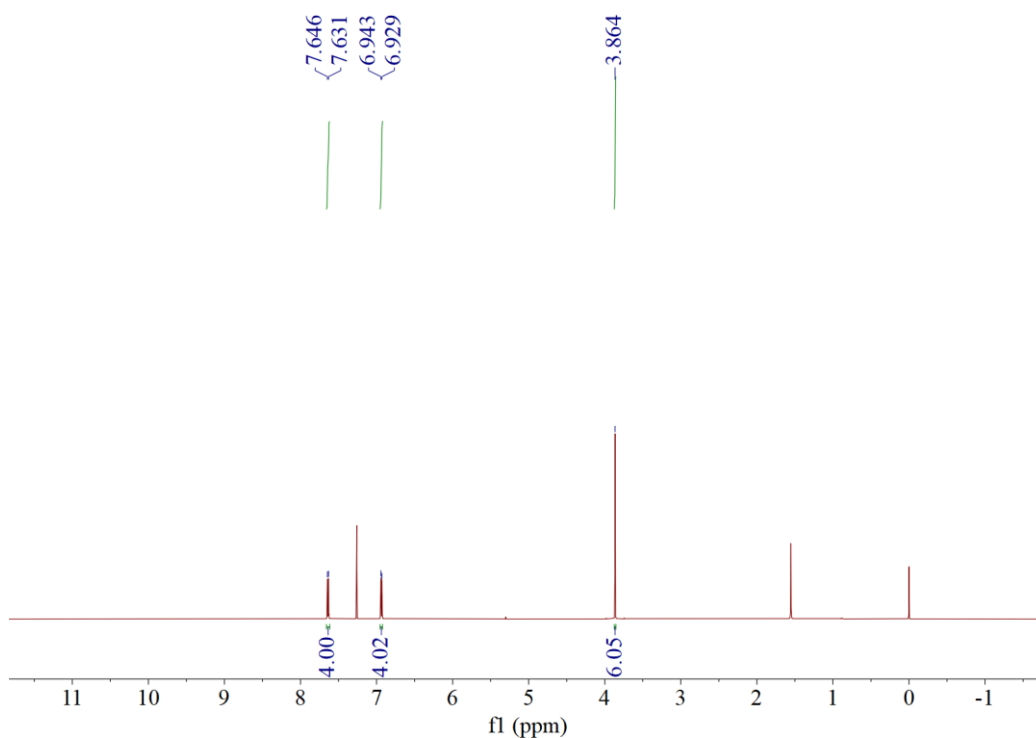


Fig. S21. ^1H NMR spectrum of compound **3f**.

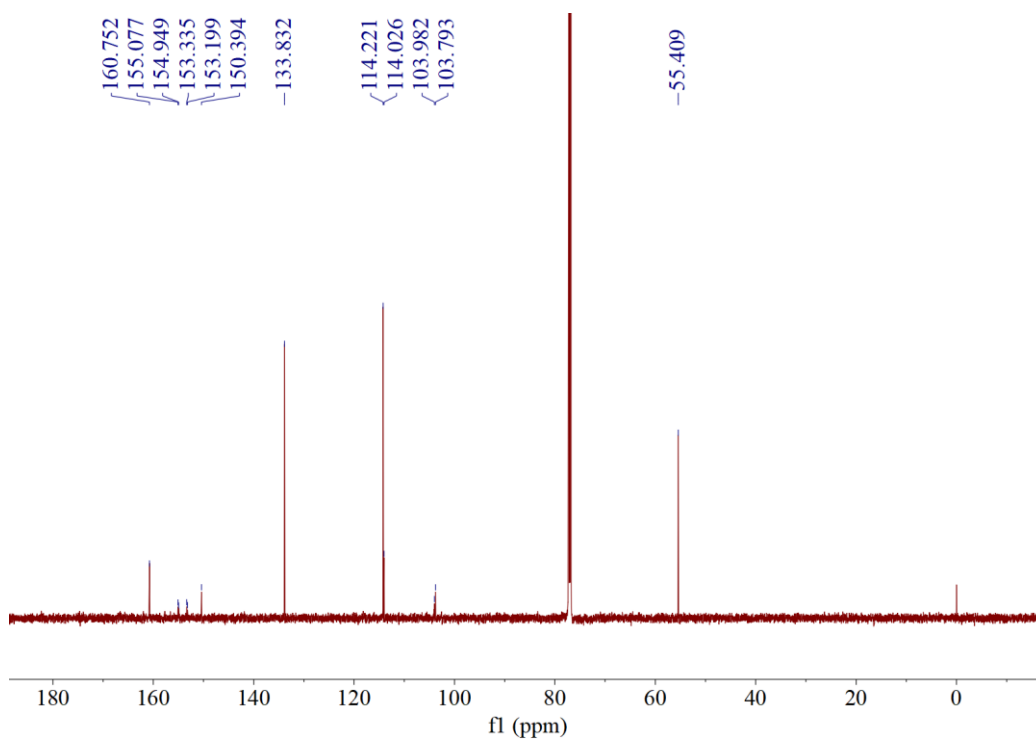


Fig. S22. ^{13}C NMR spectrum of compound **3f**.

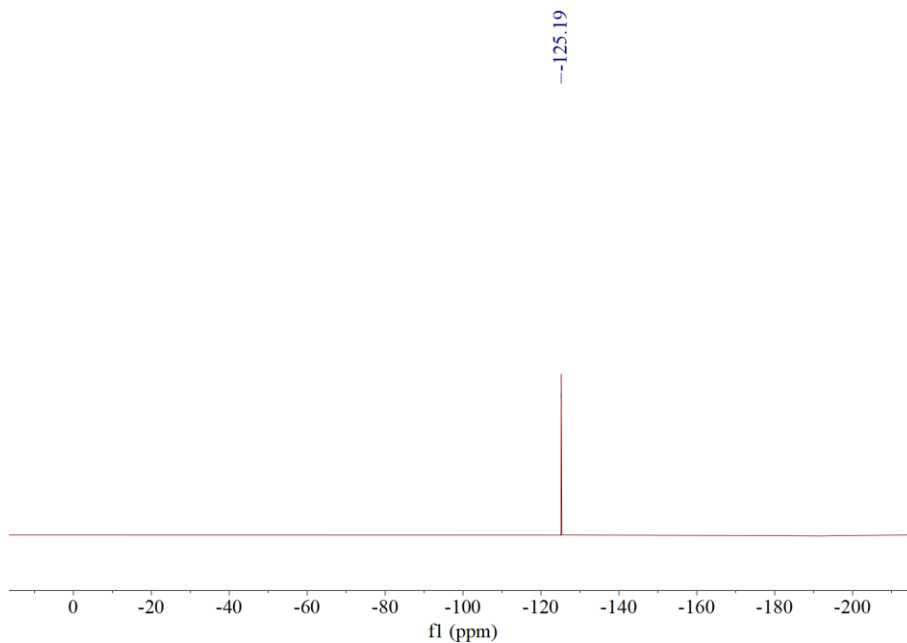


Fig. S23. ^{19}F NMR spectrum of compound **3f**.

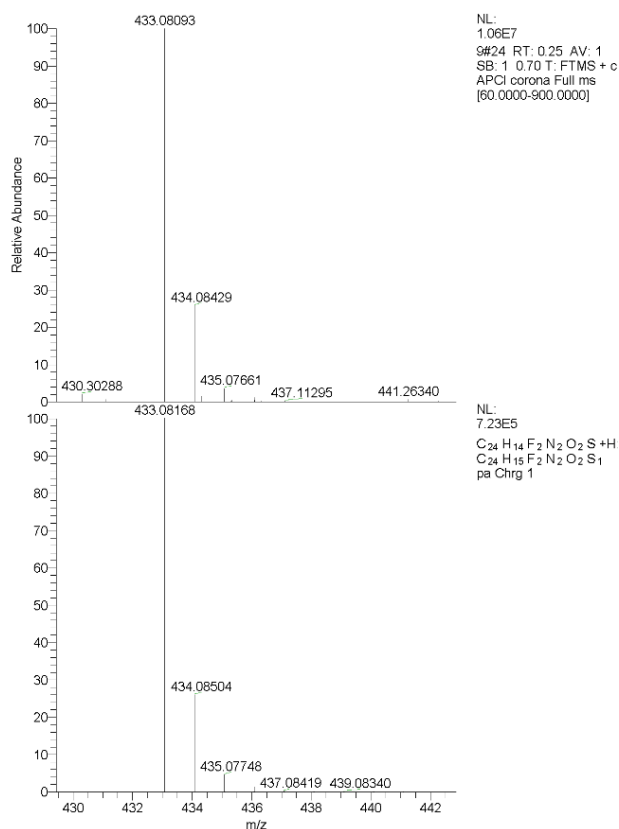


Fig. S24. HRMS spectrum of compound **3f**.

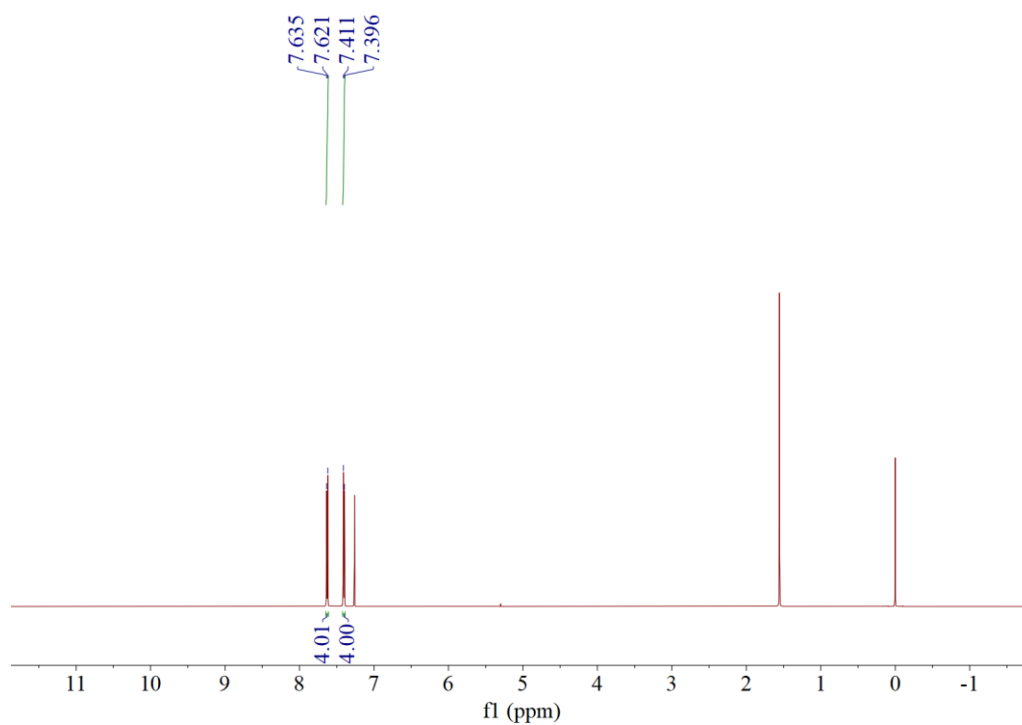


Fig. S25. ^1H NMR spectrum of compound **3g**.

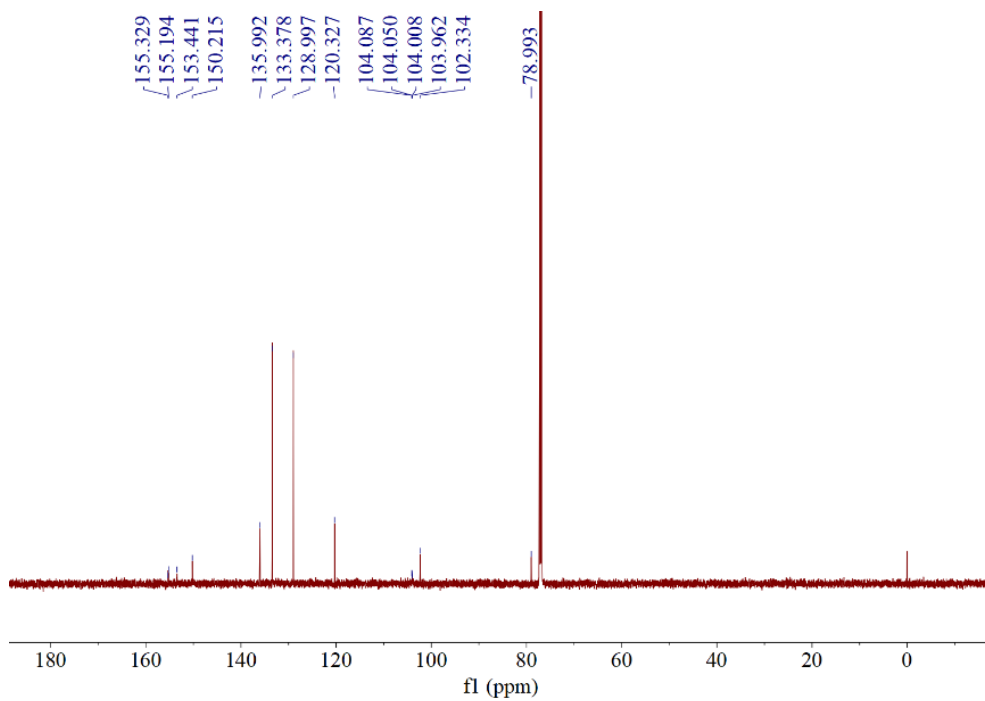


Fig. S26. ^{13}C NMR spectrum of compound **3g**.

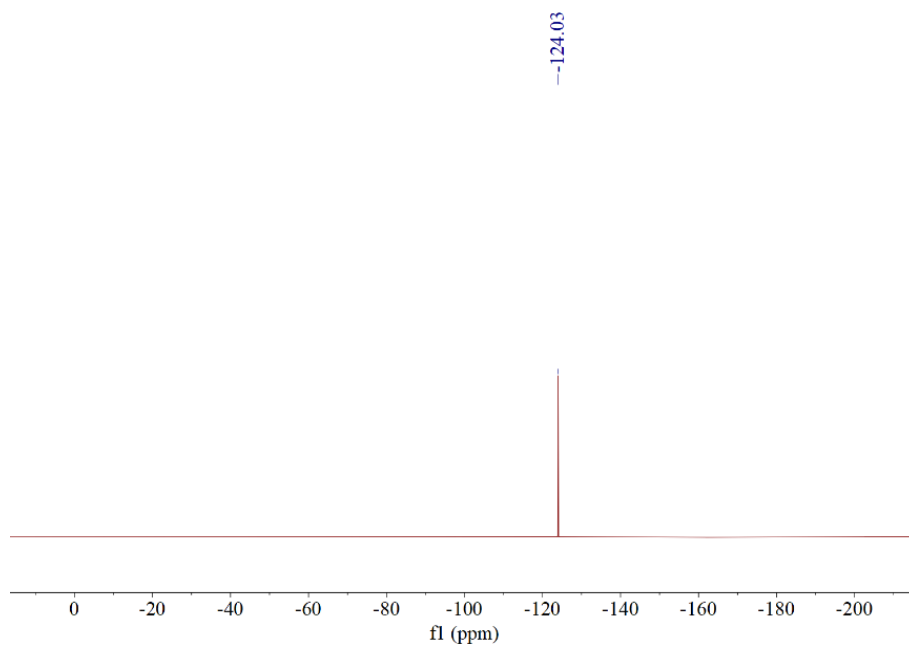


Fig. S27. ^{19}F NMR spectrum of compound **3g**.

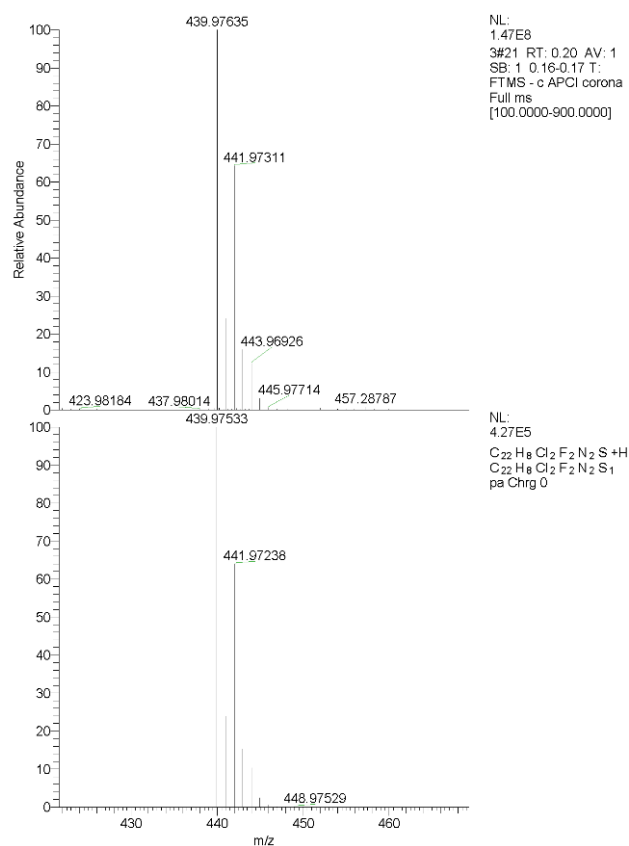


Fig. S28. HRMS spectrum of compound **3g**.

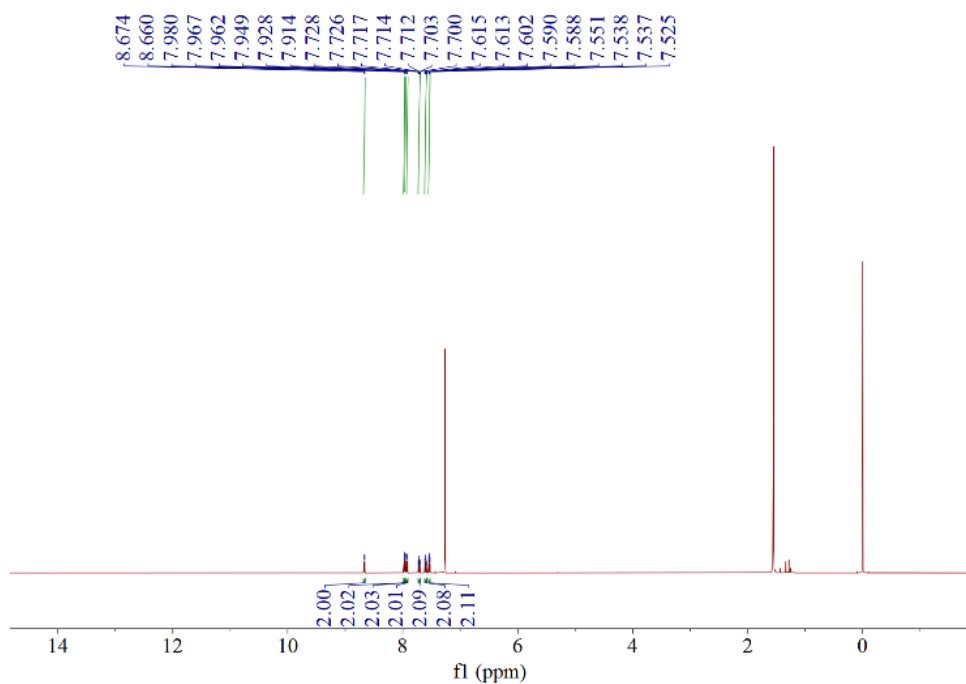


Fig. S29. ^1H NMR spectrum of compound **3h**.

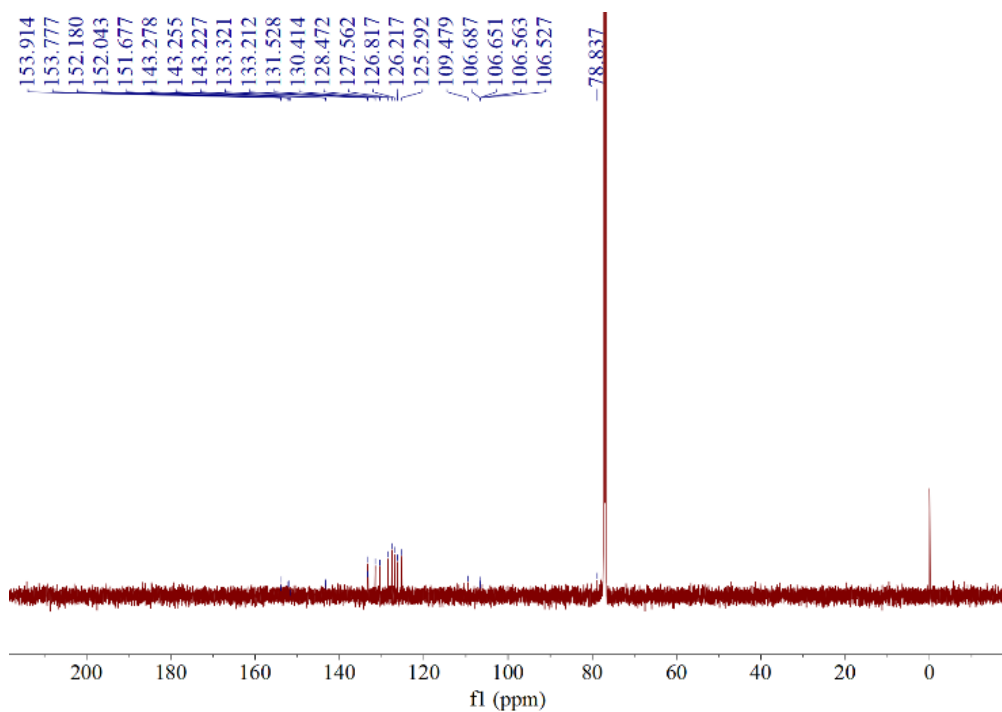


Fig. S30. ^{13}C NMR spectrum of compound **3h**.

--124.53

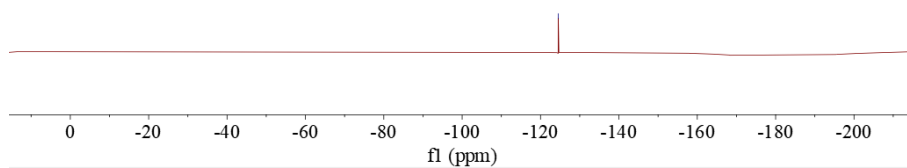


Fig. S31. ^{19}F NMR spectrum of compound **3h**.

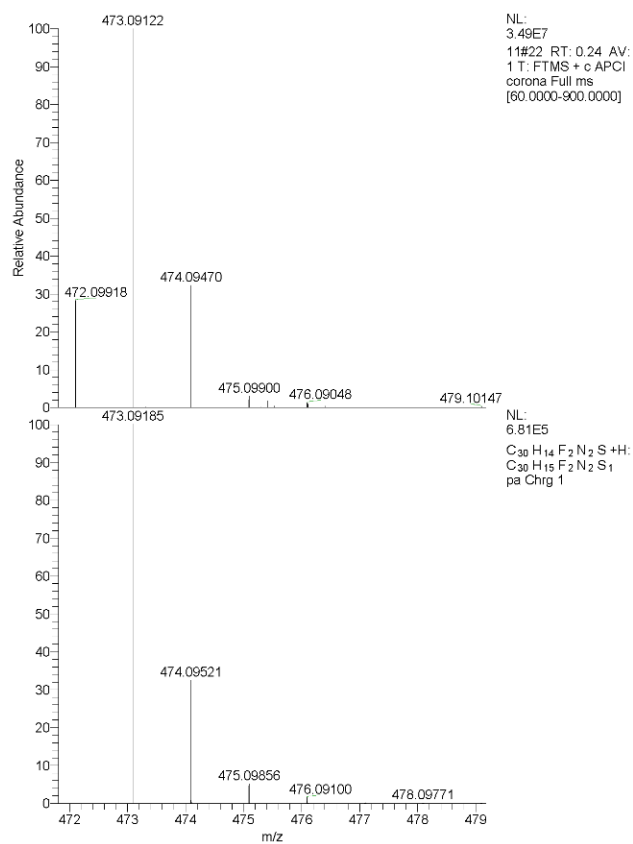


Fig. S32. HRMS spectrum of compound **3h**.

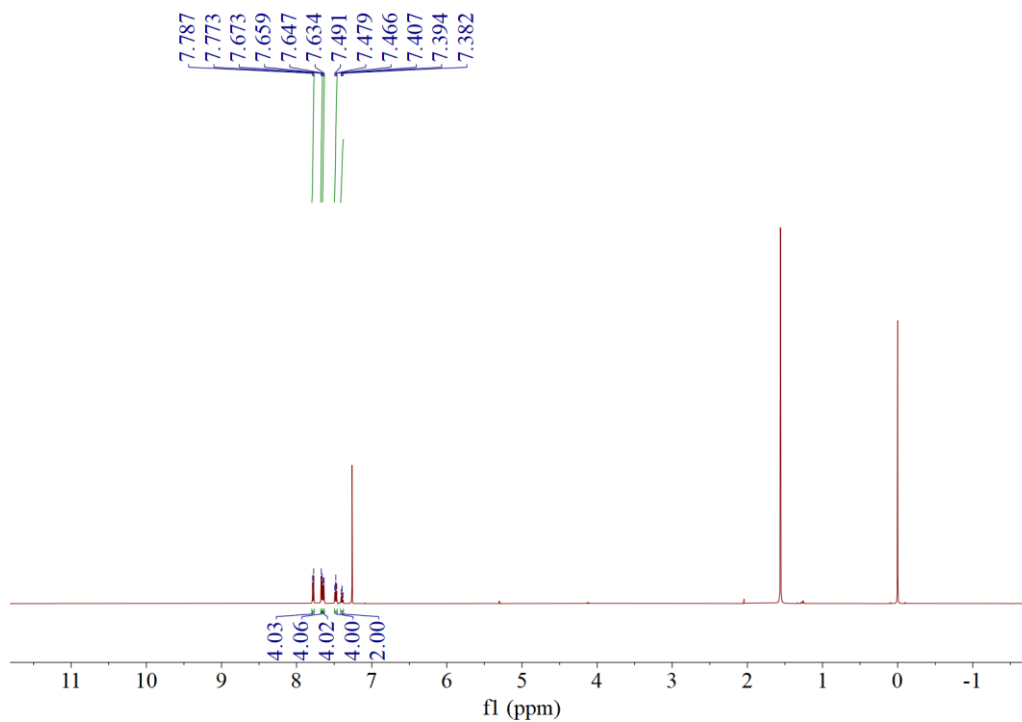


Fig. S33. ^1H NMR spectrum of compound **3i**.

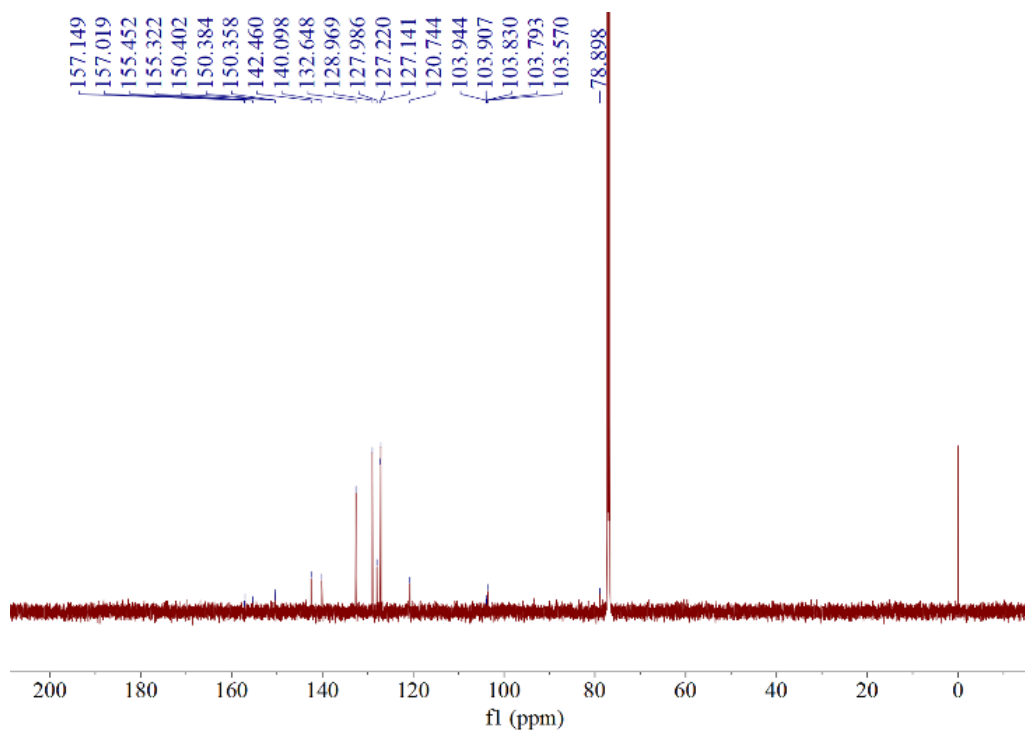


Fig. S34. ^{13}C NMR spectrum of compound **3i**.

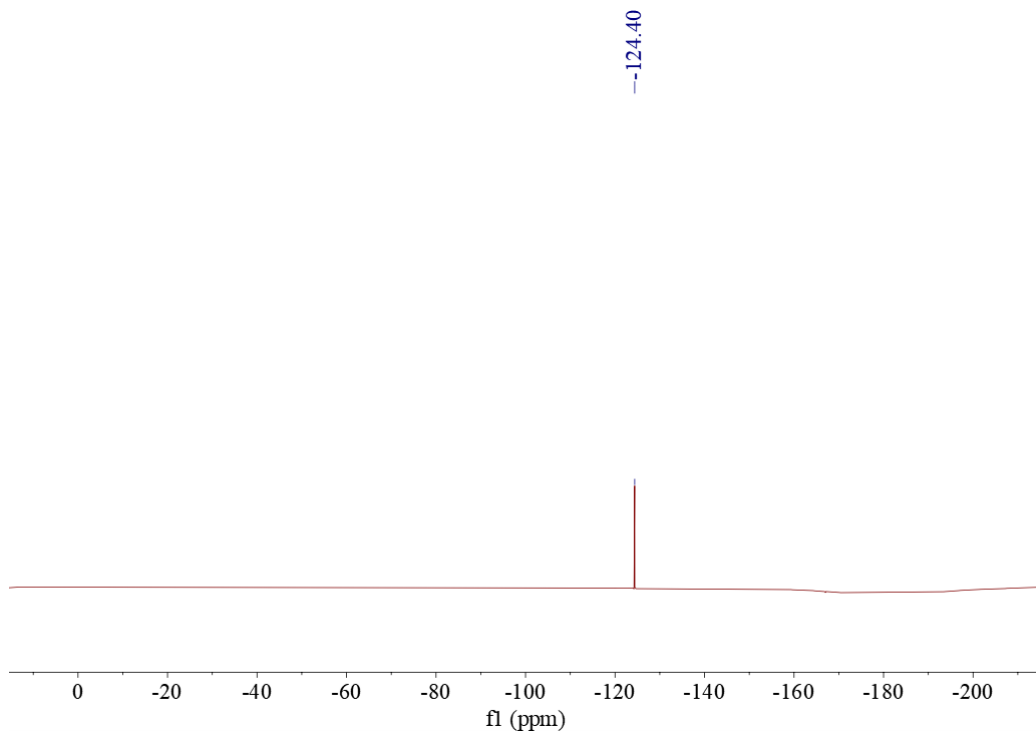


Fig. S35. ^{19}F NMR spectrum of compound **3i**.

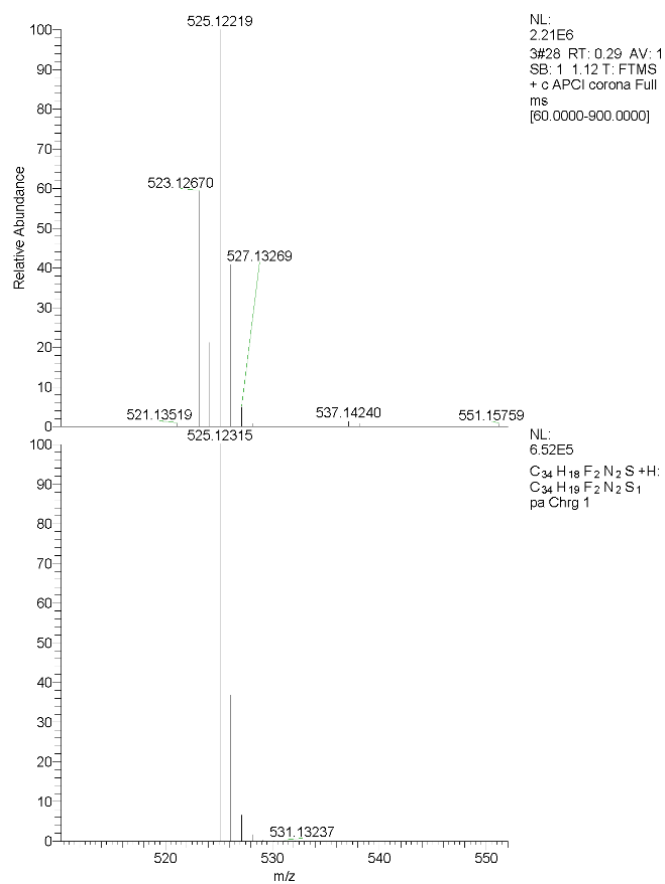


Fig. S36. HRMS spectrum of compound **3i**.

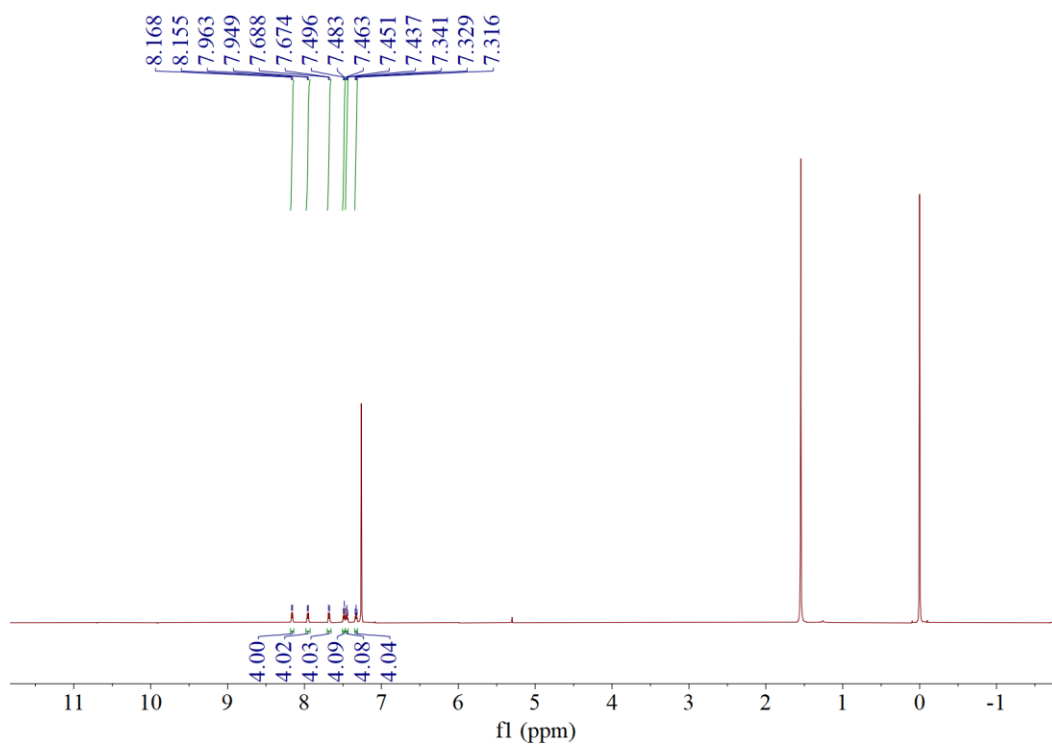


Fig. S37. ^1H NMR spectrum of compound **3j**.

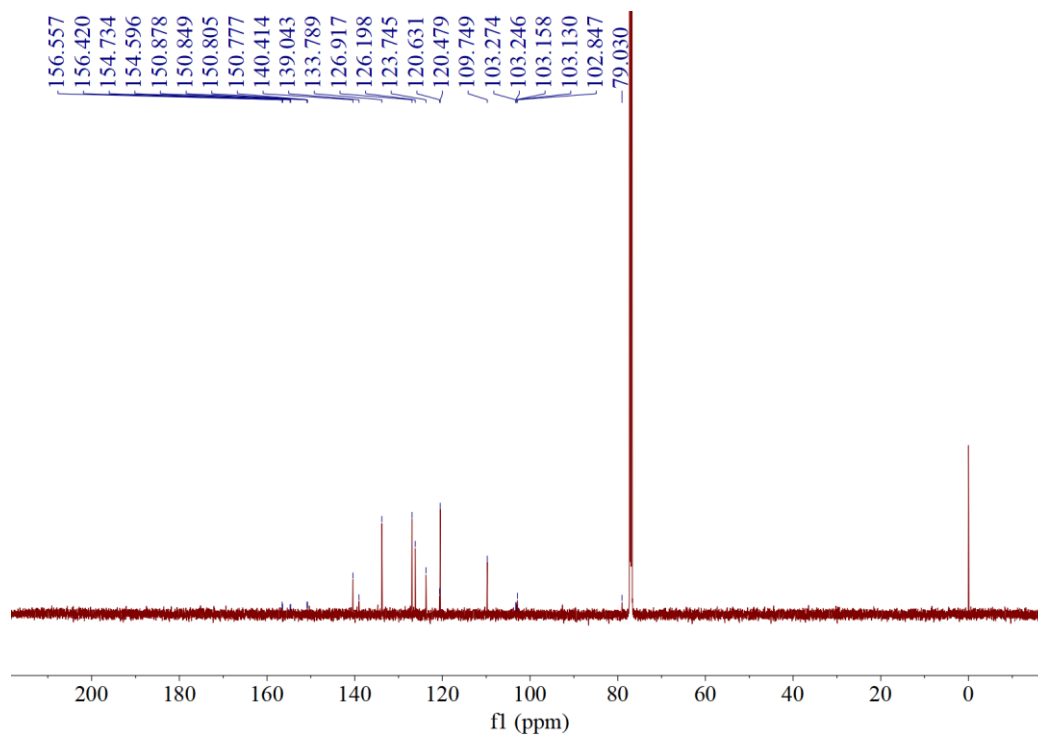


Fig. S38. ^{13}C NMR spectrum of compound **3j**.

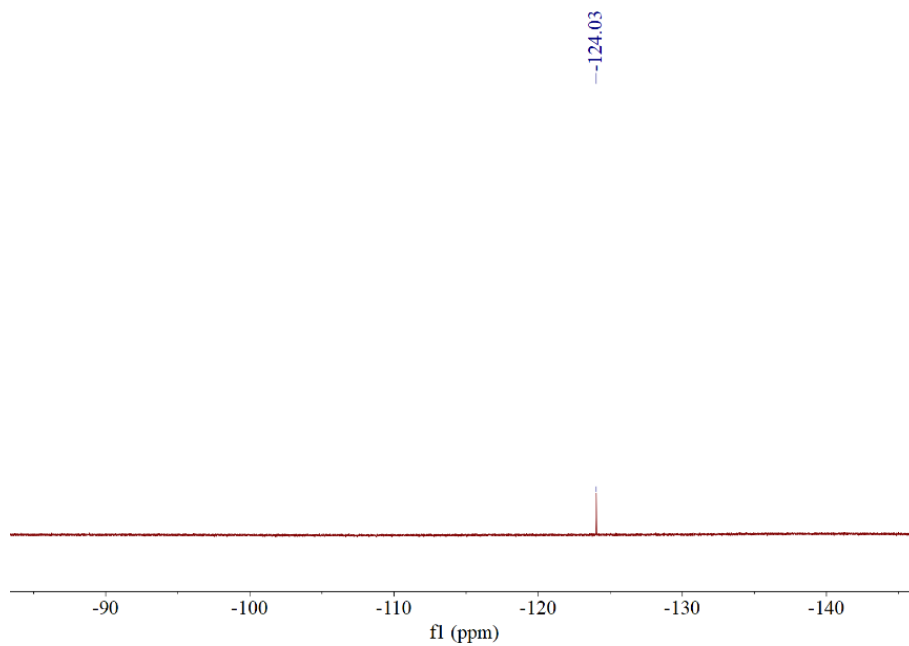


Fig. S39. ^{19}F NMR spectrum of compound **3j**.

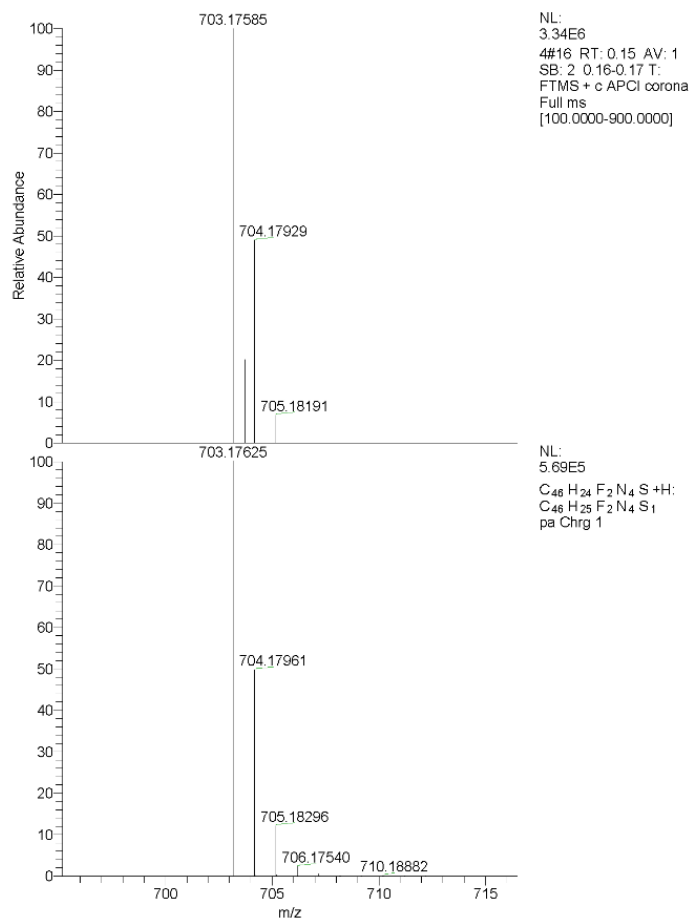


Fig. S40. HRMS spectrum of compound **3j**.

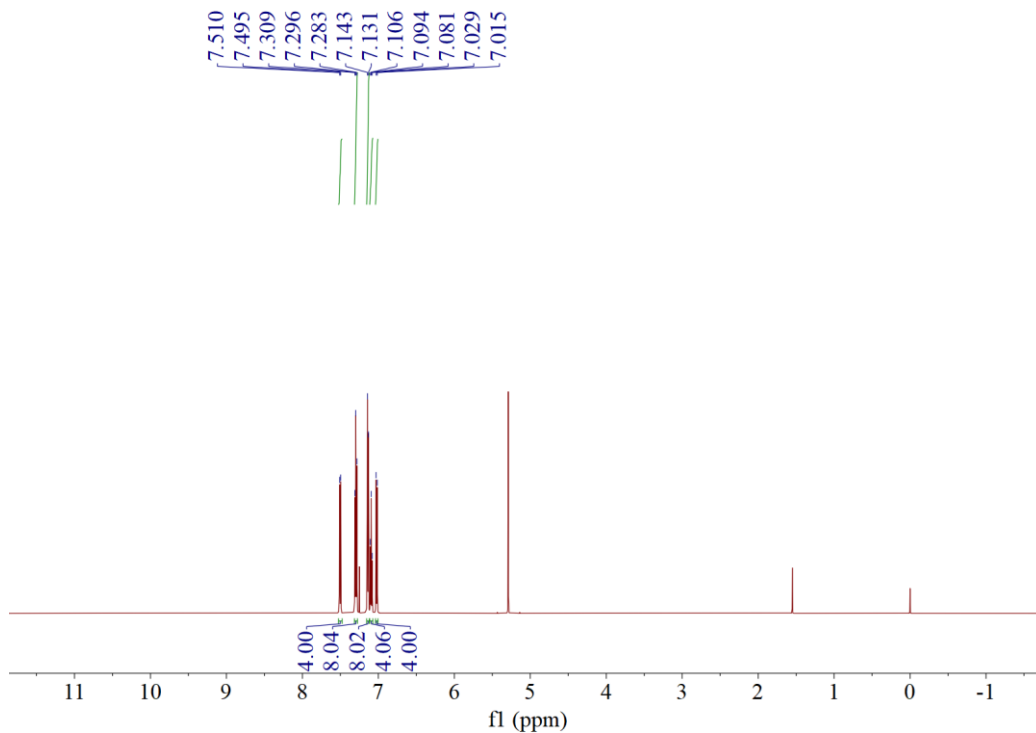


Fig. S41. ^1H NMR spectrum of compound **3k**.

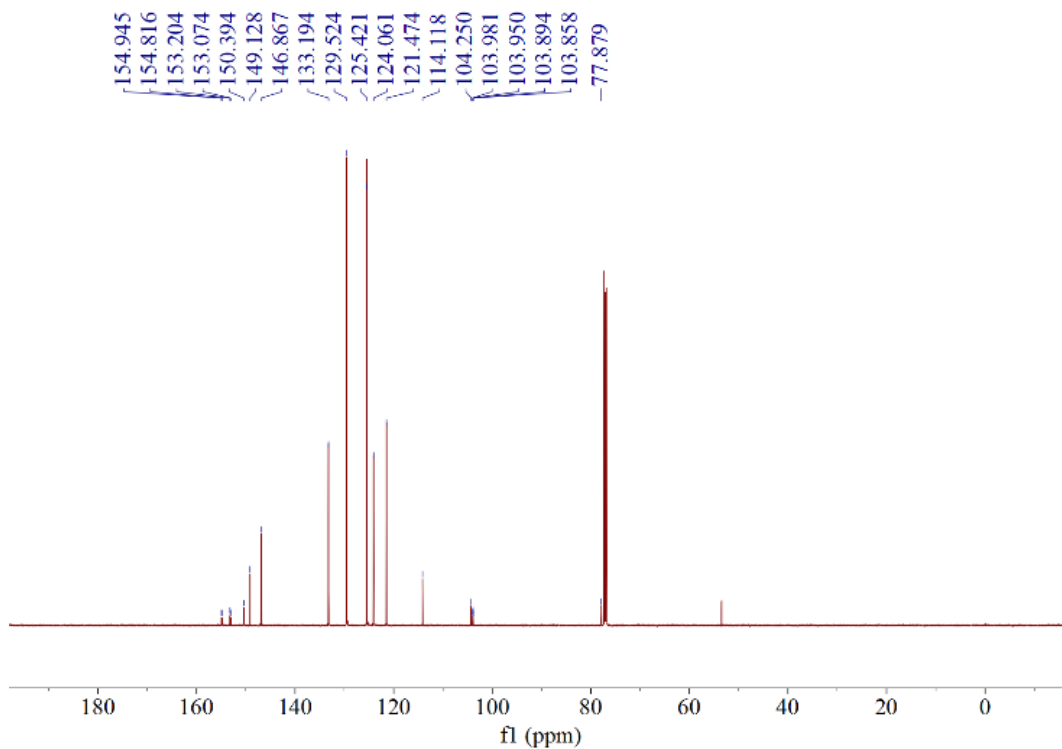


Fig. S42. ^{13}C NMR spectrum of compound **3k**.

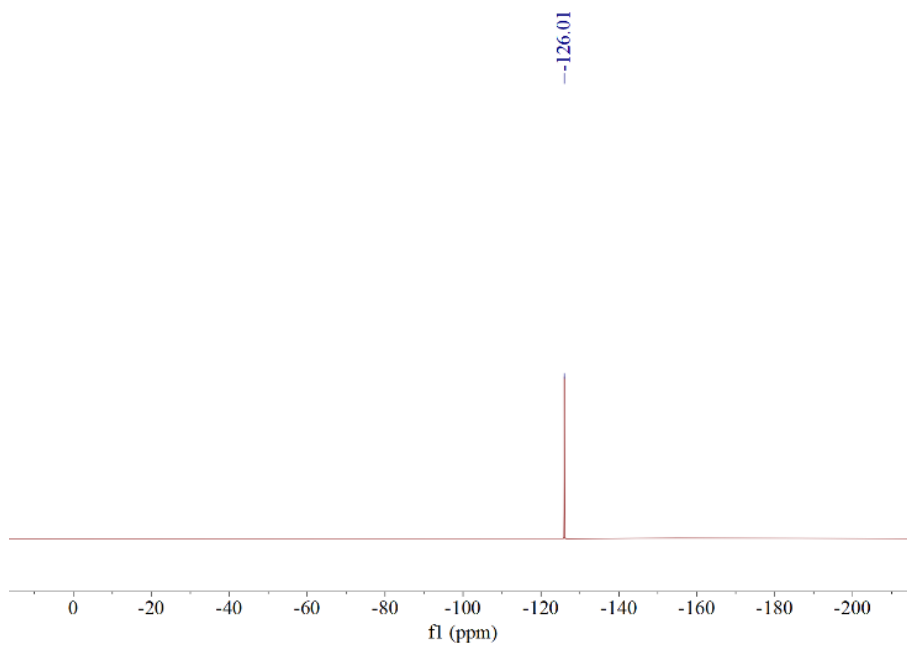


Fig. S43. ^{19}F NMR spectrum of compound **3k**.

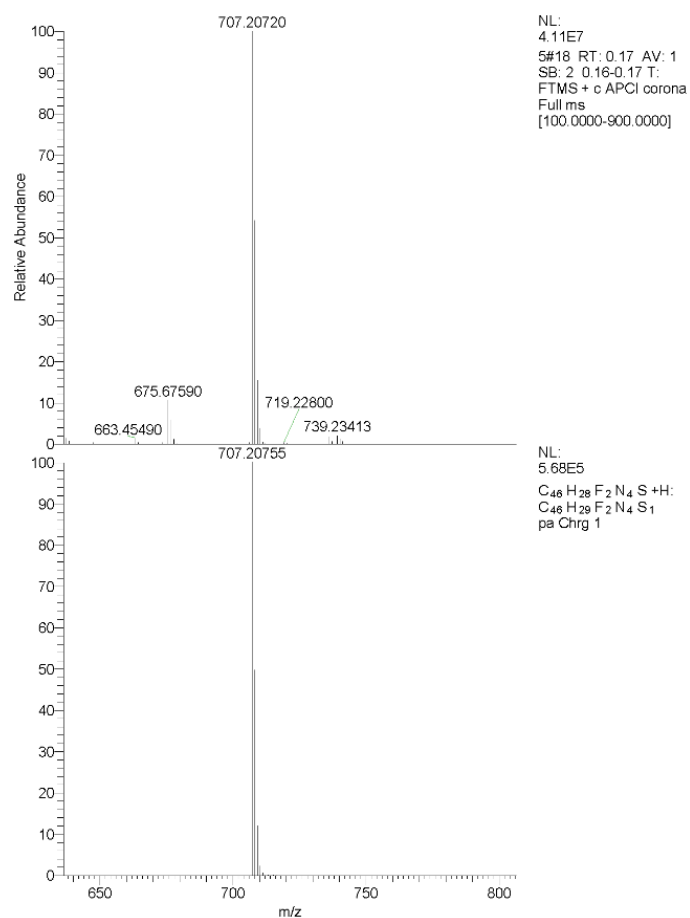


Fig. S44. HRMS spectrum of compound **3k**.

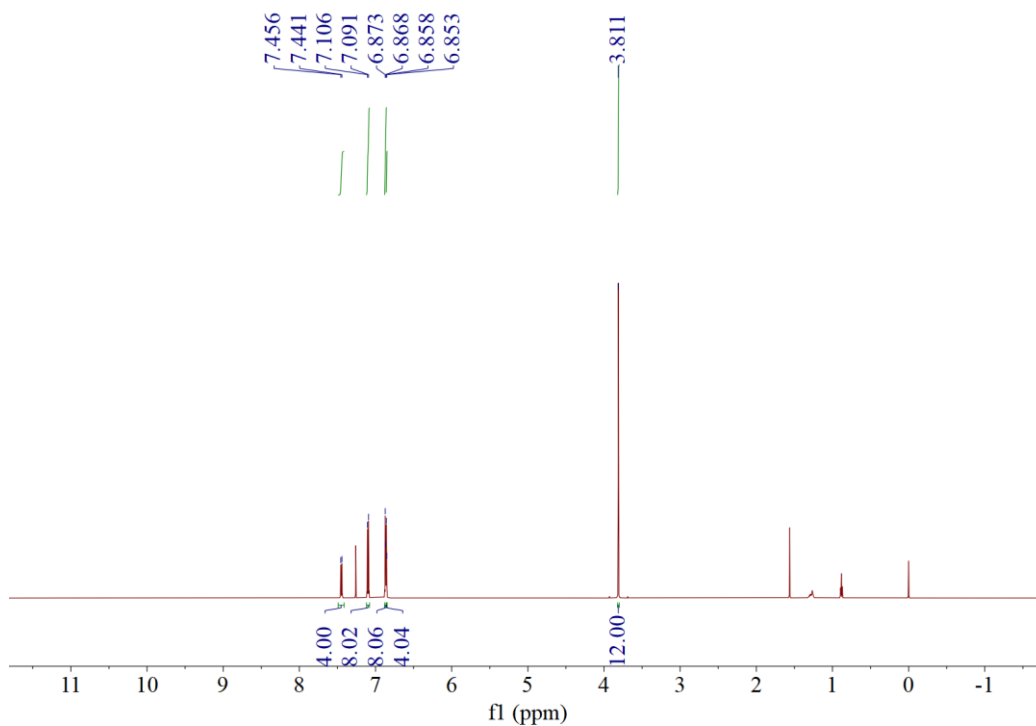


Fig. S45. ^1H NMR spectrum of compound **3I**.

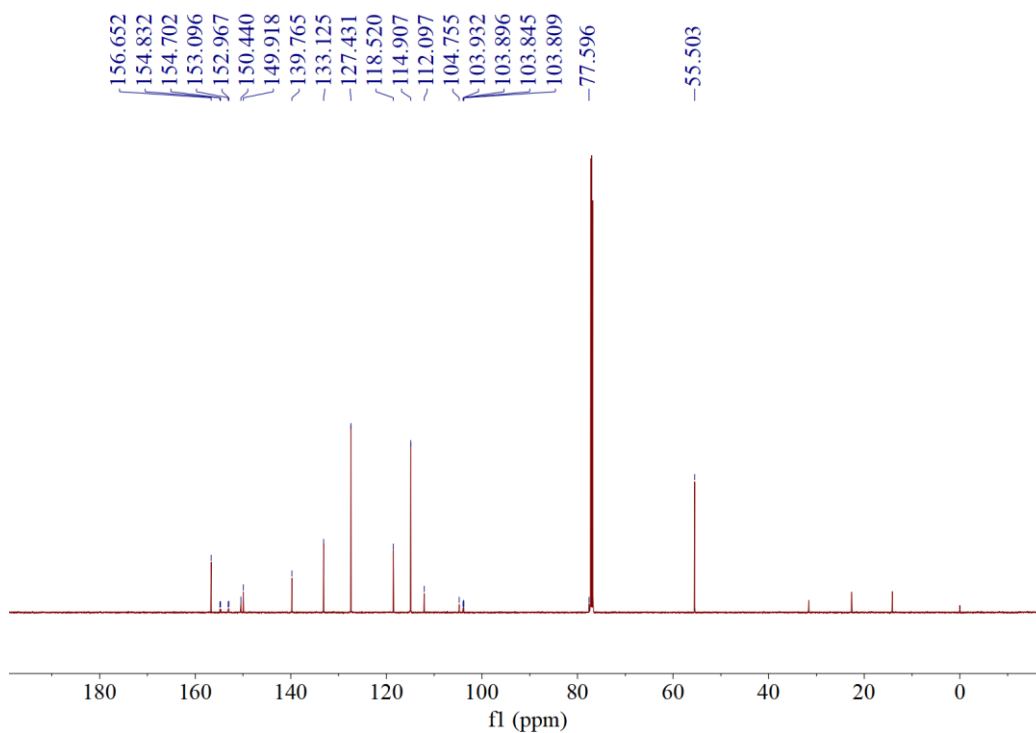


Fig. S46. ^{13}C NMR spectrum of compound **3I**.

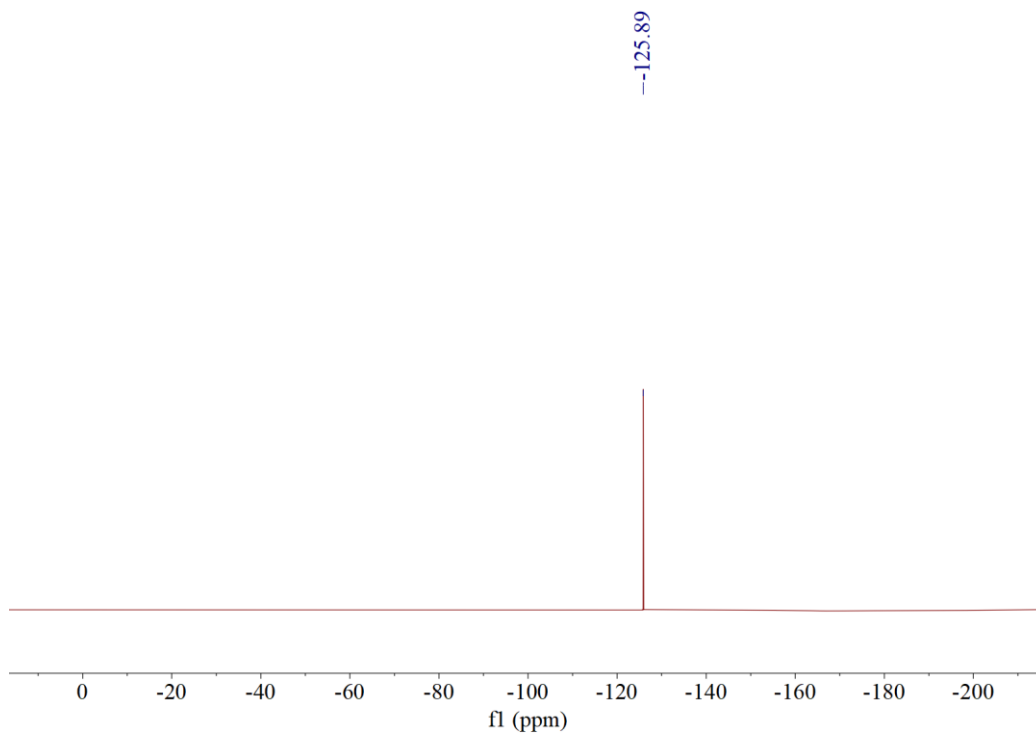


Fig. S47. ^{19}F NMR spectrum of compound **3I**.

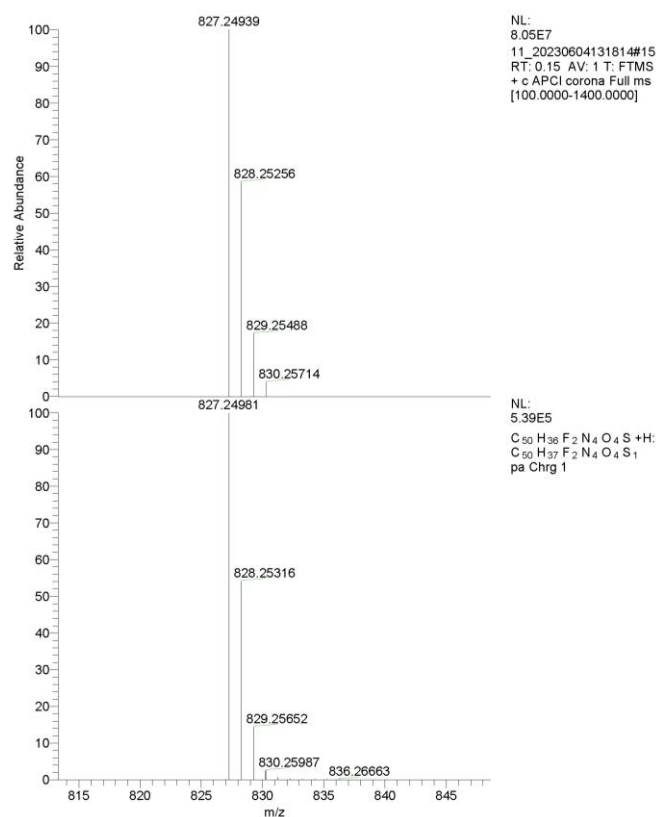


Fig. S48. HRMS spectrum of compound **3I**.

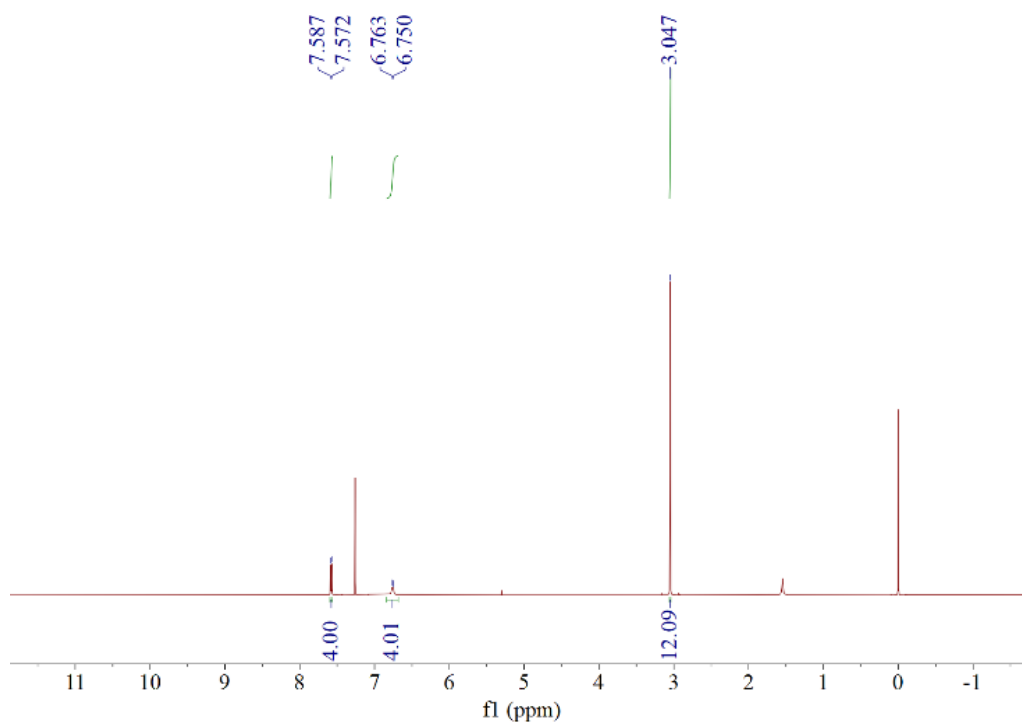


Fig. S49. ^1H NMR spectrum of compound **3m**.

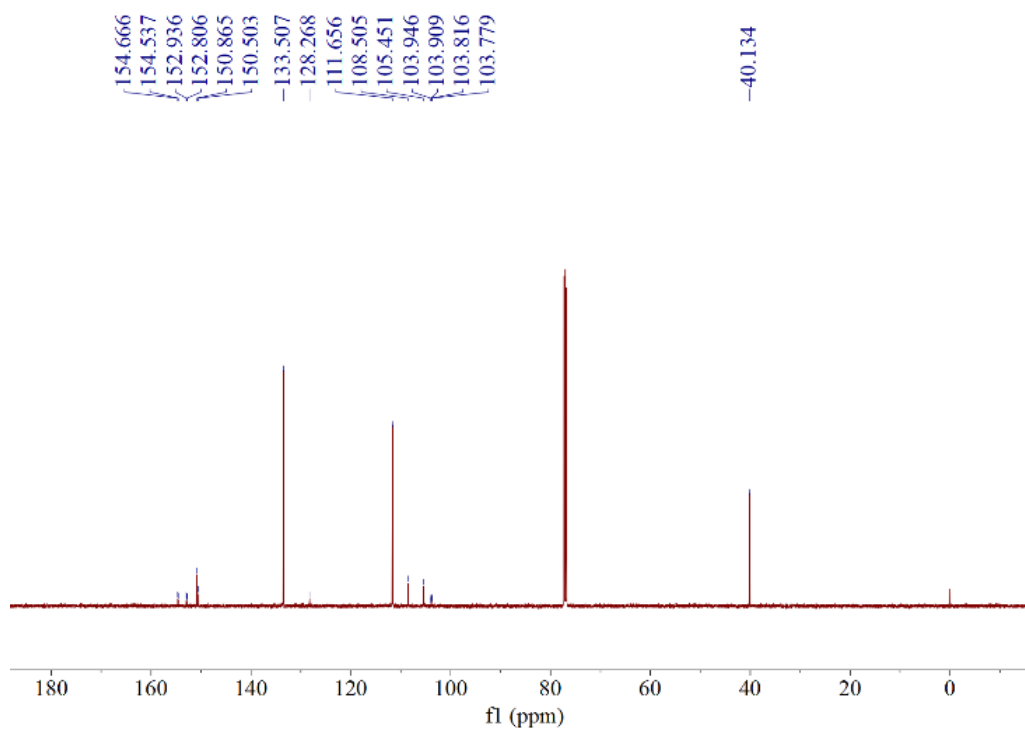


Fig. S50. ^{13}C NMR spectrum of compound **3m**.

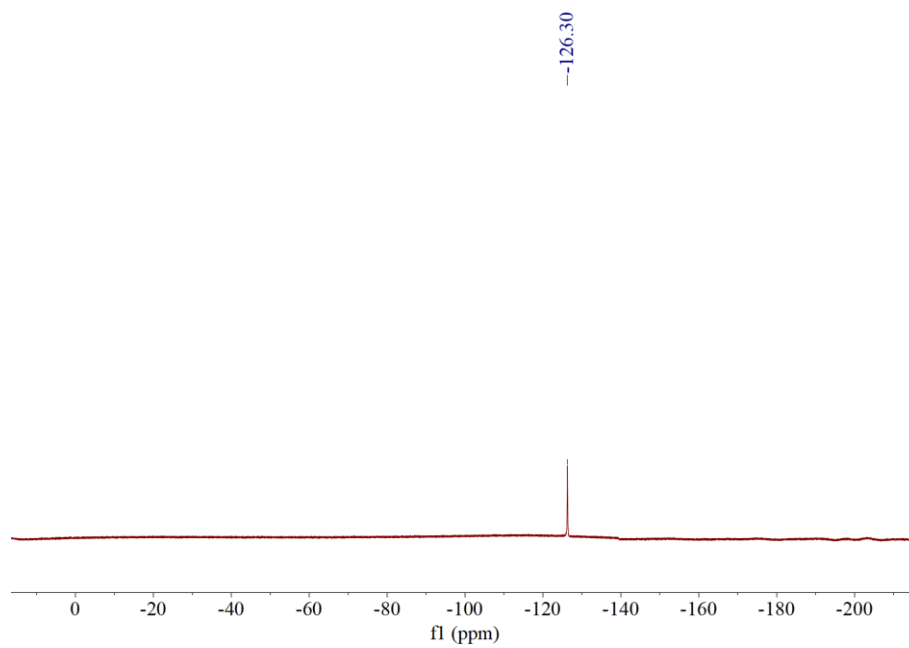


Fig. S51. ^{19}F NMR spectrum of compound **3m**.

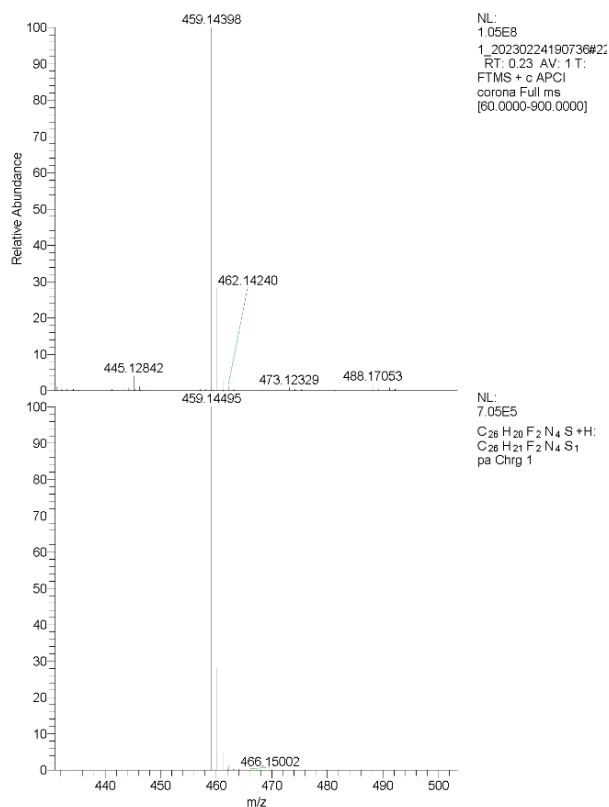


Fig. S52. HRMS spectrum of compound **3m**.

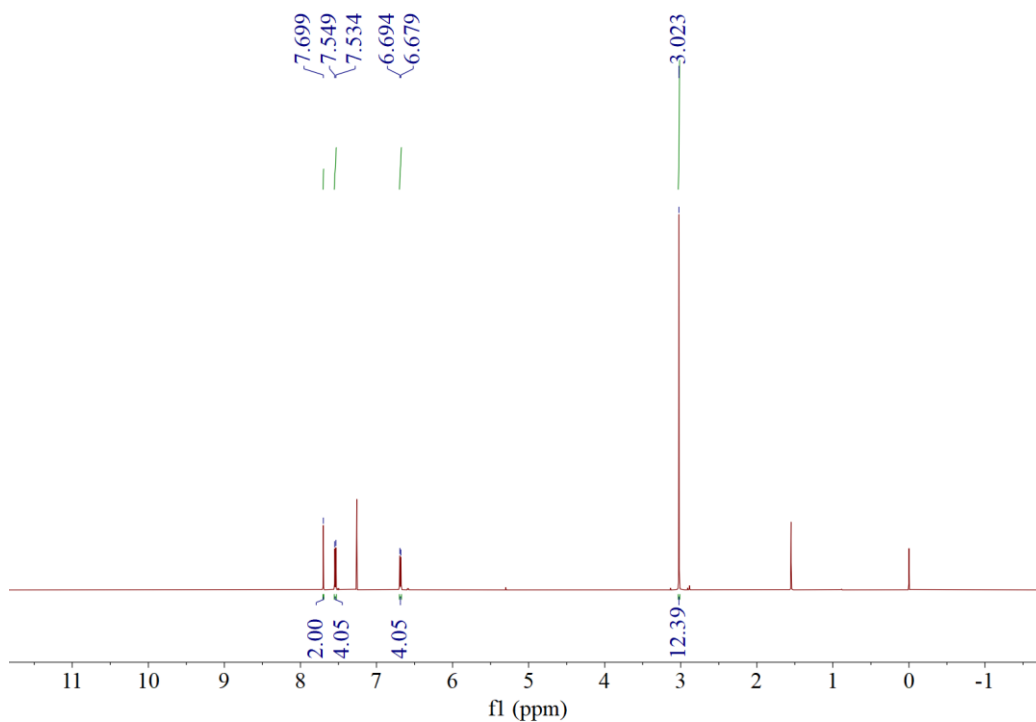


Fig. S53. ^1H NMR spectrum of compound **3n**.

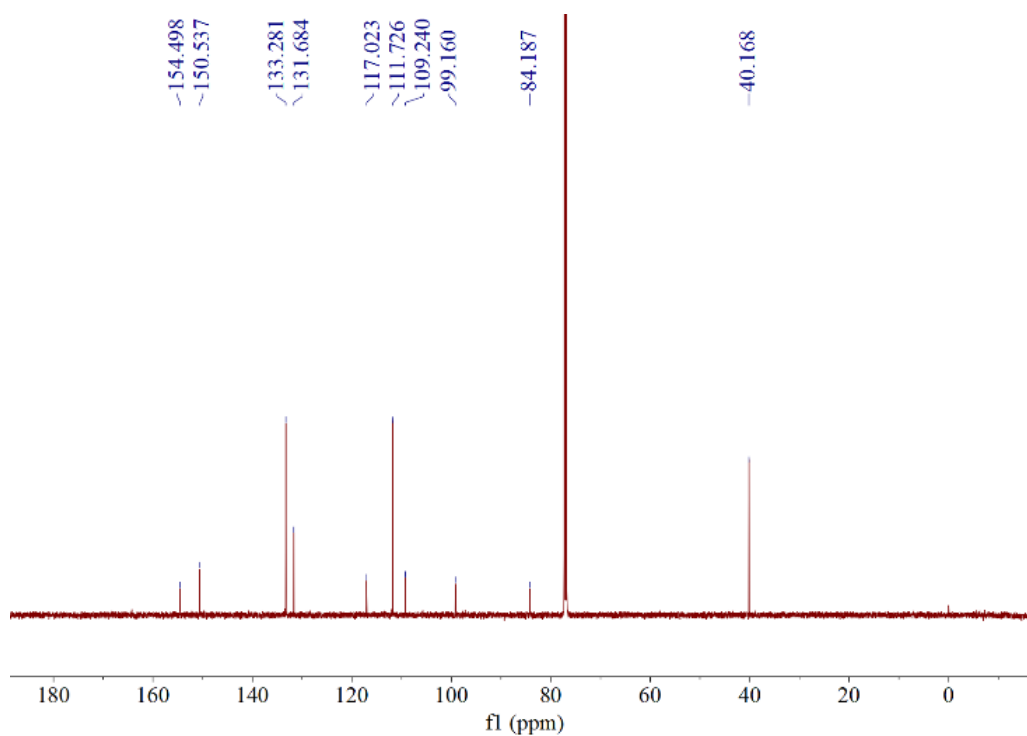


Fig. S54. ^{13}C NMR spectrum of compound **3n**.

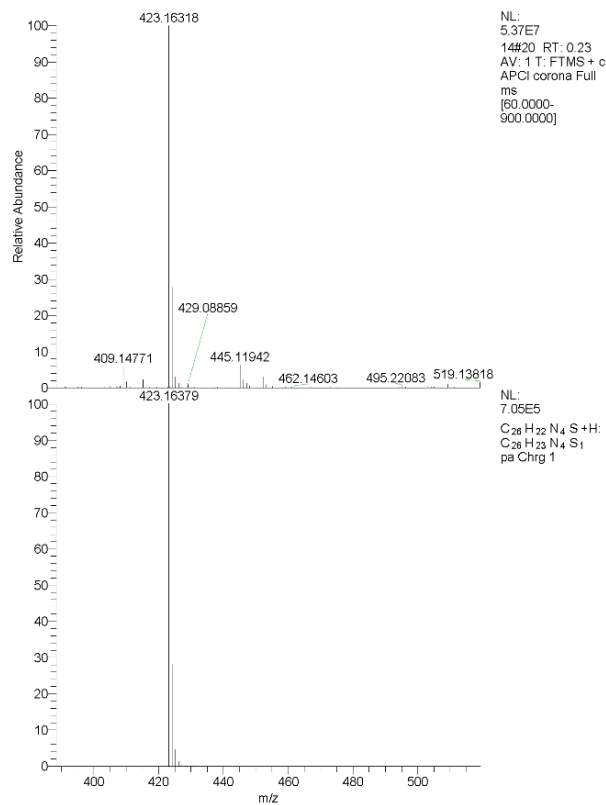


Fig. S55. HRMS spectrum of compound **3n**.

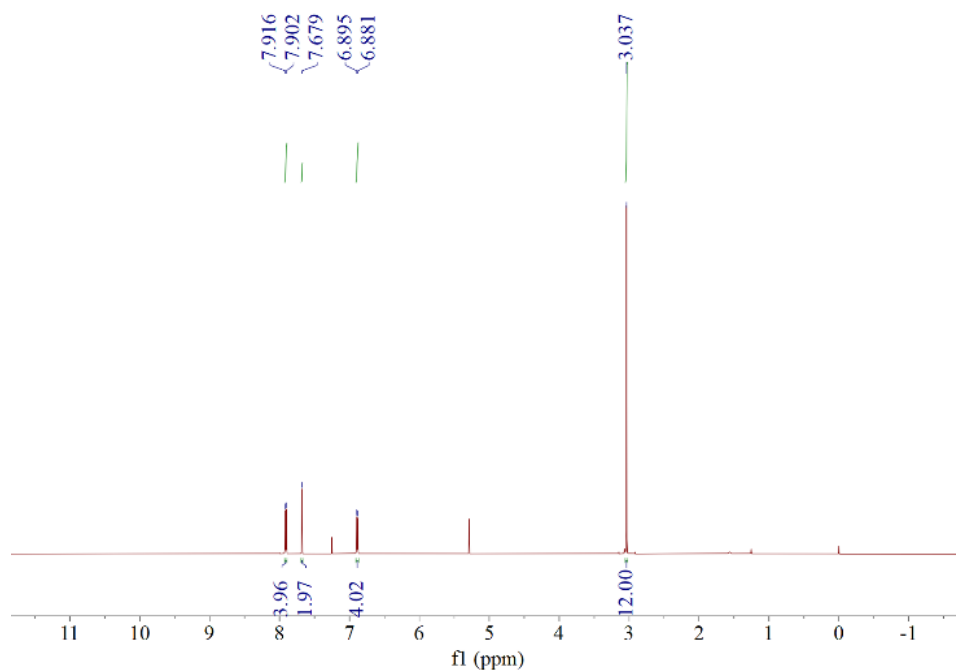


Fig. S56. ¹H NMR spectrum of compound **3o**.

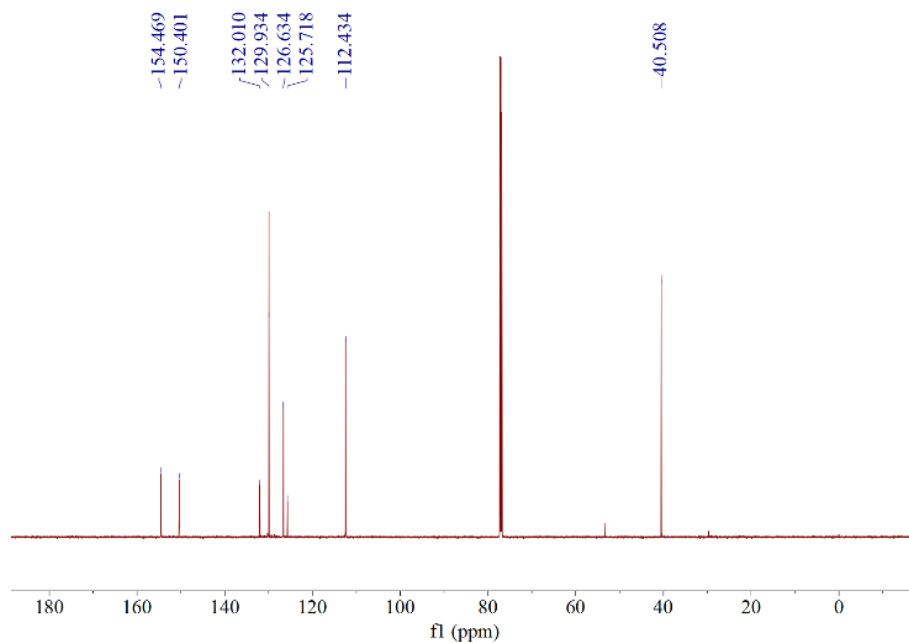


Fig. S57. ^{13}C NMR spectrum of compound **30**.

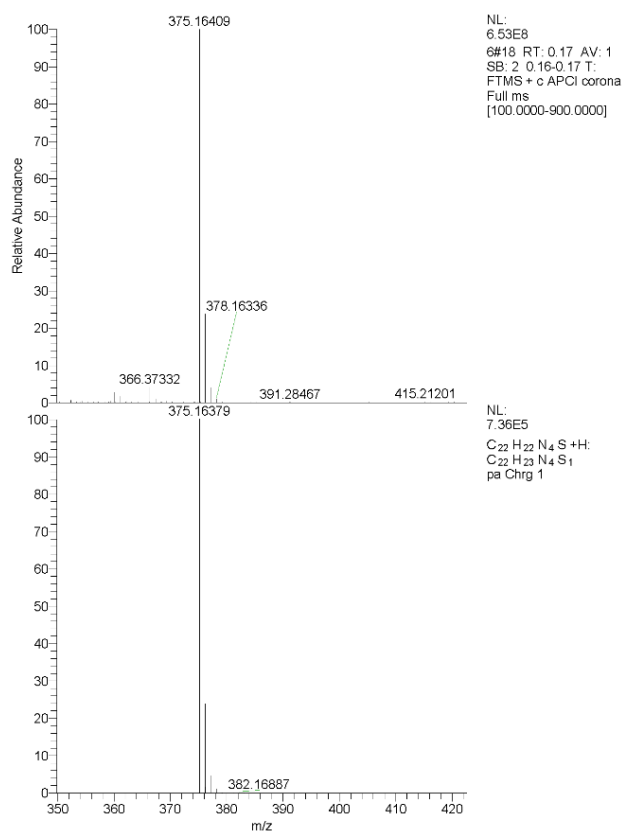


Fig. S58. HRMS spectrum of compound **30**.

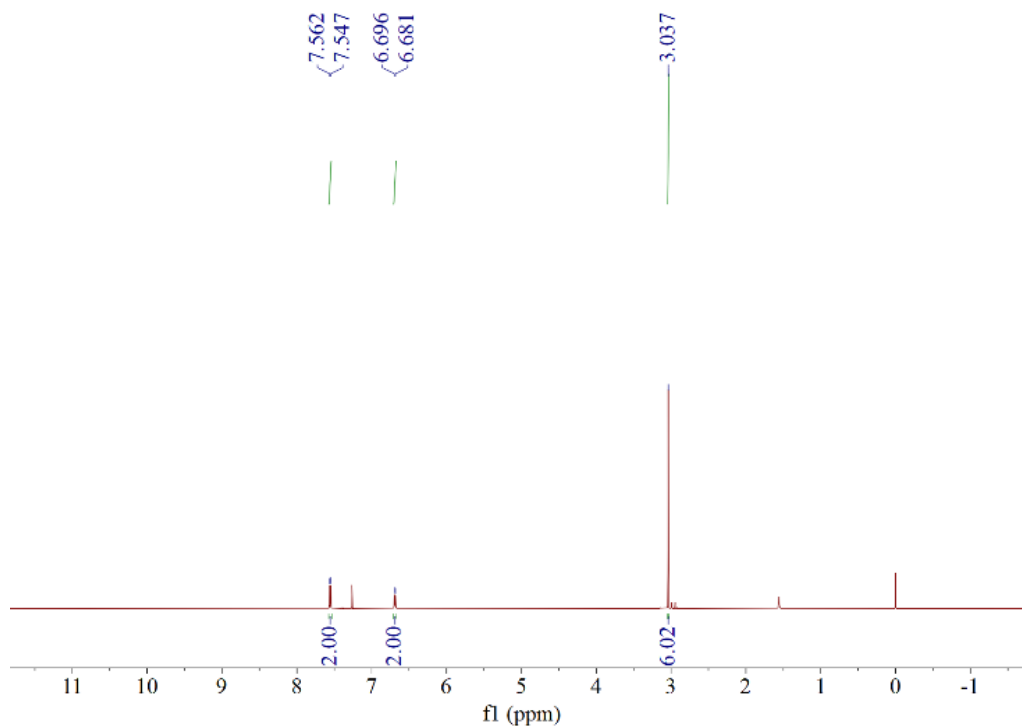


Fig. S59. ^1H NMR spectrum of compound **3p**.

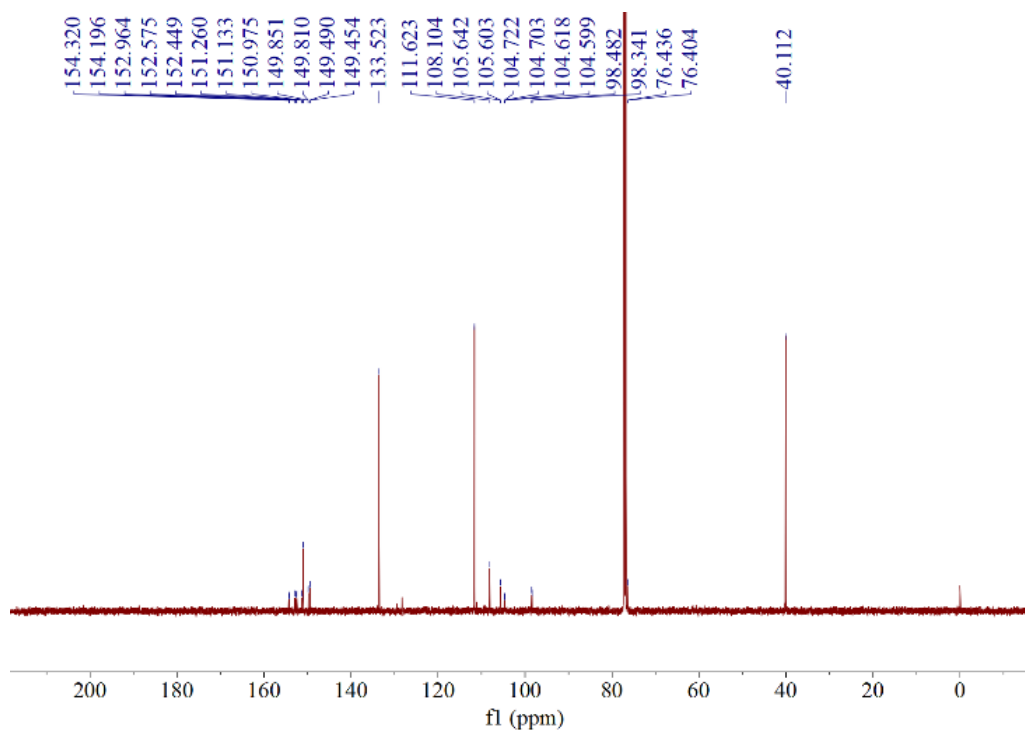


Fig. S60. ^{13}C NMR spectrum of compound **3p**.

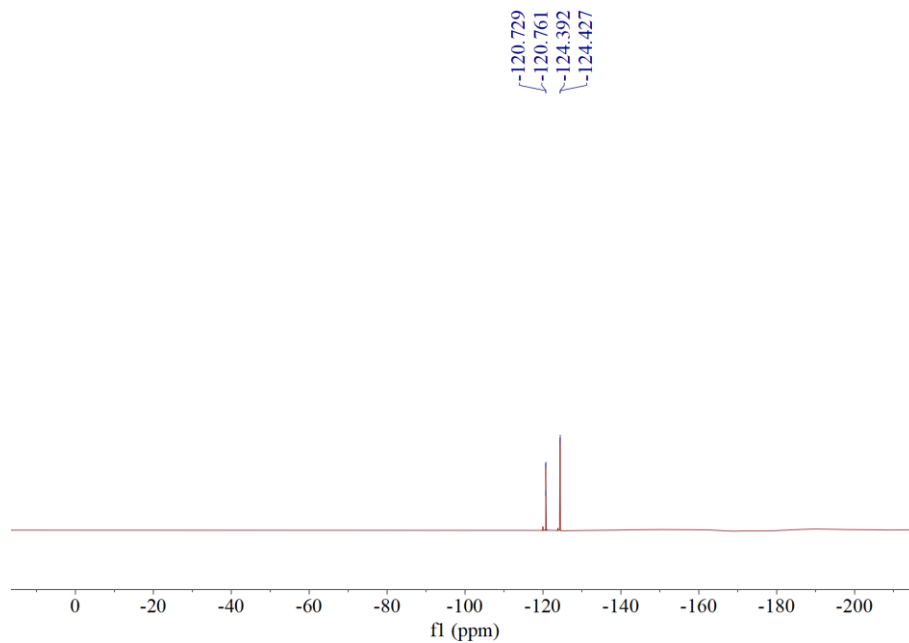


Fig. S61. ^{19}F NMR spectrum of compound **3p**.

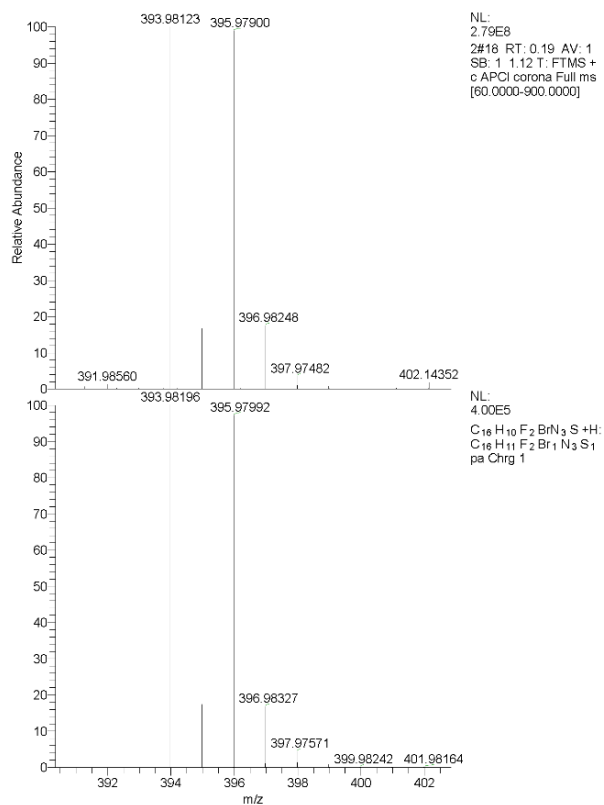


Fig. S62. HRMS spectrum of compound **3p**.

5. Single crystal data of compounds 3e, 3f, 3m and 3p

Table S1. Single crystal data of compound **3e**.

Identification code	3e	
Empirical formula	C ₂₄ H ₁₄ F ₂ N ₂ S	
Formula weight	400.43	
Temperature/K	297	
Crystal system	monoclinic	
Space group	P2 ₁ /c	
Unit cell dimensions	a = 6.7170(11) Å	α = 90 °
	b = 18.272(3) Å	β = 108.832(18) °
	c = 8.3004(14) Å	γ = 90 °
Volume	964.2(3) Å ³	
Z	2	
ρ _{calc}	1.379 g/cm ³	
Absorption coefficient	0.199 mm ⁻¹	
F(000)	412.0	
Crystal size	0.4 × 0.3 × 0.15 mm ³	
Radiation	Mo Kα (λ = 0.71073)	
2θ range for data collection	7.176 to 49.998 °	
Index ranges	-5 ≤ h ≤ 7, -21 ≤ k ≤ 18, -9 ≤ l ≤ 7	
Reflections collected	3746	
Independent reflections	1684 [R _{int} = 0.0266, R _{sigma} = 0.0429]	
Data/restraints/parameters	1684/43/200	
Goodness-of-fit on F ²	1.131	
Final R indexes [I ≥ 2σ(I)]	R ₁ = 0.0595, wR ₂ = 0.1162	
Final R indexes [all data]	R ₁ = 0.1045, wR ₂ = 0.1357	
Largest diff. peak/hole	0.16/-0.15 e.Å ⁻³	

Table S2. Single crystal data of compound **3f**.

Identification code	3f	
Empirical formula	C ₂₄ H ₁₄ F ₂ N ₂ O ₂ S	
Formula weight	432.43	
Temperature/K	297	
Crystal system	monoclinic	

Space group	C2/c
Unit cell dimensions	a = 18.920(3) Å α = 90 ° b = 12.160(2) Å β = 102.902(17) ° c = 9.0331(17) Å γ = 90 °
Volume	2025.8(6) Å ³
Z	4
ρ _{calc}	1.418 g/cm ³
Absorption coefficient	0.202 mm ⁻¹
F(000)	888.0
Crystal size	0.3 × 0.08 × 0.08 mm ³
Radiation	Mo Kα (λ = 0.71073)
2θ range for data collection	7.428 to 50 °
Index ranges	-22 ≤ h ≤ 22, -14 ≤ k ≤ 10, -10 ≤ l ≤ 10
Reflections collected	4643
Independent reflections	1789 [R _{int} = 0.0433, R _{sigma} = 0.0632]
Data/restraints/parameters	1789/0/142
Goodness-of-fit on F ²	1.022
Final R indexes [I ≥ 2σ(I)]	R ₁ = 0.0594, wR ₂ = 0.1163
Final R indexes [all data]	R ₁ = 0.0987, wR ₂ = 0.1331
Largest diff. peak/hole	0.16/-0.28 e.Å ⁻³

Table S3. Single crystal data of compound **3m**.

Identification code	3m
Empirical formula	C ₂₆ H ₂₀ F ₂ N ₄ S
Formula weight	458.52
Temperature/K	297
Crystal system	monoclinic
Space group	P2 ₁ /n
Unit cell dimensions	a = 7.7592(10) Å α = 90 ° b = 15.080(2) Å β = 93.781(11) ° c = 19.199(2) Å γ = 90 °
Volume	2241.6(5) Å ³
Z	4
ρ _{calc}	1.359 g/cm ³
Absorption coefficient	0.183 mm ⁻¹
F(000)	952.0
Crystal size	0.08 × 0.03 × 0.09 mm ³
Radiation	Mo Kα (λ = 0.71073)
2θ range for data collection	7.082 to 58.978 °
Index ranges	-10 ≤ h ≤ 10, -13 ≤ k ≤ 20, -16 ≤ l ≤ 24

Reflections collected	12199
Independent reflections	5194 [$R_{\text{int}} = 0.0399$, $R_{\text{sigma}} = 0.0656$]
Data/restraints/parameters	5194/114/312
Goodness-of-fit on F^2	1.098
Final R indexes [$I \geq 2\sigma(I)$]	$R_1 = 0.0749$, $wR_2 = 0.1267$
Final R indexes [all data]	$R_1 = 0.1415$, $wR_2 = 0.1552$
Largest diff. peak/hole	0.18/-0.21 e. \AA^{-3}

Table S4. Single crystal data of compound **3p**.

Identification code	3p	
Empirical formula	$\text{C}_{16}\text{H}_{10.16}\text{Br}_{0.84}\text{F}_2\text{N}_3\text{S}$	
Formula weight	381.62	
Temperature/K	297	
Crystal system	triclinic	
Space group	P-1	
Unit cell dimensions	$a = 7.0240(8) \text{ \AA}$ $b = 10.3191(9) \text{ \AA}$ $c = 11.3416(14) \text{ \AA}$	$\alpha = 90.378(9)^\circ$ $\beta = 105.741(10)^\circ$ $\gamma = 98.561(8)^\circ$
Volume	$781.46(15) \text{ \AA}^3$	
Z	2	
ρ_{calc}	1.622 g/cm^3	
Absorption coefficient	2.376 mm^{-1}	
F(000)	381.0	
Crystal size	$0.2 \times 0.2 \times 0.1 \text{ mm}^3$	
Radiation	Mo $K\alpha$ ($\lambda = 0.71073$)	
2θ range for data collection	6.752 to 49.998°	
Index ranges	$-8 \leq h \leq 8$, $-12 \leq k \leq 11$, $-13 \leq l \leq 13$	
Reflections collected	5693	
Independent reflections	2757 [$R_{\text{int}} = 0.0433$, $R_{\text{sigma}} = 0.0632$]	
Data/restraints/parameters	2757/0/211	
Goodness-of-fit on F^2	1.081	
Final R indexes [$I \geq 2\sigma(I)$]	$R_1 = 0.0515$, $wR_2 = 0.0904$	
Final R indexes [all data]	$R_1 = 0.0823$, $wR_2 = 0.1000$	
Largest diff. peak/hole	0.28/-0.35 e. \AA^{-3}	

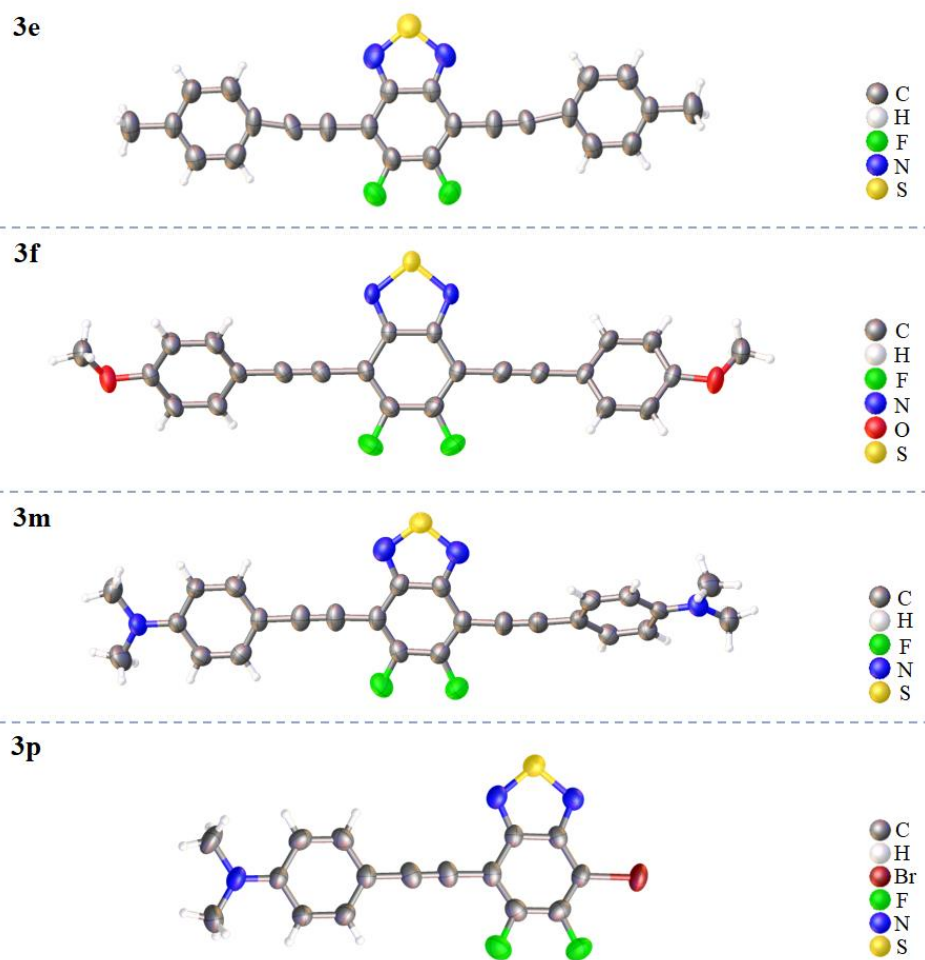


Fig. S63. Crystal structures of compound **3e**, **3f**, **3m** and **3p** (CCDC: 2282710, 2282714, 2282717, 2282718).

6. Thermogravimetric analyses of compounds 3a-3p

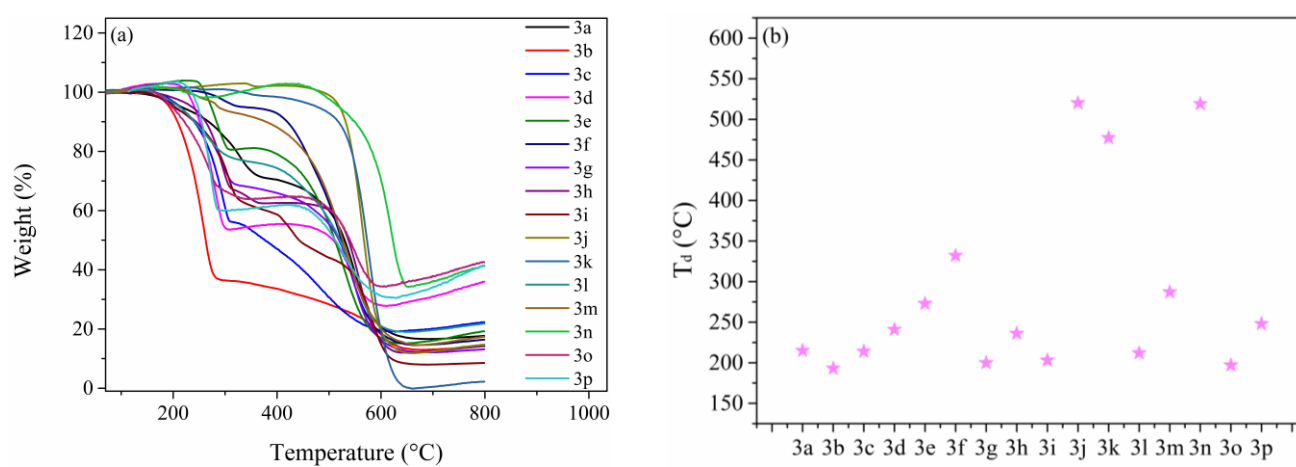


Fig. S64. (a) The thermogravimetric analyses (TGA) diagrams and (b) thermal decomposition temperature of compounds **3a-3p** at a heating rate of 10 °C/min in air atmosphere.

7. Fluorescent lifetime of compounds 3a-3p

Table S5. The fluorescence lifetime data of compounds **3a-3p**.

Compound	τ_1	Rel ₁ %	τ_2	Rel ₂ %	τ^a
3a	1.4198	86.55%	6.4488	13.45%	2.10
3b	1.8463	49.84%	4.3634	50.16%	3.11
3c	1.6426	55.52%	4.4814	44.48%	2.91
3d	2.4471	12.51%	6.7837	87.49%	6.24
3e	2.5736	63.47%	5.0303	36.53%	3.47
3f	1.6476	67.61%	4.103	32.39%	2.44
3g	2.4676	10.44%	3.9959	89.56%	3.84
3h	1.8551	64.09%	4.8718	35.91%	2.94
3i	1.5362	76.94%	4.9953	23.06%	2.33
3j	3.4046	76.34%	10.6215	23.66%	5.11
3k	1.4029	55.95%	3.001	44.05%	2.11
3l	1.1121	65.12%	3.9692	34.88%	2.11
3m	1.2798	52.34%	2.8227	47.66%	2.02
3n	0.823	85.96%	2.4159	14.04%	1.05
3o	1.4621	38.75%	2.4094	61.25%	2.04
3p	0.7513	44.62%	2.0322	55.38%	1.46

^a Fluorescence lifetime is obtained by double exponential fitting. $\tau = \tau_1 \times \text{Rel}_1 \% + \tau_2 \times \text{Rel}_2 \%$.

8. Fluorescence spectra of 3a-3p in different states

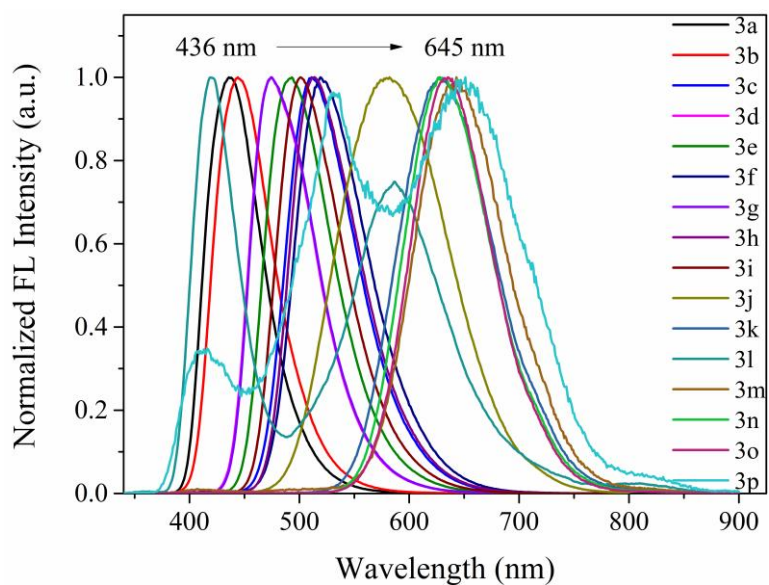


Fig. S65. The normalized emission spectra of compounds **3a-3p** in THF (10^{-5} M).

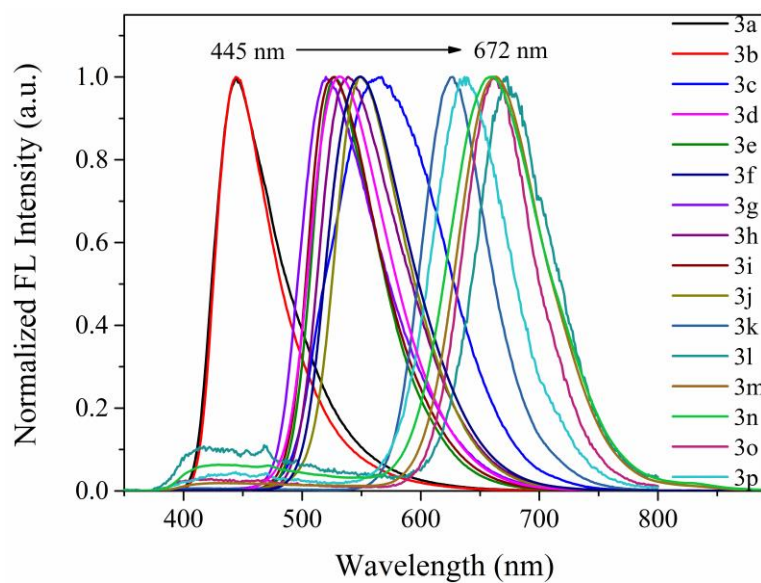


Fig. S66. The normalized emission spectra of compounds **3a-3p** in solid state.

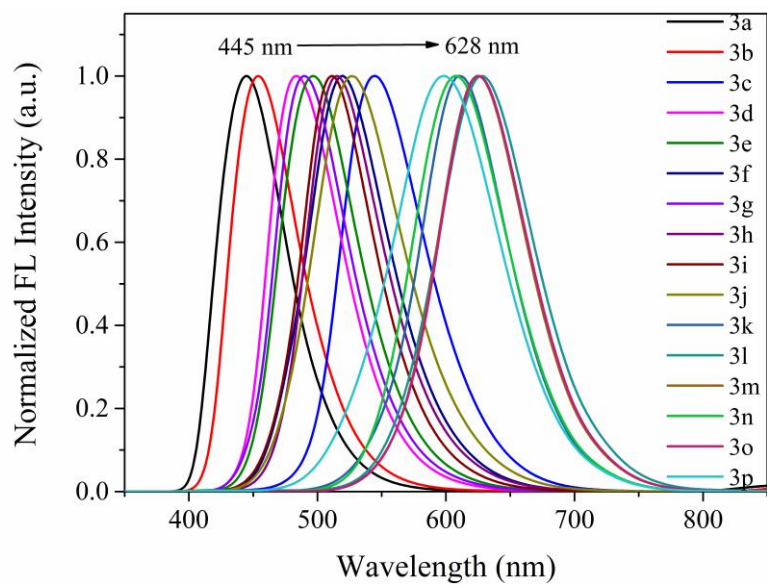


Fig. S67. The normalized emission spectra of compounds **3a-3p** in film state.

9. Fluorescence spectra of compounds 3a-3p in various solvents

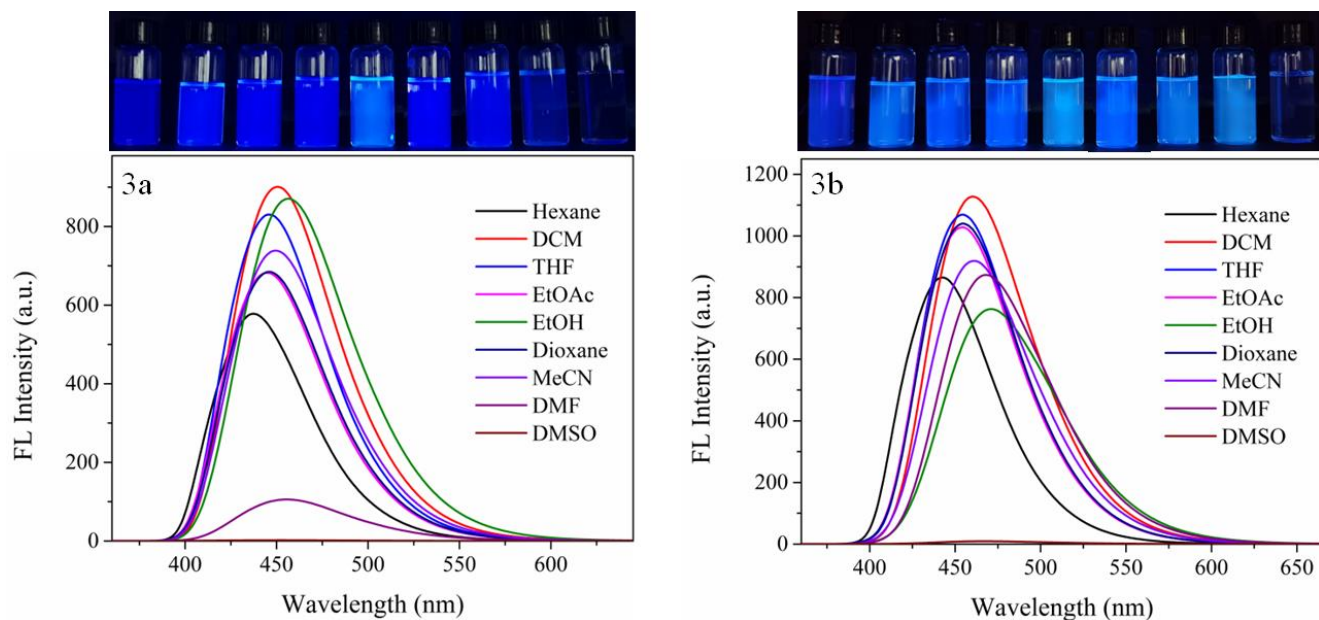


Fig. S68. Fluorescence spectra and representative images (under 365 nm irradiation) of compounds **3a** and **3b** (10^{-5} M) in solvents of different polarities.

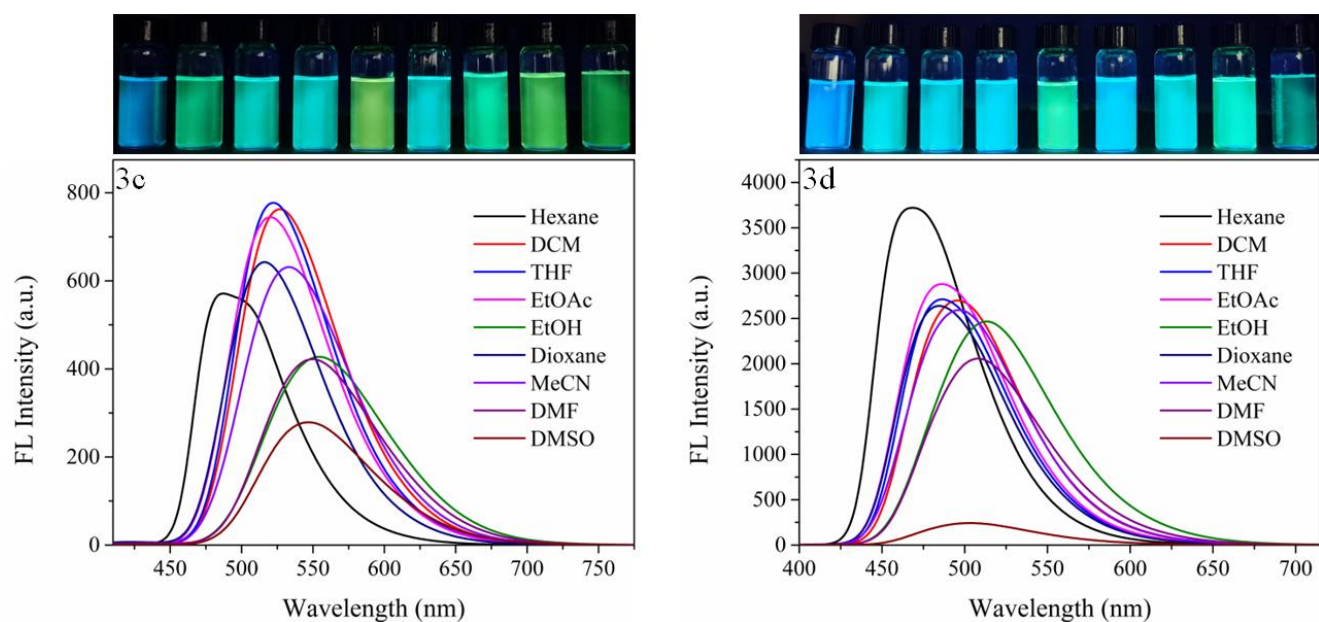


Fig. S69. Fluorescence spectra and representative images (under 365 nm irradiation) of compounds **3c** and **3d** (10^{-5} M) in solvents of different polarities.

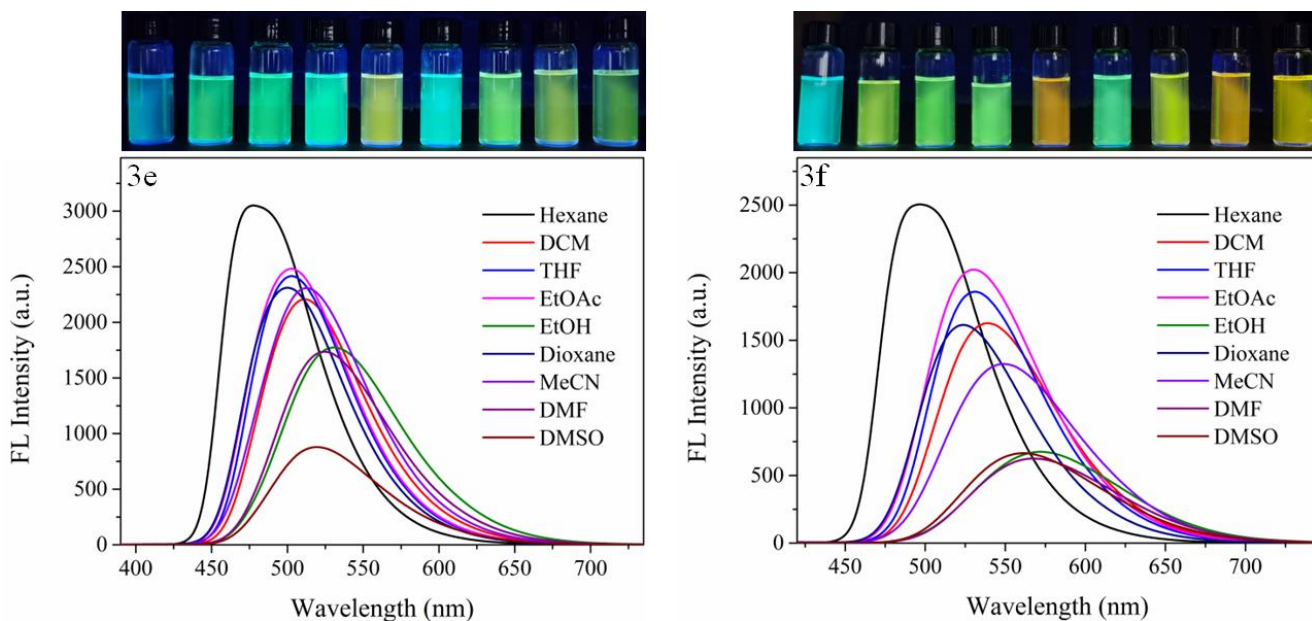


Fig. S70. Fluorescence spectra and representative images (under 365 nm irradiation) of compounds **3e** and **3f** (10^{-5} M) in solvents of different polarities.

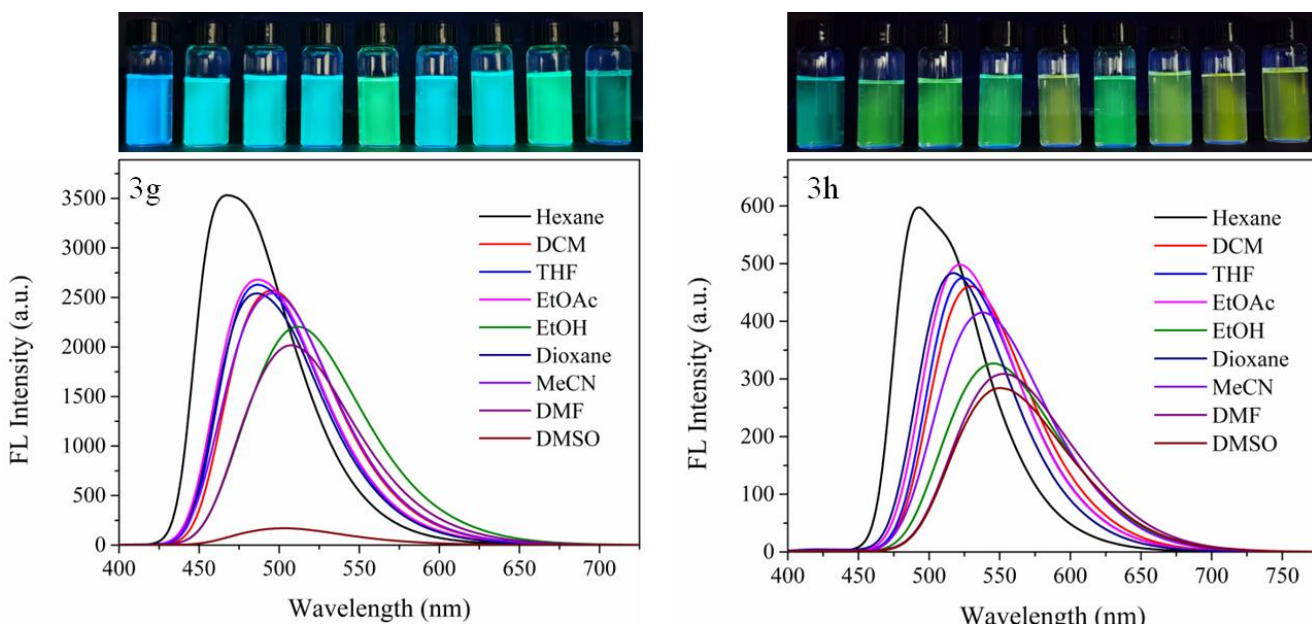


Fig. S71. Fluorescence spectra and representative images (under 365 nm irradiation) of compounds **3g** and **3h** (10^{-5} M) in solvents of different polarities.

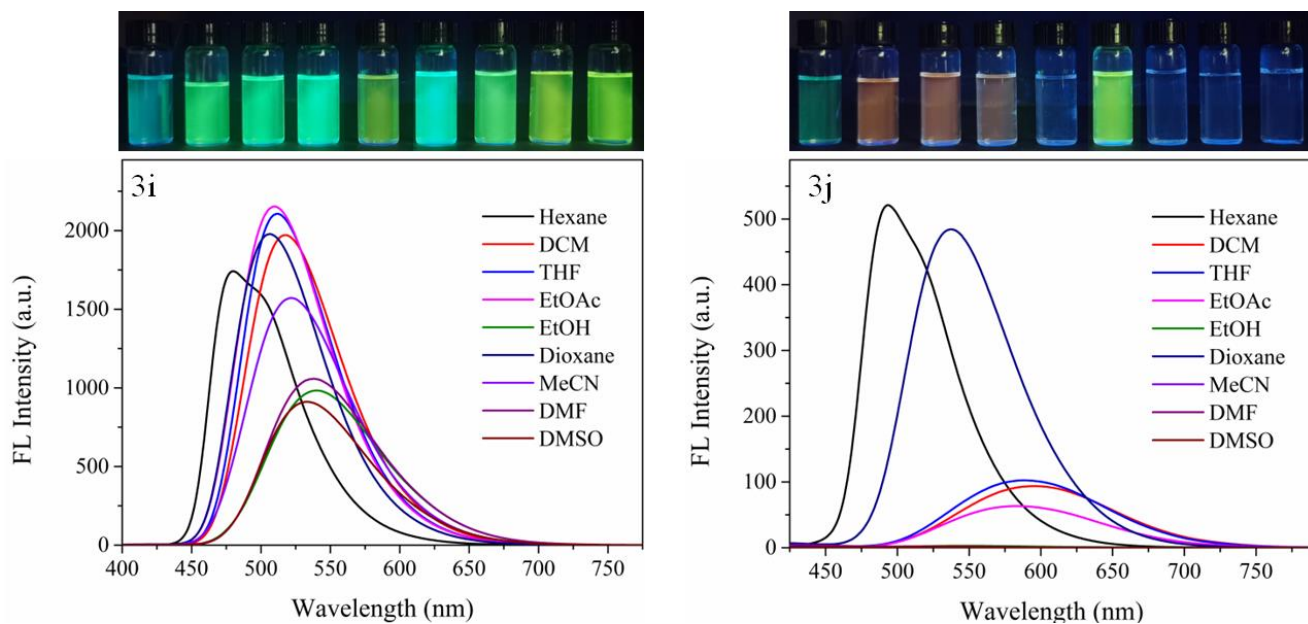


Fig. S72. Fluorescence spectra and representative images (under 365 nm irradiation) of compounds **3i** and **3j** (10^{-5} M) in solvents of different polarities.

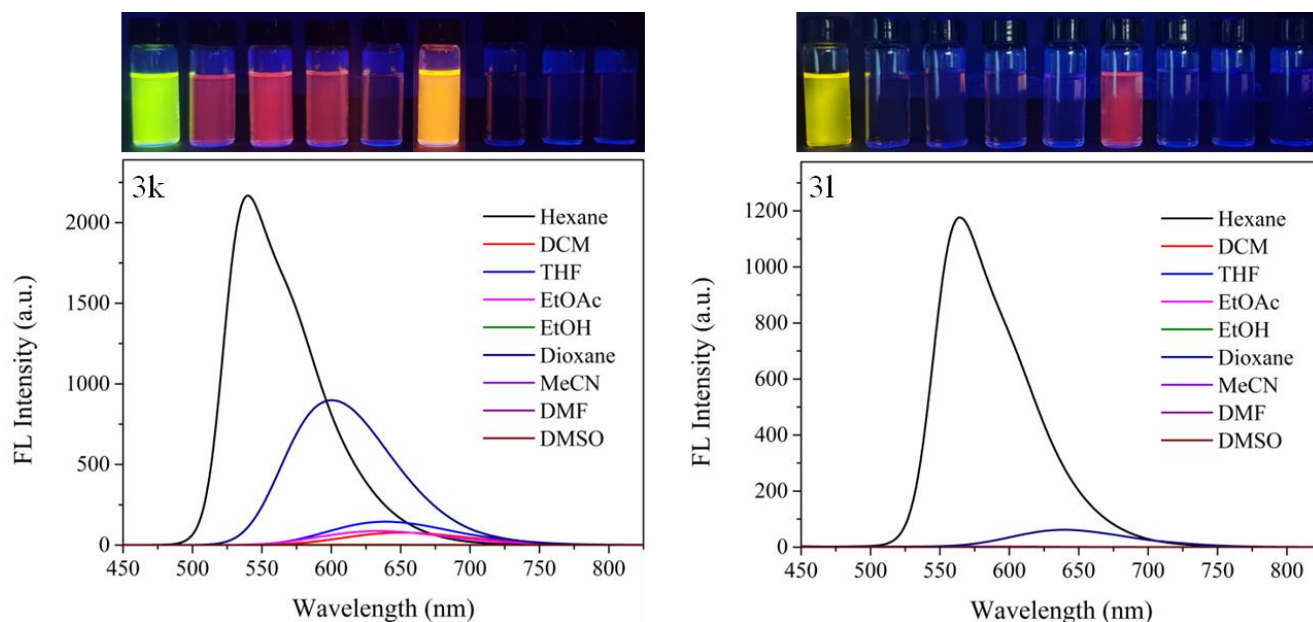


Fig. S73. Fluorescence spectra and representative images (under 365 nm irradiation) of compounds **3k** and **3l** (10^{-5} M) in solvents of different polarities.

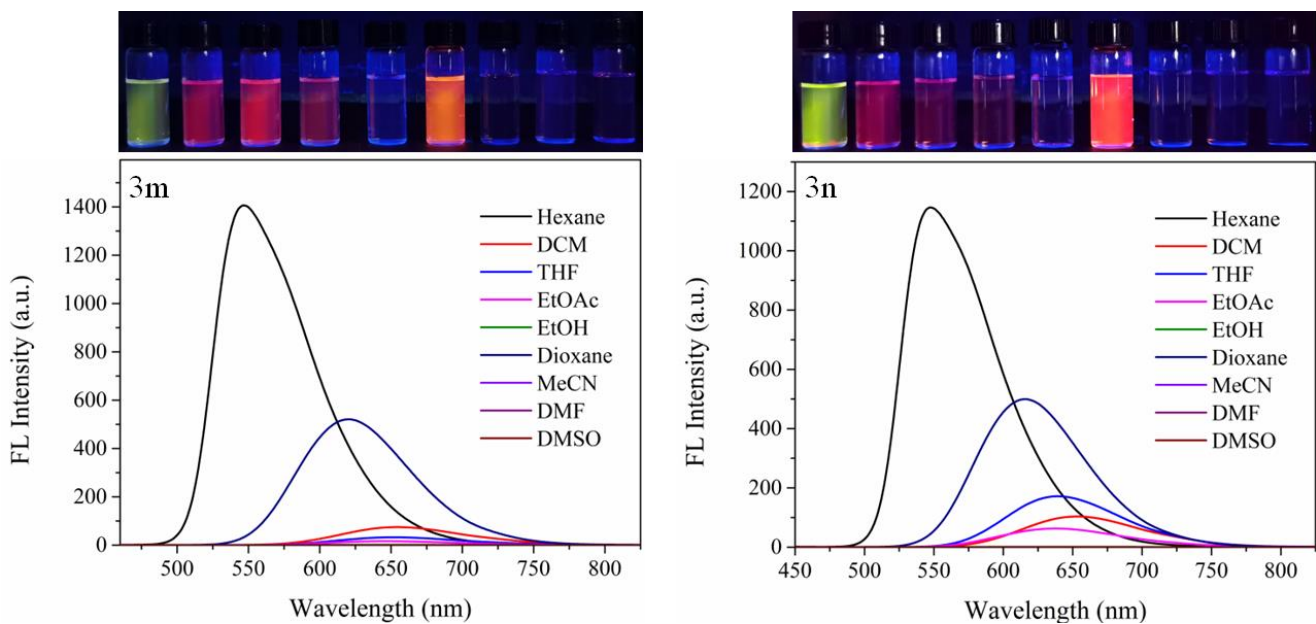


Fig. S74. Fluorescence spectra and representative images (under 365 nm irradiation) of compounds **3m** and **3n** (10^{-5} M) in solvents of different polarities.

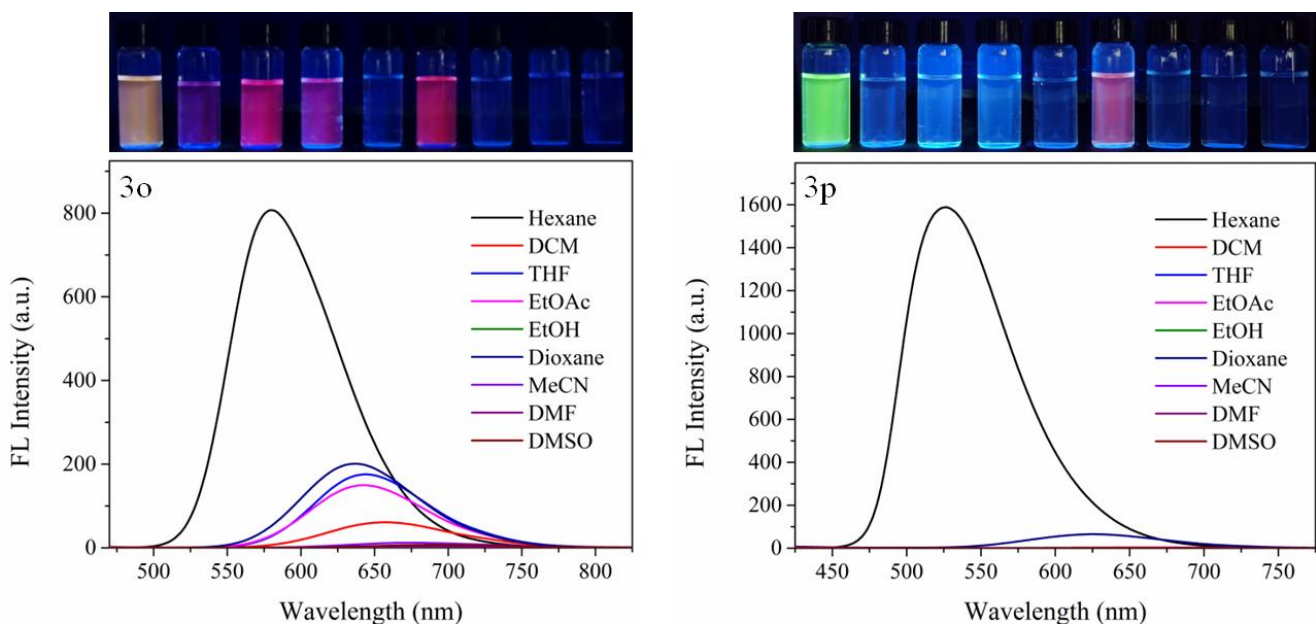


Fig. S75. Fluorescence spectra and representative images (under 365 nm irradiation) of compounds **3o** and **3p** (10^{-5} M) in solvents of different polarities.

Table S6. Polarity data for common organic solvents.

Solvent	Abbreviation of solvent name	Polarity
<i>n</i> -Hexane	Hexane	0.06
Dichloromethane	DCM	3.4
Tetrahydrofuran	THF	4.2
Ethyl acetate	EtOAc	4.3
Ethanol	EtOH	4.3
1,4-Dioxane	Dioxane	4.8
Acetonitrile	MeCN	6.2
<i>N,N</i> -Dimethylformamide	DMF	6.4
Dimethyl sulfoxide	DMSO	7.2

Table S7. The maximum emission peak of **3a-3p** (10^{-5} M) in solvents of different polarities.

Sol. Comp.	3a	3b	3c	3d	3e	3f	3g	3h	3i	3j	3k	3l	3m	3n	3o	3p
Hexane	437	443	487	469	478	497	468	493	480	493	540	564	547	548	580	526
DCM	451	460	527	496	512	539	496	529	518	596	651	-	655	654	656	661
THF	436	444	511	475	493	519	474	514	501	582	628	569	643	630	635	-
EtOAc	445	454	520	486	503	530	487	521	510	583	634	572	646	639	642	-
EtOH	456	471	555	514	531	573	512	546	540	547	627	-	-	-	-	-
Dioxane	446	455	516	484	500	524	486	517	507	537	600	639	620	616	637	626
MeCN	449	461	533	496	513	549	497	538	522	541	-	-	-	-	-	-
DMF	455	468	550	508	524	568	508	552	538	-	-	-	-	-	-	-
DMSO	452	467	547	504	519	562	502	550	533	-	-	-	-	-	-	-
Red shift	19	28	68	45	53	71	44	59	58	103	111	75	108	106	76	135
DM(10^2) ^a	47	76	51	47	46	40	57	40	46	84	38	27	1	226	227	890

^a Dipole moment obtained by theoretical calculation.

10. Fluorescent behaviors of 3a-3p in solution and aggregation states

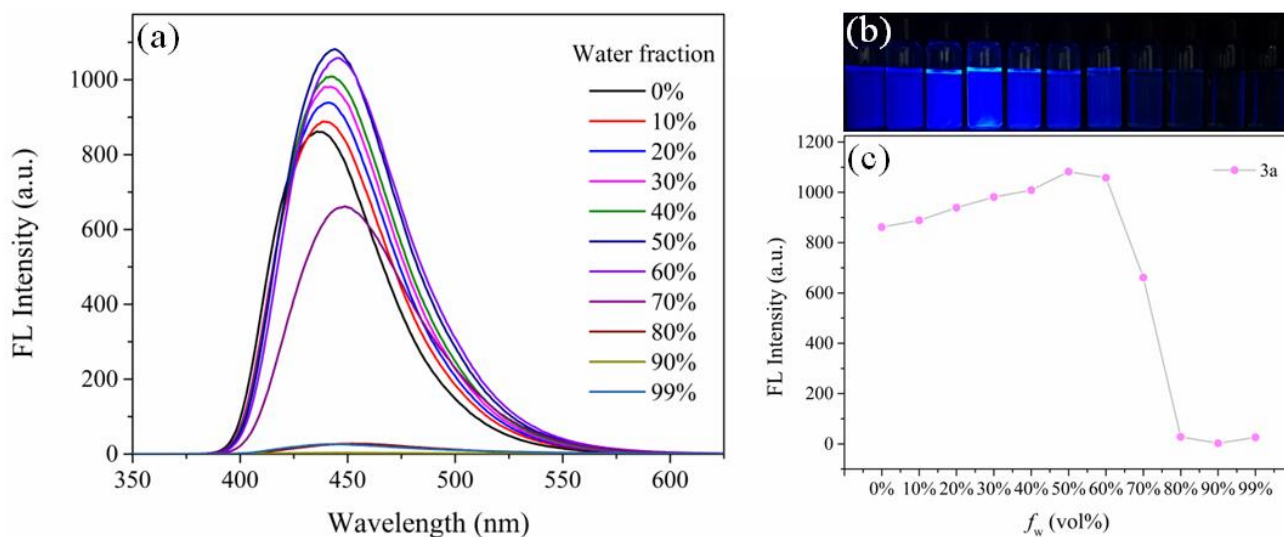


Fig. S76. (a) The fluorescence spectra and (b) photos of compound **3a** (10^{-5} M) and (c) plot of maximum emission intensity versus water fraction (f_w) in THF/H₂O mixtures.

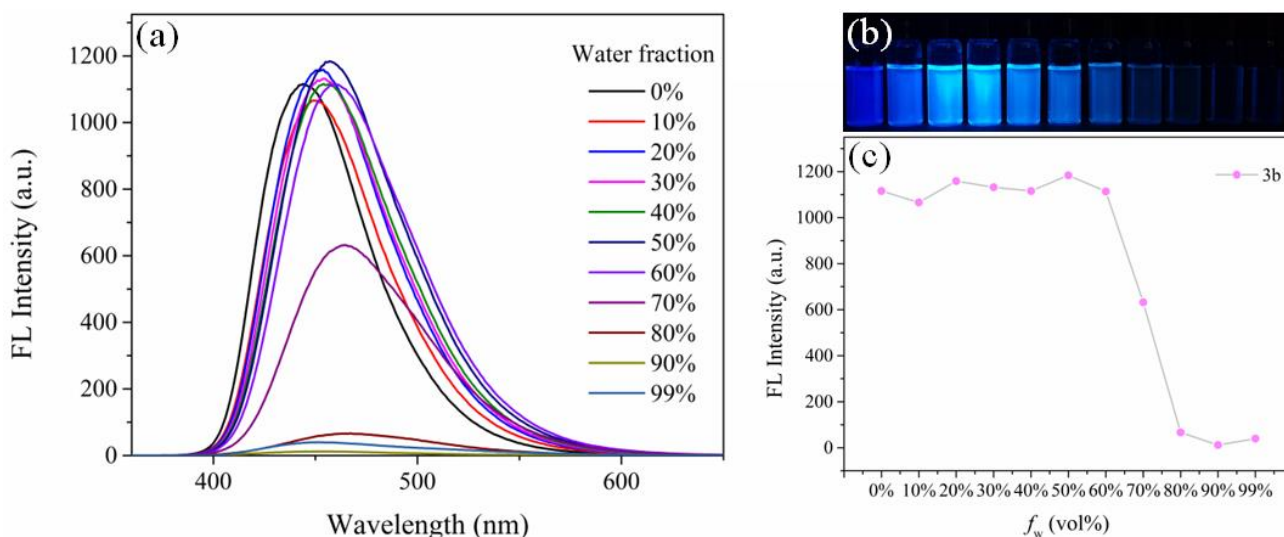


Fig. S77. (a) The fluorescence spectra and (b) photos of compound **3b** (10^{-5} M) and (c) plot of maximum emission intensity versus water fraction (f_w) in THF/H₂O mixtures.

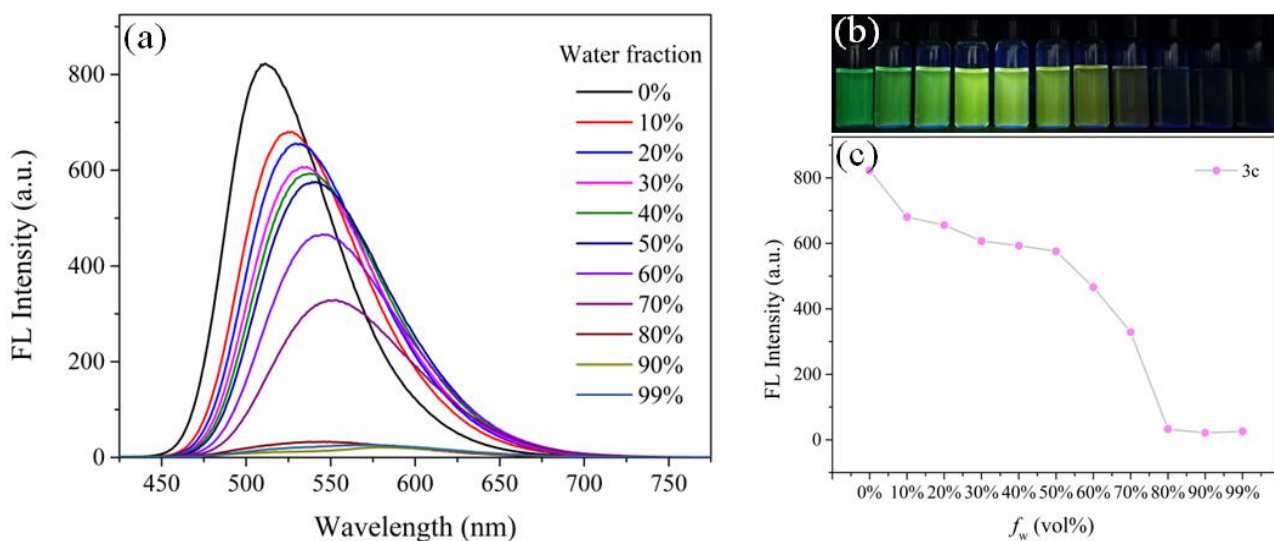


Fig. S78. (a) The fluorescence spectra and (b) photos of compound **3c** (10^{-5} M) and (c) plot of maximum emission intensity versus water fraction (f_w) in THF/H₂O mixtures.

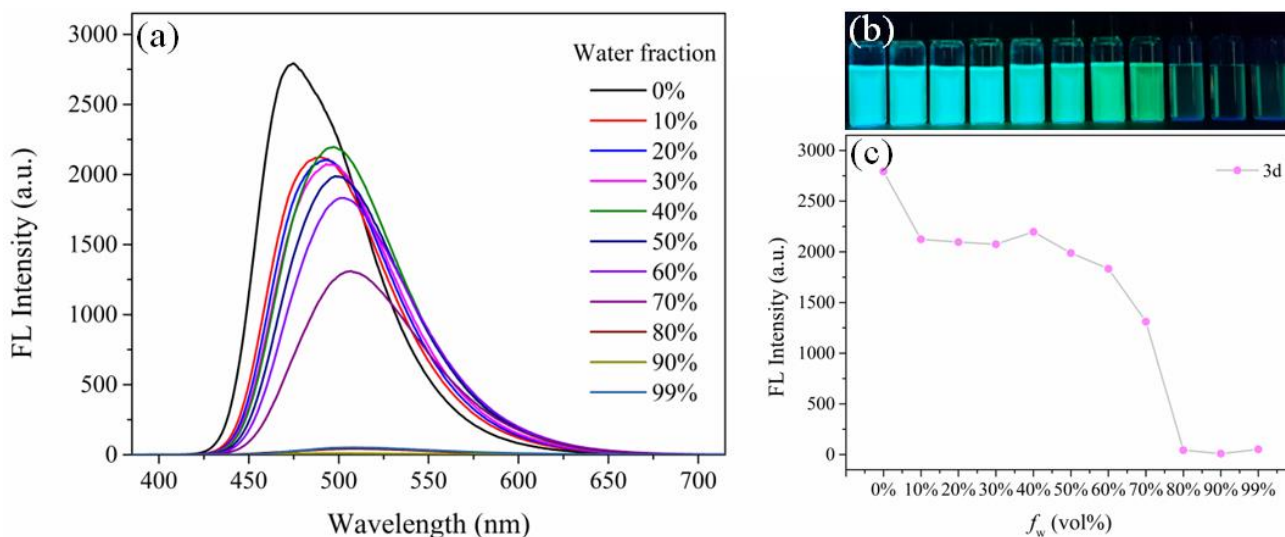


Fig. S79. (a) The fluorescence spectra and (b) photos of compound **3d** (10^{-5} M) and (c) plot of maximum emission intensity versus water fraction (f_w) in THF/H₂O mixtures.

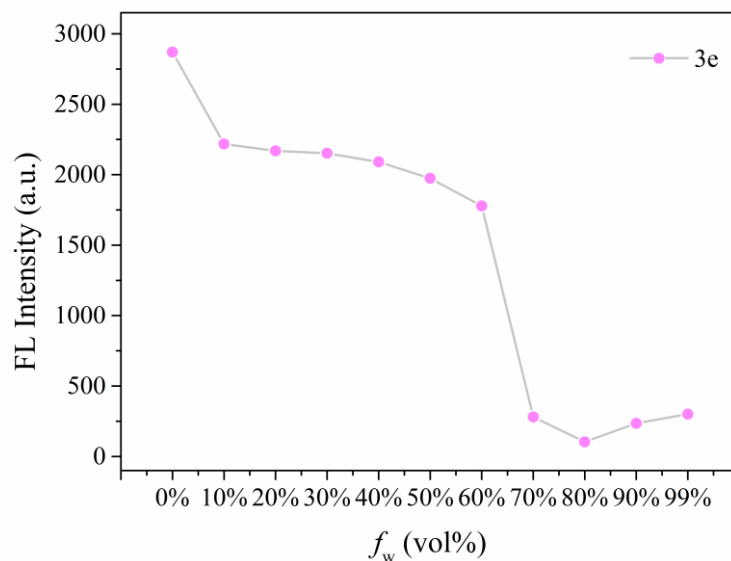


Fig. S80. The plot of maximum emission intensity of compound **3e** (10^{-5} M) versus water fraction (f_w) in THF/H₂O mixtures.

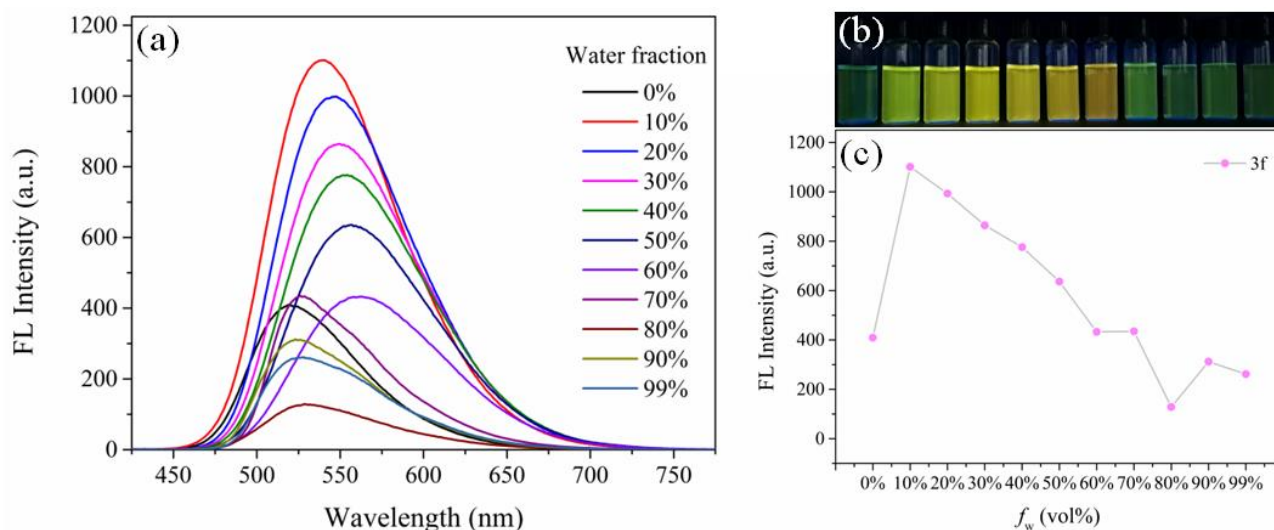


Fig. S81. (a) The fluorescence spectra and (b) photos of compound **3f** (10^{-5} M) and (c) plot of maximum emission intensity versus water fraction (f_w) in THF/H₂O mixtures.

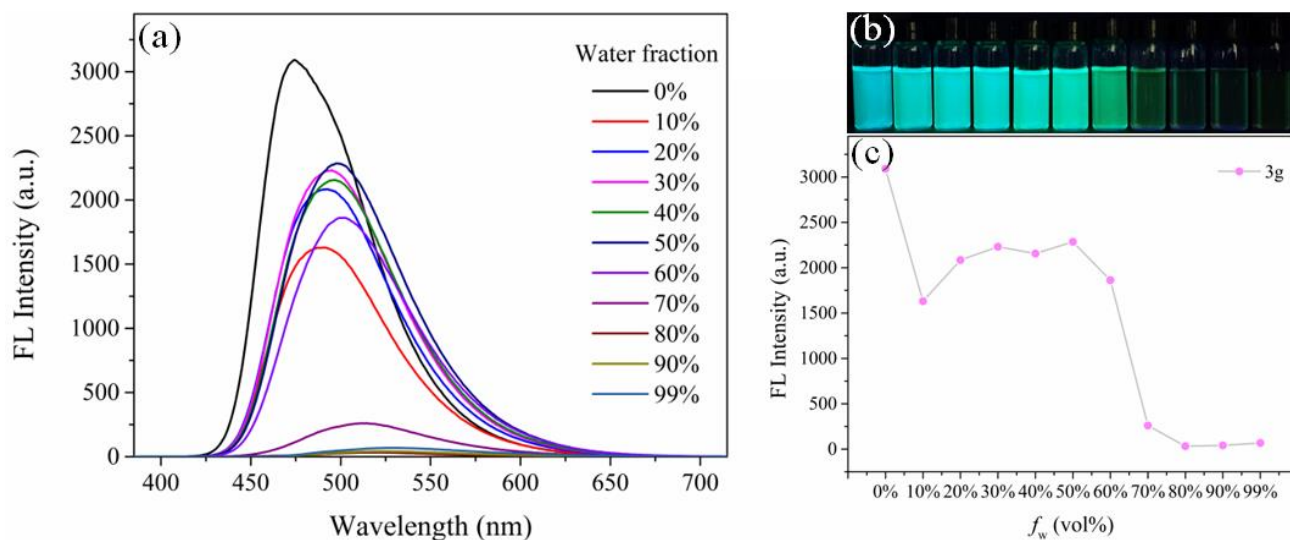


Fig. S82. (a) The fluorescence spectra and (b) photos of compound **3g** (10^{-5} M) and (c) plot of maximum emission intensity versus water fraction (f_w) in THF/H₂O mixtures.

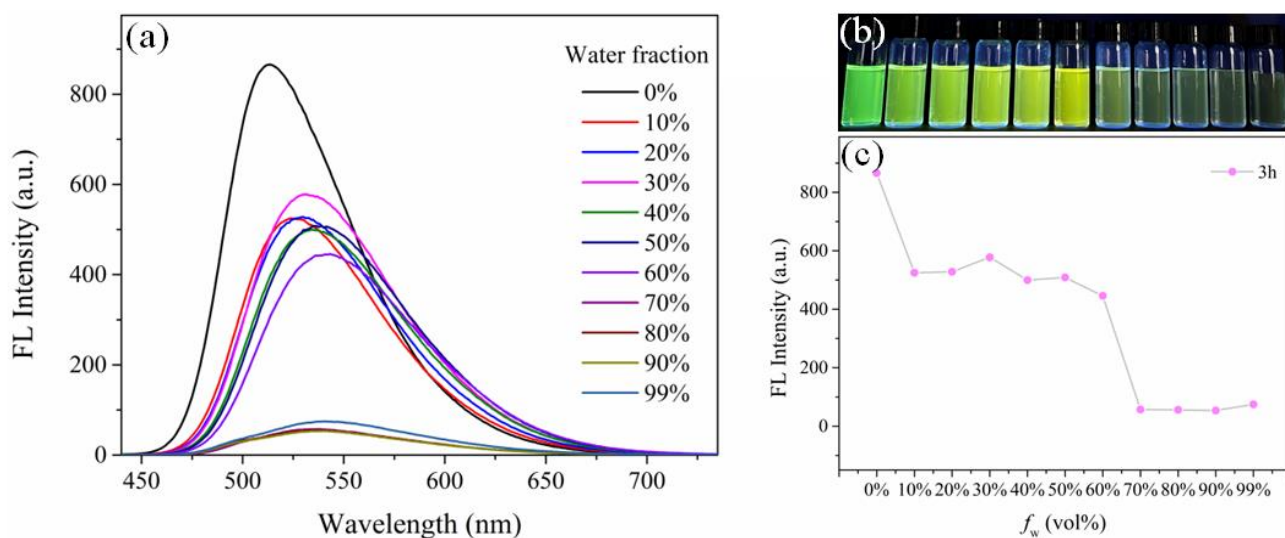


Fig. S83. (a) The fluorescence spectra and (b) photos of compound **3h** (10^{-5} M) and (c) plot of maximum emission intensity versus water fraction (f_w) in THF/H₂O mixtures.

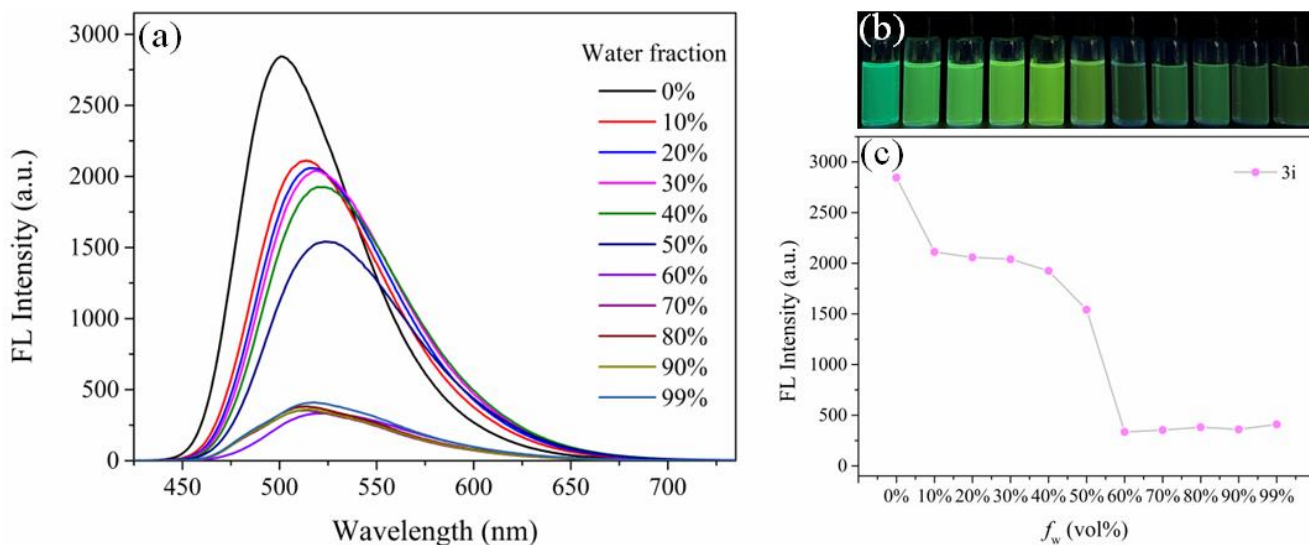


Fig. S84. (a) The fluorescence spectra and (b) photos of compound **3i** (10^{-5} M) and (c) plot of maximum emission intensity versus water fraction (f_w) in THF/H₂O mixtures.

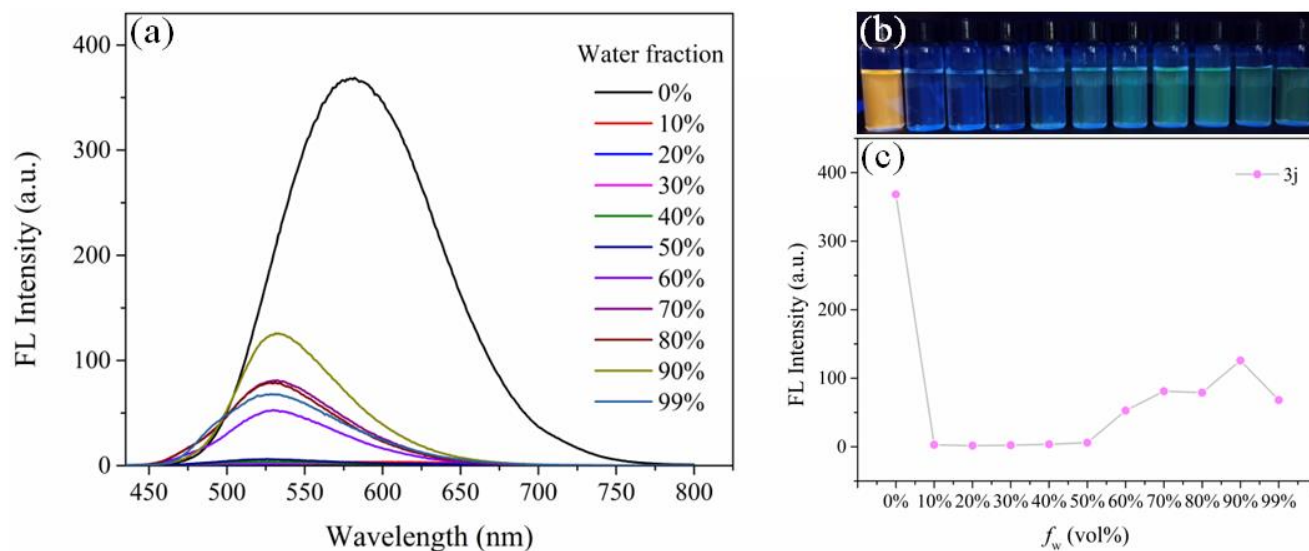


Fig. S85. (a) The fluorescence spectra and (b) photos of compound **3j** (10^{-5} M) and (c) plot of maximum emission intensity versus water fraction (f_w) in THF/H₂O mixtures.

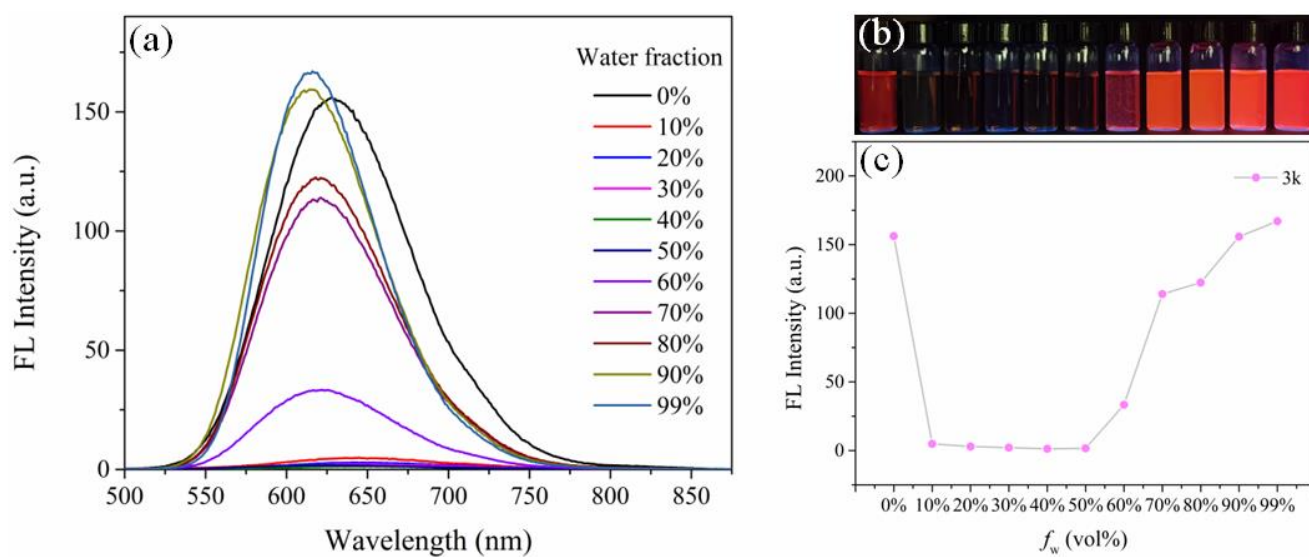


Fig. S86. (a) The fluorescence spectra and (b) photos of compound **3k** (10^{-5} M) and (c) plot of maximum emission intensity versus water fraction (f_w) in THF/H₂O mixtures.

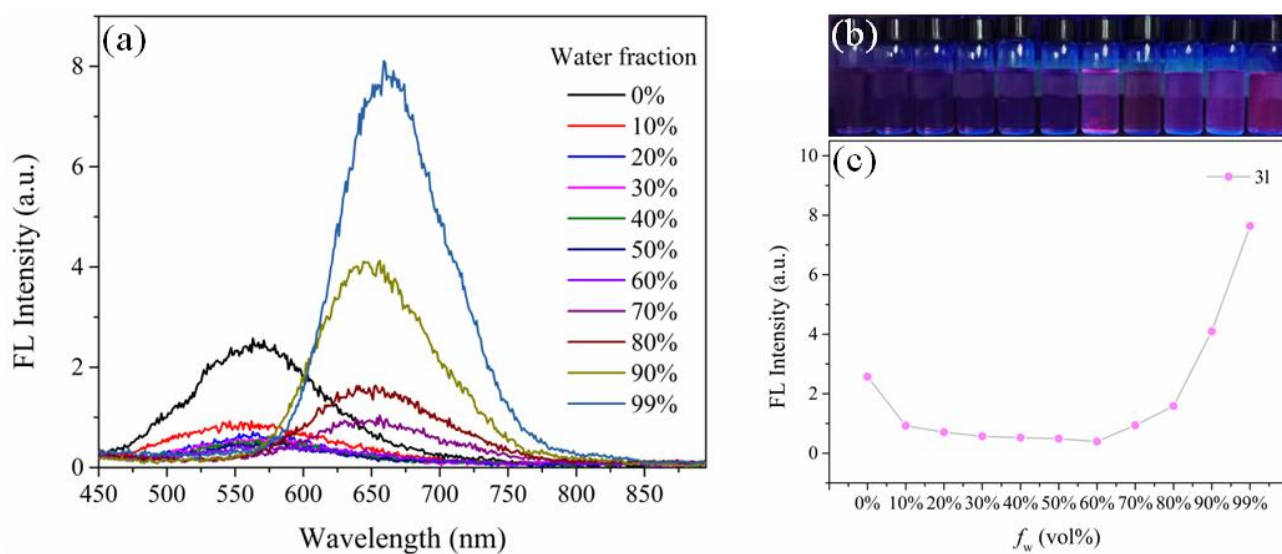


Fig. S87. (a) The fluorescence spectra and (b) photos of compound **31** (10^{-5} M) and (c) plot of maximum emission intensity versus water fraction (f_w) in THF/H₂O mixtures.

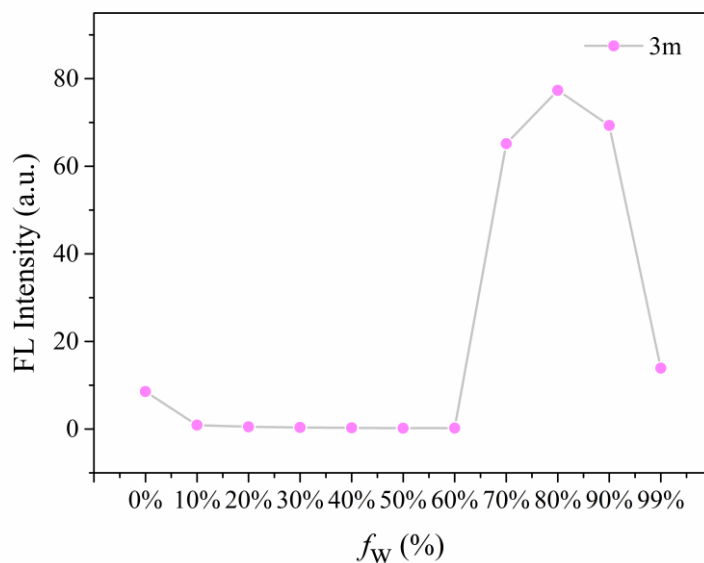


Fig. S88. The plot of maximum emission intensity of compound **3m** (10^{-5} M) versus water fraction (f_w) in THF/H₂O mixtures.

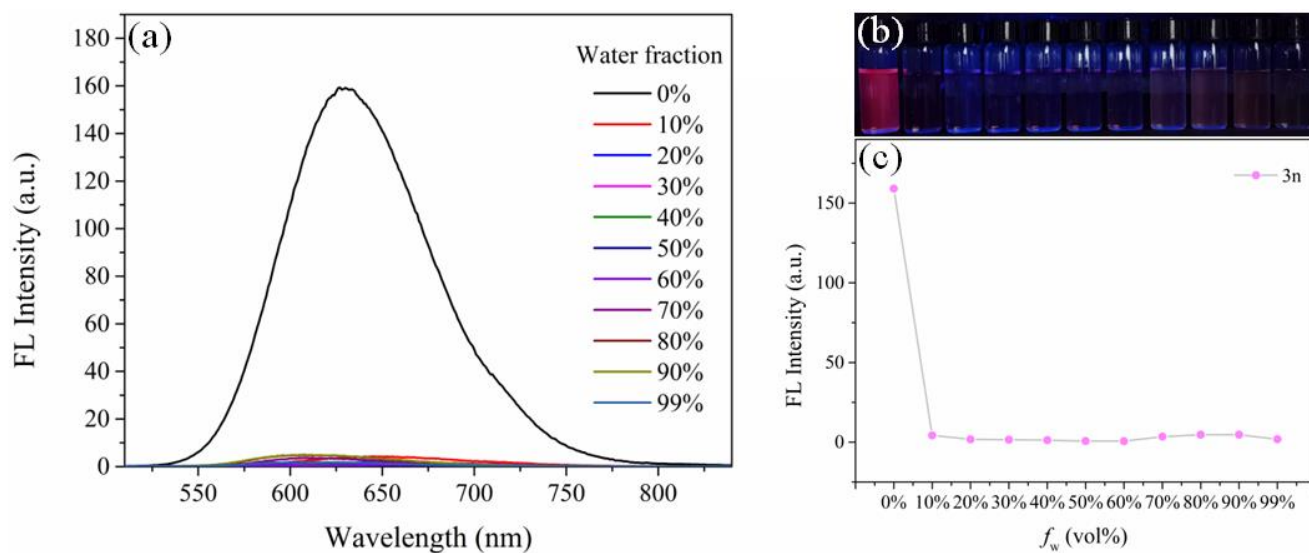


Fig. S89. (a) The fluorescence spectra and (b) photos of compound **3n** (10^{-5} M) and (c) plot of maximum emission intensity versus water fraction (f_w) in THF/H₂O mixtures.

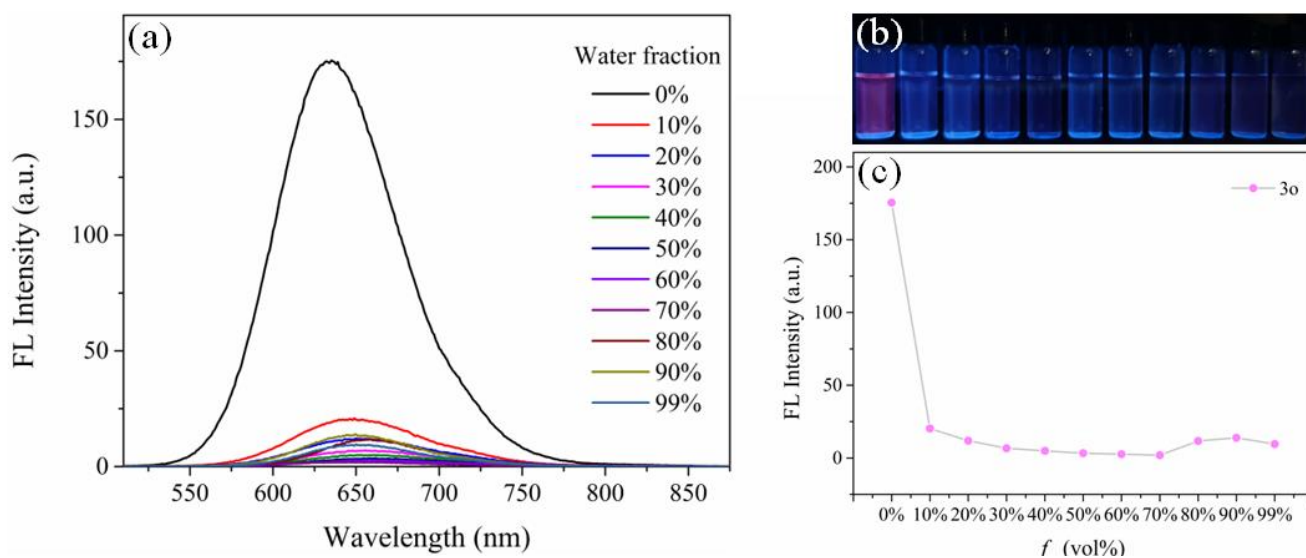


Fig. S90. (a) The fluorescence spectra and (b) photos of compound **3o** (10^{-5} M) and (c) plot of maximum emission intensity versus water fraction (f_w) in THF/H₂O mixtures.

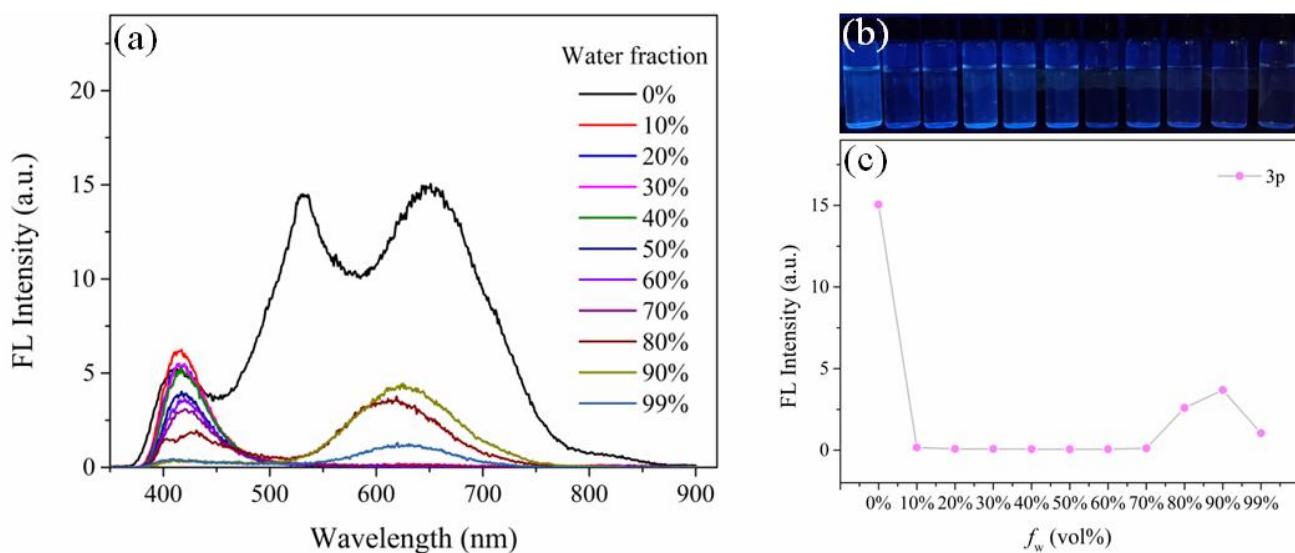


Fig. S91. (a) The fluorescence spectra and (b) photos of compound **3p** (10^{-5} M) and (c) plot of maximum emission intensity versus water fraction (f_w) in THF/H₂O mixtures.

11. AIE behaviors of compounds **3k** and **3m**

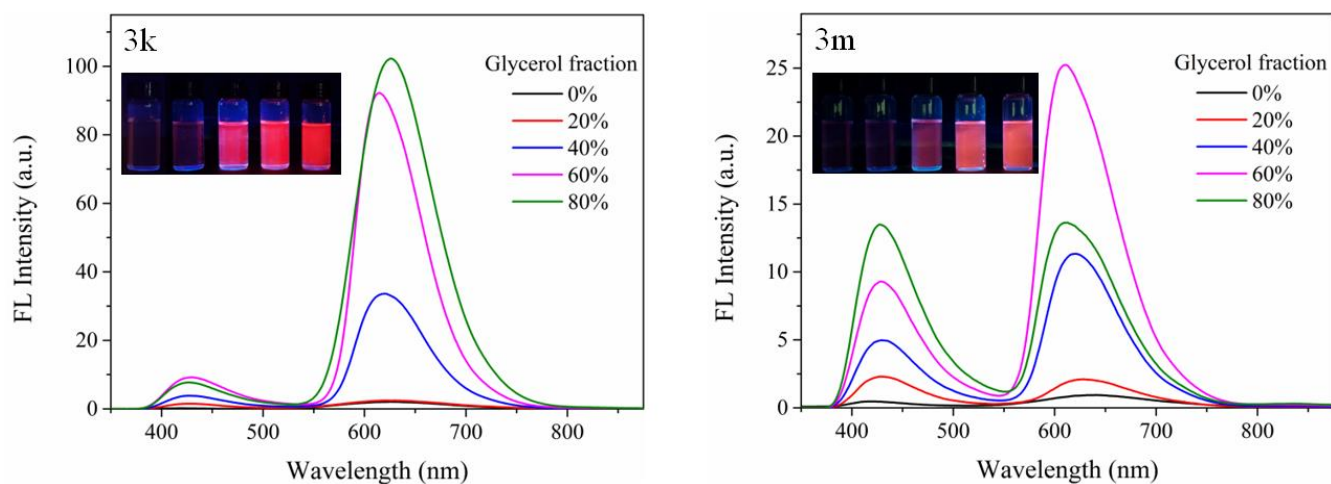


Fig. S92. The fluorescence spectra and photos of compounds **3k** and **3m** (10^{-5} M) in ethanol/glycerol mixtures with increasing glycerol fraction (f_w) from 0% to 80%.

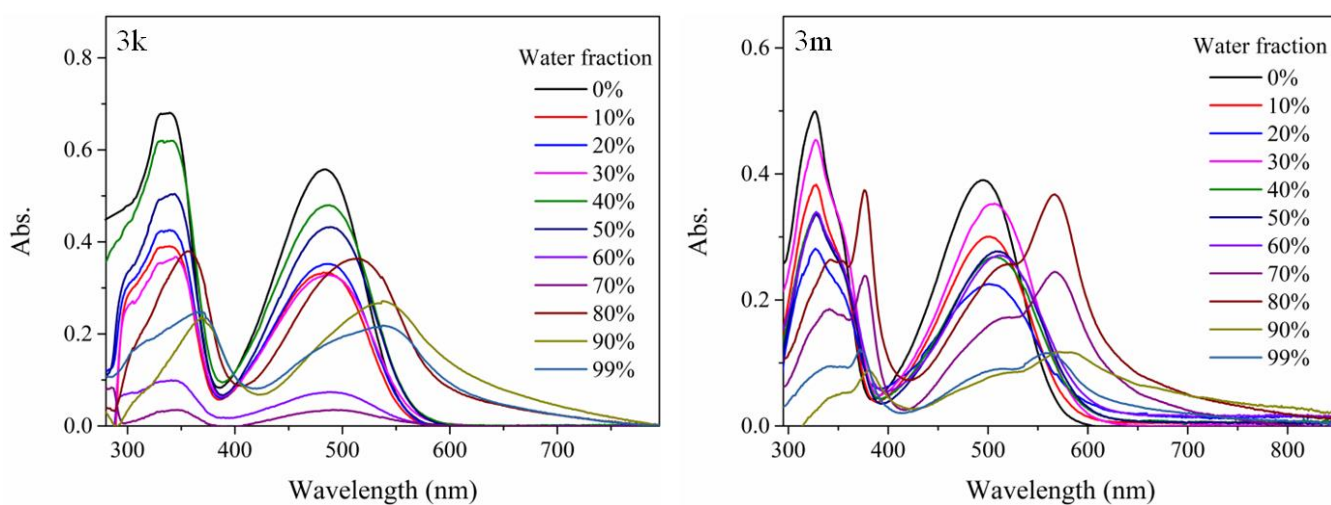


Fig. S93. The UV-vis spectra of compounds **3k** and **3m** (10^{-5} M) in THF/H₂O mixtures with increasing water fraction (f_w) from 0% to 99%.

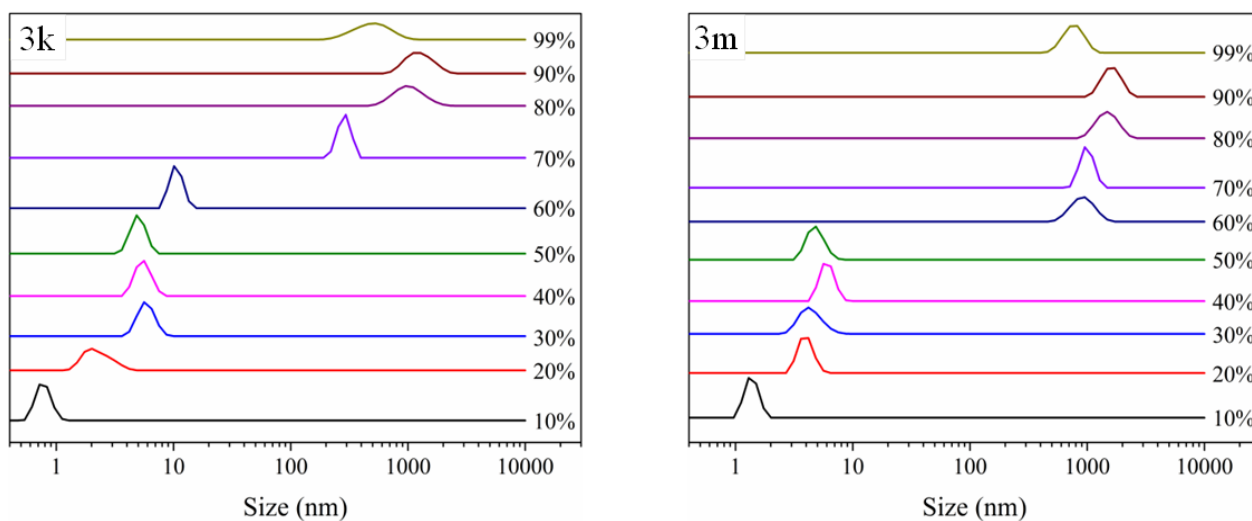


Fig. S94. The dynamic light scattering spectra of compounds **3k** and **3m** (10^{-5} M) in THF/H₂O mixtures with increasing water fraction (f_w) from 0% to 99%.

12. Photostability of compounds 3a-3p

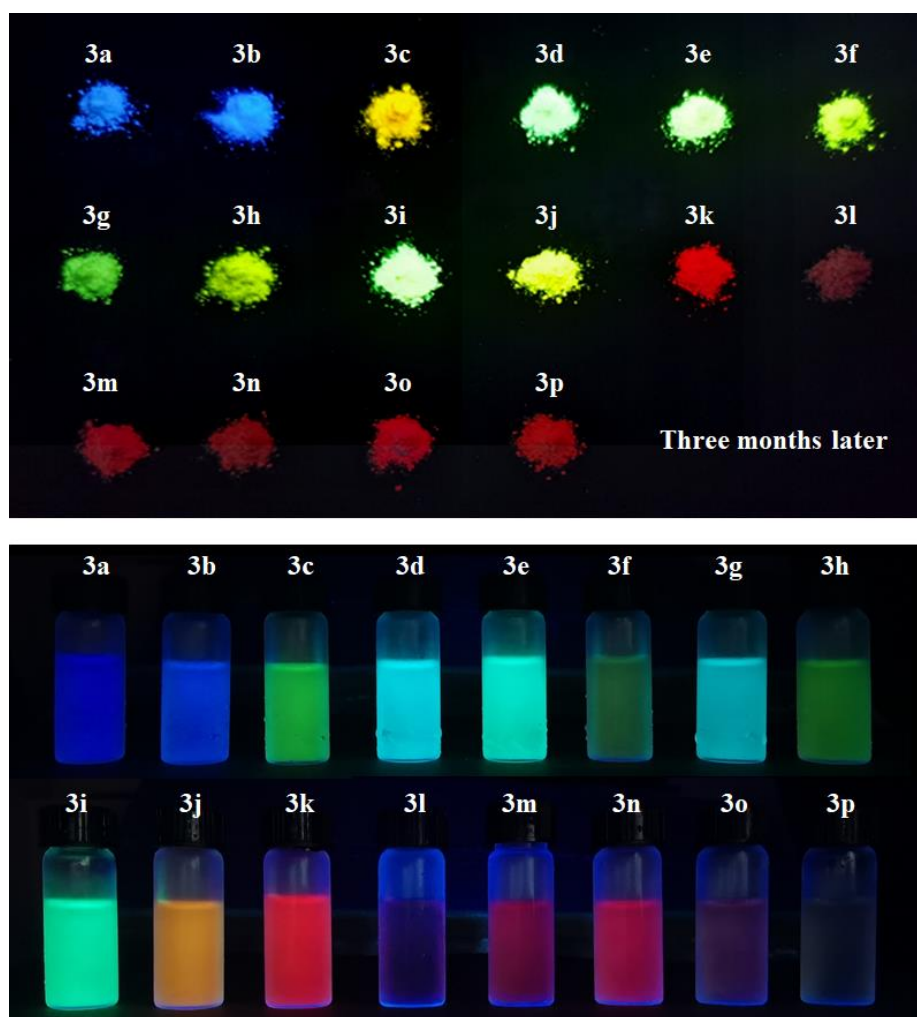


Fig. S95. Fluorescence pictures of solid powder and solution of compounds **3a-3p** after more than 3 months of storage.

13. Computational results of 3a-3p

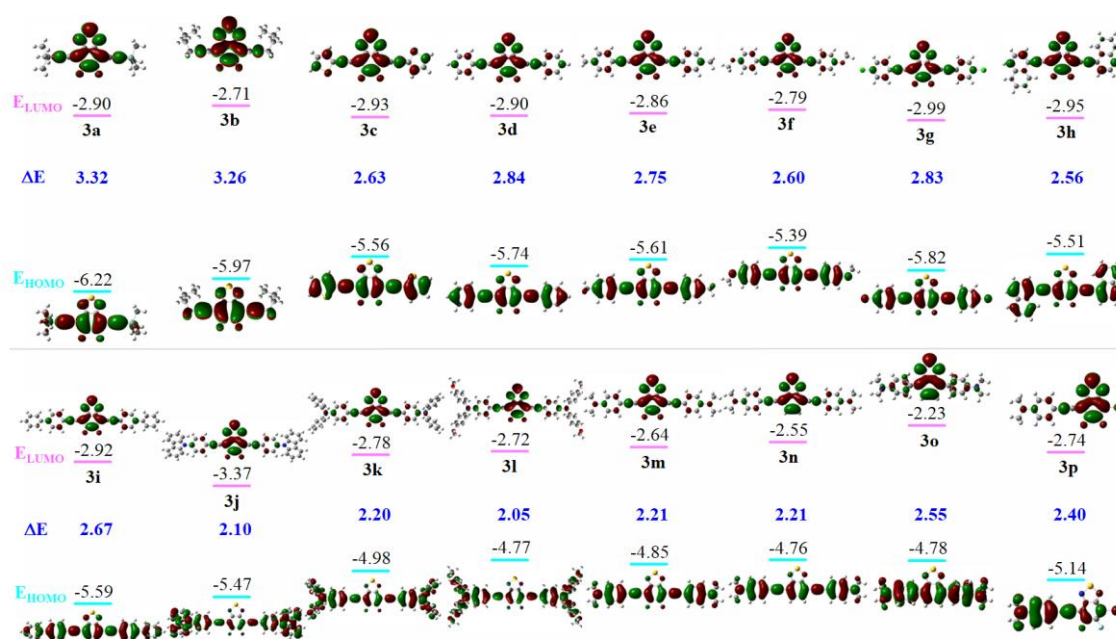


Fig. S96. The frontier orbitals of compounds **3a-3p** generated on B3LYP/6-31G(d,p) optimized geometries in the THF.

Table S8. Computational result of optimized structure of **3a**.

Center number	Atomic number	Atomic type	Coordinates (Angstroms)		
			X	Y	Z
1	6	0	0.711572	-1.352885	-0.002299
2	6	0	-0.709852	-1.353766	-0.001135
3	6	0	-1.469625	-0.200874	-0.000533
4	6	0	-0.725301	1.032870	-0.000979
5	6	0	0.724141	1.033771	-0.002251
6	6	0	1.469965	-0.199065	-0.002815
7	7	0	-1.260162	2.254213	-0.000293
8	16	0	-0.001998	3.314577	-0.001326
9	7	0	1.257473	2.255785	-0.002578
10	6	0	2.885478	-0.233303	-0.002874
11	9	0	1.305393	-2.551076	-0.002648
12	9	0	-1.302219	-2.552672	-0.000643
13	6	0	-2.885093	-0.236513	0.000294
14	6	0	-4.106208	-0.265135	0.000589
15	14	0	-5.958633	-0.311995	0.000858
16	6	0	4.106604	-0.261526	-0.002049
17	14	0	5.958952	-0.310138	0.001731
18	6	0	6.505485	-1.613120	1.251663
19	6	0	6.536011	-0.768245	-1.735240
20	6	0	6.588318	1.398651	0.492040
21	6	0	-6.546298	-0.242903	1.792322
22	6	0	-6.582410	1.182272	-0.966231
23	6	0	-6.500205	-1.920761	-0.821733
24	1	0	7.599158	-1.674634	1.280687
25	1	0	6.155734	-1.370111	2.259999

26	1	0	6.120120	-2.603370	0.988735
27	1	0	7.630543	-0.806931	-1.771764
28	1	0	6.200505	-0.033911	-2.474324
29	1	0	6.154636	-1.749628	-2.034557
30	1	0	6.236947	1.680274	1.489716
31	1	0	7.683962	1.409905	0.505335
32	1	0	6.252513	2.164722	-0.213972
33	1	0	-7.640989	-0.272886	1.831732
34	1	0	-6.165577	-1.090610	2.370724
35	1	0	-6.217273	0.678318	2.283438
36	1	0	-7.678032	1.190410	-0.986259
37	1	0	-6.227409	1.163391	-2.001482
38	1	0	-6.247236	2.119237	-0.510276
39	1	0	-6.120661	-2.792759	-0.279722
40	1	0	-7.593804	-1.987082	-0.841963
41	1	0	-6.140883	-1.980742	-1.853961

Table S9. Computational result of optimized structure of **3b**.

Center number	Atomic number	Atomic type	Coordinates (Angstroms)		
			X	Y	Z
1	6	0	0.710825	2.008466	0.062002
2	6	0	-0.710724	2.008456	0.061982
3	6	0	-1.473038	0.880907	-0.166942
4	6	0	-0.725241	-0.326322	-0.412396
5	6	0	0.725379	-0.326315	-0.412356
6	6	0	1.473156	0.880917	-0.166851
7	7	0	-1.258843	-1.524521	-0.654365
8	16	0	0.000095	-2.563676	-0.864305
9	7	0	1.259008	-1.524505	-0.654304
10	6	0	2.888980	0.910543	-0.162797
11	6	0	-2.888864	0.910530	-0.162902
12	6	0	4.103071	0.913494	-0.151235
13	6	0	-4.102955	0.913576	-0.151448
14	6	0	5.564542	0.934006	-0.184735
15	6	0	-5.564425	0.934114	-0.184725
16	6	0	6.242404	-0.440900	-0.408424
17	6	0	6.310432	-1.358601	0.822245
18	6	0	4.965844	-1.885060	1.335680
19	6	0	-6.242261	-0.440785	-0.408638
20	6	0	-6.310817	-1.358573	0.821946
21	6	0	-4.966490	-1.884980	1.336147
22	9	0	1.303120	3.185803	0.301846
23	9	0	-1.303041	3.185780	0.301831
24	1	0	5.870815	1.614764	-0.990013
25	1	0	5.942509	1.382350	0.744422

26	1	0	-5.942265	1.382292	0.744563
27	1	0	-5.870830	1.615020	-0.989828
28	1	0	7.266263	-0.238230	-0.743420
29	1	0	5.740173	-0.956571	-1.235739
30	1	0	6.950978	-2.211714	0.564550
31	1	0	6.828864	-0.827416	1.632345
32	1	0	5.118391	-2.600379	2.150868
33	1	0	4.329725	-1.080266	1.713963
34	1	0	4.409062	-2.394335	0.541362
35	1	0	-7.265994	-0.238105	-0.744012
36	1	0	-5.739738	-0.956451	-1.235775
37	1	0	-6.951106	-2.211735	0.563772
38	1	0	-6.829798	-0.827552	1.631799
39	1	0	-5.119544	-2.600999	2.150627
40	1	0	-4.330966	-1.080327	1.715741
41	1	0	-4.408822	-2.393437	0.541929

Table S10. Computational result of optimized structure of **3c**.

Center number	Atomic number	Atomic type	Coordinates (Angstroms)		
			X	Y	Z
1	6	0	0.637183	-1.402684	-0.000247
2	6	0	-0.777517	-1.332097	-0.000034
3	6	0	-1.482429	-0.140286	0.000053
4	6	0	-0.674704	1.054516	0.000070
5	6	0	0.773078	0.982233	-0.000083
6	6	0	1.457436	-0.287143	-0.000213
7	7	0	-1.146644	2.301051	0.000131
8	16	0	0.163264	3.297805	0.000191
9	7	0	1.367370	2.175237	-0.000044
10	6	0	2.861897	-0.387733	-0.000448
11	9	0	1.174908	-2.628980	-0.000325
12	9	0	-1.434520	-2.498914	-0.000016
13	6	0	-2.889984	-0.100640	0.000171
14	6	0	4.077739	-0.476932	-0.000084
15	6	0	-4.107767	-0.043639	0.000080
16	6	0	5.477804	-0.556713	0.000043
17	6	0	-5.509412	0.001819	0.000049
18	16	0	6.472005	0.897535	-0.000382
19	6	0	7.923465	-0.044387	0.000076
20	6	0	7.664333	-1.391143	0.000572
21	6	0	6.276195	-1.687605	0.000548
22	6	0	-6.333826	1.113818	-0.000042
23	6	0	-7.714689	0.785160	-0.000077
24	6	0	-7.942704	-0.567195	0.000001
25	16	0	-6.469613	-1.475114	0.000077

26	1	0	8.884252	0.451690	-0.000009
27	1	0	8.441348	-2.146227	0.000953
28	1	0	5.863931	-2.689261	0.000913
29	1	0	-5.944485	2.124578	-0.000075
30	1	0	-8.509027	1.522002	-0.000139
31	1	0	-8.891668	-1.085486	0.000025

Table S11. Computational result of optimized structure of **3d**.

Center number	Atomic number	Atomic type	Coordinates (Angstroms)		
			X	Y	Z
1	6	0	0.709089	-1.369354	-0.000084
2	6	0	-0.709067	-1.369365	-0.000087
3	6	0	-1.471950	-0.215298	-0.000085
4	6	0	-0.724882	1.018032	-0.000078
5	6	0	0.724869	1.018043	-0.000041
6	6	0	1.471958	-0.215277	-0.000065
7	7	0	-1.258776	2.239543	-0.000047
8	16	0	-0.000023	3.300074	-0.000019
9	7	0	1.258748	2.239560	-0.000061
10	6	0	2.882064	-0.247305	-0.000051
11	9	0	1.304758	-2.568182	-0.000059
12	9	0	-1.304719	-2.568200	-0.000100
13	6	0	-2.882059	-0.247352	-0.000090
14	6	0	4.099201	-0.265491	-0.000001
15	6	0	-4.099196	-0.265543	-0.000007
16	6	0	5.521957	-0.285368	0.000034
17	6	0	-5.521959	-0.285389	0.000034
18	6	0	6.219423	-1.511270	0.000002
19	6	0	7.611195	-1.523136	0.000034
20	6	0	8.326305	-0.322048	0.000105
21	6	0	7.642861	0.897377	0.000140
22	6	0	6.251300	0.921889	0.000102
23	6	0	-6.251279	0.921877	0.000000
24	6	0	-7.642843	0.897387	0.000037
25	6	0	-8.326303	-0.322027	0.000116

26	6	0	-7.611210	-1.523129	0.000151
27	6	0	-6.219441	-1.511285	0.000109
28	1	0	5.660165	-2.440973	-0.000053
29	1	0	8.139953	-2.471289	0.000007
30	1	0	9.411863	-0.336291	0.000132
31	1	0	8.196235	1.831376	0.000193
32	1	0	5.715978	1.865523	0.000128
33	1	0	-5.715946	1.865506	-0.000056
34	1	0	-8.196201	1.831395	0.000011
35	1	0	-9.411861	-0.336254	0.000145
36	1	0	-8.139985	-2.471272	0.000206
37	1	0	-5.660194	-2.440994	0.000132

Table S12. Computational result of optimized structure of **3e**.

Center number	Atomic number	Atomic type	Coordinates (Angstroms)		
			X	Y	Z
1	6	0	0.709553	-1.340202	-0.000378
2	6	0	-0.708157	-1.340938	-0.000390
3	6	0	-1.472586	-0.187562	-0.000315
4	6	0	-0.725512	1.045969	-0.000279
5	6	0	0.724547	1.046717	-0.000274
6	6	0	1.472843	-0.186035	-0.000307
7	7	0	-1.259908	2.267286	-0.000230
8	16	0	-0.001651	3.328674	-0.000252
9	7	0	1.257704	2.268579	-0.000183
10	6	0	2.882603	-0.217645	-0.000249
11	9	0	1.306015	-2.539233	-0.000418
12	9	0	-1.303426	-2.540572	-0.000445
13	6	0	-2.882326	-0.220070	-0.000292
14	6	0	4.100136	-0.237239	-0.000090
15	6	0	-4.099882	-0.238103	-0.000103
16	6	0	5.521699	-0.259828	0.000062
17	6	0	-5.521499	-0.257285	0.000052
18	6	0	6.222061	-1.481957	0.000185
19	6	0	7.613593	-1.493424	0.000352
20	6	0	8.352414	-0.302054	0.000406
21	6	0	7.648194	0.913693	0.000272
22	6	0	6.259730	0.943120	0.000106
23	6	0	-6.255693	0.944851	0.000300
24	6	0	-7.646983	0.917591	0.000495
25	6	0	-8.352293	-0.293960	0.000442

26	6	0	-7.614430	-1.489581	0.000184
27	6	0	-6.225662	-1.480336	-0.000004
28	6	0	-9.860840	-0.322138	0.000621
29	6	0	9.861177	-0.316287	0.000646
30	1	0	5.667137	-2.414405	0.000144
31	1	0	8.137122	-2.445436	0.000443
32	1	0	8.199800	1.850131	0.000297
33	1	0	5.731154	1.890737	0.000004
34	1	0	-5.726401	1.892028	0.000360
35	1	0	-8.196801	1.854683	0.000703
36	1	0	-8.139735	-2.441037	0.000141
37	1	0	-5.671429	-2.413235	-0.000193
38	1	0	-10.279739	0.687124	0.001292
39	1	0	-10.246549	-0.847924	-0.880089
40	1	0	-10.246329	-0.849019	0.880768
41	1	0	10.251285	-1.337016	0.000230
42	1	0	10.261595	0.199419	-0.879450
43	1	0	10.261291	0.198562	0.881388

Table S13. Computational result of optimized structure of **3f**.

Center number	Atomic number	Atomic type	Coordinates (Angstroms)		
			X	Y	Z
1	6	0	0.674487	-1.339698	-0.000236
2	6	0	-0.742021	-1.304669	-0.000224
3	6	0	-1.478404	-0.132608	-0.000175
4	6	0	-0.699329	1.081264	-0.000160
5	6	0	0.750736	1.045393	-0.000193
6	6	0	1.468350	-0.205693	-0.000202
7	7	0	-1.202437	2.315825	-0.000162
8	16	0	0.082172	3.345404	-0.000203
9	7	0	1.314486	2.253418	-0.000131
10	6	0	2.876227	-0.272785	-0.000198
11	9	0	1.241038	-2.554097	-0.000277
12	9	0	-1.368022	-2.489573	-0.000238
13	6	0	-2.887864	-0.127728	-0.000145
14	6	0	4.093438	-0.324190	-0.000071
15	6	0	-4.106040	-0.110505	-0.000052
16	6	0	5.511880	-0.385791	0.000032
17	6	0	-5.525609	-0.084843	0.000053
18	6	0	6.182806	-1.630638	0.000059
19	6	0	7.565467	-1.687490	0.000167
20	6	0	8.325107	-0.503787	0.000251
21	6	0	7.675470	0.739862	0.000230
22	6	0	6.284679	0.791082	0.000119
23	6	0	-6.225372	1.144110	0.000207
24	6	0	-7.608922	1.168792	0.000318
25	6	0	-8.340827	-0.032286	0.000275

26	6	0	-7.662462	-1.260409	0.000131
27	6	0	-6.270768	-1.279324	0.000019
28	8	0	9.672794	-0.669583	0.000372
29	6	0	10.502730	0.491957	0.000148
30	8	0	-9.692022	0.102147	0.000420
31	6	0	-10.494891	-1.078238	0.000031
32	1	0	5.603134	-2.547714	-0.000014
33	1	0	8.086478	-2.639029	0.000181
34	1	0	8.239831	1.664078	0.000307
35	1	0	5.784788	1.754018	0.000101
36	1	0	-5.666653	2.074043	0.000226
37	1	0	-8.151895	2.107974	0.000424
38	1	0	-8.205329	-2.197388	0.000119
39	1	0	-5.749222	-2.230765	-0.000101
40	1	0	11.528828	0.124483	0.000019
41	1	0	10.334373	1.101904	-0.894301
42	1	0	10.334654	1.102050	0.894552
43	1	0	-11.529211	-0.734572	-0.000103
44	1	0	-10.312528	-1.684018	-0.894521
45	1	0	-10.312876	-1.684376	0.894412

Table S14. Computational result of optimized structure of **3g**.

Center number	Atomic number	Atomic type	Coordinates (Angstroms)		
			X	Y	Z
1	6	0	0.709109	-1.325021	-0.000058
2	6	0	-0.709145	-1.325002	-0.000069
3	6	0	-1.470904	-0.170212	-0.000052
4	6	0	-0.724647	1.063429	-0.000041
5	6	0	0.724678	1.063408	-0.000040
6	6	0	1.470902	-0.170255	-0.000046
7	7	0	-1.258608	2.284820	-0.000050
8	16	0	0.000048	3.345222	-0.000021
9	7	0	1.258675	2.284783	-0.000012
10	6	0	2.880951	-0.202050	-0.000036
11	9	0	1.305093	-2.523028	-0.000069
12	9	0	-1.305164	-2.522990	-0.000080
13	6	0	-2.880957	-0.201972	-0.000069
14	6	0	4.097798	-0.218809	-0.000004
15	6	0	-4.097804	-0.218716	-0.000008
16	6	0	5.519407	-0.236059	0.000013
17	6	0	-5.519419	-0.235992	0.000009
18	6	0	6.221449	-1.458652	0.000009
19	6	0	7.611991	-1.476788	0.000025
20	6	0	8.307663	-0.266924	0.000045
21	6	0	7.638953	0.958088	0.000049
22	6	0	6.248412	0.970734	0.000034
23	6	0	-6.248448	0.970782	-0.000009
24	6	0	-7.638992	0.958102	0.000011
25	6	0	-8.307669	-0.266925	0.000048

26	6	0	-7.611969	-1.476775	0.000068
27	6	0	-6.221429	-1.458606	0.000051
28	17	0	10.066784	-0.286363	0.000065
29	17	0	-10.066792	-0.286410	0.000070
30	1	0	5.669890	-2.392416	-0.000006
31	1	0	8.150171	-2.417687	0.000022
32	1	0	8.197842	1.886826	0.000065
33	1	0	5.717085	1.916119	0.000038
34	1	0	-5.717147	1.916180	-0.000038
35	1	0	-8.197901	1.886827	-0.000004
36	1	0	-8.150129	-2.417686	0.000099
37	1	0	-5.669844	-2.392353	0.000068

Table S15. Computational result of optimized structure of **3h**.

Center number	Atomic number	Atomic type	Coordinates (Angstroms)		
			X	Y	Z
1	6	0	0.391961	-1.368291	-0.000095
2	6	0	-0.991671	-1.063098	-0.000201
3	6	0	-1.489674	0.228778	-0.000193
4	6	0	-0.497059	1.273761	-0.000149
5	6	0	0.918502	0.962103	-0.000029
6	6	0	1.383955	-0.402897	-0.000023
7	7	0	-0.756273	2.581436	-0.000109
8	16	0	0.700601	3.347425	0.000012
9	7	0	1.701857	2.040691	0.000000
10	6	0	2.755159	-0.726919	0.000045
11	9	0	0.719058	-2.666475	-0.000158
12	9	0	-1.834457	-2.105437	-0.000379
13	6	0	-2.875491	0.482320	-0.000324
14	6	0	3.948039	-0.973219	0.000044
15	6	0	-4.080608	0.658390	-0.000104
16	6	0	5.340365	-1.251616	0.000059
17	6	0	-5.489709	0.829402	-0.000025
18	6	0	6.297569	-0.173803	0.000060
19	6	0	7.692657	-0.499279	0.000080
20	6	0	8.093294	-1.862450	0.000106
21	6	0	7.157968	-2.874843	0.000106
22	6	0	5.782148	-2.572389	0.000080
23	6	0	-6.036861	2.109866	0.000022
24	6	0	-7.432795	2.299099	0.000107
25	6	0	-8.282539	1.213848	0.000162

26	6	0	-7.772448	-0.112302	0.000135
27	6	0	-6.355736	-0.323225	0.000036
28	6	0	-8.635590	-1.241952	0.000210
29	6	0	-8.125021	-2.520268	0.000194
30	6	0	-6.724334	-2.725054	0.000097
31	6	0	-5.858967	-1.652211	0.000020
32	6	0	5.911217	1.191311	0.000040
33	6	0	6.861397	2.189963	0.000044
34	6	0	8.240754	1.871884	0.000065
35	6	0	8.645109	0.556160	0.000082
36	1	0	9.154647	-2.094739	0.000122
37	1	0	7.474826	-3.912871	0.000135
38	1	0	5.051328	-3.374131	0.000084
39	1	0	-5.373283	2.968079	-0.000019
40	1	0	-7.833232	3.307810	0.000131
41	1	0	-9.359268	1.358692	0.000227
42	1	0	-9.709394	-1.076193	0.000281
43	1	0	-8.794202	-3.375259	0.000260
44	1	0	-6.329934	-3.736689	0.000099
45	1	0	-4.785479	-1.811930	-0.000034
46	1	0	4.854427	1.439312	-0.000001
47	1	0	6.550588	3.230366	0.000031
48	1	0	8.977535	2.669363	0.000062
49	1	0	9.701785	0.303304	0.000101

Table S16. Computational result of optimized structure of **3i**.

Center number	Atomic number	Atomic type	Coordinates (Angstroms)		
			X	Y	Z
1	6	0	-0.708844	-1.261493	-0.003300
2	6	0	0.708753	-1.261555	-0.002416
3	6	0	1.472162	-0.107257	-0.001368
4	6	0	0.724966	1.126188	-0.001608
5	6	0	-0.724849	1.126252	-0.002956
6	6	0	-1.472153	-0.107129	-0.003670
7	7	0	1.258872	2.347626	-0.000934
8	16	0	0.000158	3.408380	-0.001756
9	7	0	-1.258648	2.347736	-0.003100
10	6	0	-2.881616	-0.139176	-0.004229
11	9	0	-1.305017	-2.460249	-0.003906
12	9	0	1.304822	-2.460364	-0.002355
13	6	0	2.881625	-0.139430	-0.000275
14	6	0	-4.099212	-0.157491	-0.004343
15	6	0	4.099220	-0.157783	0.000666
16	6	0	-5.519829	-0.177613	-0.003663
17	6	0	5.519843	-0.177804	0.001430
18	6	0	-6.223751	-1.399480	0.007218
19	6	0	-7.612215	-1.411410	0.008323
20	6	0	-8.354145	-0.215288	-0.000344
21	6	0	-7.644332	1.000200	-0.011244
22	6	0	-6.256072	1.025121	-0.013349
23	6	0	6.255979	1.024981	0.012767
24	6	0	7.644247	1.000148	0.012556
25	6	0	8.354108	-0.215301	0.001937

26	6	0	7.612314	-1.411477	-0.008619
27	6	0	6.223841	-1.399629	-0.009377
28	6	0	-9.837717	-0.235201	0.002366
29	6	0	9.837682	-0.235116	0.001632
30	6	0	10.546321	-1.217325	-0.713158
31	6	0	11.940315	-1.235684	-0.713750
32	6	0	12.657039	-0.273308	0.000791
33	6	0	11.967021	0.708131	0.715729
34	6	0	10.573019	0.727562	0.715968
35	6	0	-10.574391	0.728856	-0.708743
36	6	0	-11.968385	0.709370	-0.706057
37	6	0	-12.657110	-0.273526	0.008127
38	6	0	-11.939075	-1.237297	0.719459
39	6	0	-10.545092	-1.218857	0.716446
40	1	0	-5.670583	-2.332798	0.005266
41	1	0	-8.131588	-2.364103	-0.008985
42	1	0	-8.188684	1.938835	0.007233
43	1	0	-5.727324	1.972438	-0.012634
44	1	0	5.727159	1.972258	0.011931
45	1	0	8.188629	1.938797	-0.004524
46	1	0	8.131786	-2.364121	0.008689
47	1	0	5.670717	-2.332975	-0.008764
48	1	0	10.001824	-1.955706	-1.293610
49	1	0	12.467000	-1.998254	-1.279929
50	1	0	13.742761	-0.288003	0.000499
51	1	0	12.514502	1.456167	1.281566
52	1	0	10.049079	1.480443	1.296727
53	1	0	-10.051576	1.482913	-1.288981
54	1	0	-12.516894	1.458524	-1.269412

55	1	0	-13.742829	-0.288258	0.010319
56	1	0	-12.464718	-2.001023	1.285048
57	1	0	-9.999592	-1.958329	1.294555

Table S17. Computational result of optimized structure of **3j**.

Center number	Atomic number	Atomic type	Coordinates (Angstroms)		
			X	Y	Z
1	6	0	0.708353	-1.215847	-0.000185
2	6	0	-0.708422	-1.215815	-0.000408
3	6	0	-1.475668	-0.067430	0.000167
4	6	0	-0.732168	1.176033	0.000401
5	6	0	0.732236	1.175994	-0.000464
6	6	0	1.475645	-0.067497	-0.000488
7	7	0	-1.313154	2.372788	0.000736
8	16	0	0.000091	3.578903	0.000175
9	7	0	1.313284	2.372727	-0.000603
10	6	0	2.883139	-0.094810	-0.000385
11	9	0	1.327567	-2.449895	-0.000036
12	9	0	-1.327697	-2.449835	-0.000868
13	6	0	-2.883129	-0.094638	0.000067
14	6	0	4.104405	-0.113111	-0.000449
15	6	0	-4.104401	-0.112892	0.000023
16	6	0	5.525580	-0.127505	-0.000497
17	6	0	-5.525529	-0.127343	0.000158
18	6	0	6.235958	-1.349285	0.050824
19	6	0	7.627943	-1.359983	0.058750
20	6	0	8.347351	-0.152675	-0.000807
21	6	0	7.649586	1.067340	-0.060215
22	6	0	6.257726	1.081480	-0.051999
23	6	0	-6.235903	-1.349140	-0.050919
24	6	0	-7.627880	-1.359890	-0.058722
25	6	0	-8.347359	-0.152606	0.000720

26	6	0	-7.649595	1.067444	0.059854
27	6	0	-6.257750	1.081623	0.051491
28	7	0	9.768065	-0.165316	-0.001114
29	6	0	10.601925	0.596270	0.847280
30	6	0	10.587839	-0.941318	-0.850180
31	7	0	-9.768031	-0.165307	0.001185
32	6	0	-10.602054	0.596682	-0.846728
33	6	0	-10.587694	-0.941770	0.849981
34	6	0	10.232025	-1.816524	-1.883103
35	6	0	11.262759	-2.441656	-2.591680
36	6	0	12.616785	-2.197571	-2.286503
37	6	0	12.966460	-1.310031	-1.266070
38	6	0	11.950572	-0.670584	-0.541554
39	6	0	11.959492	0.301874	0.537464
40	6	0	12.986983	0.923420	1.261183
41	6	0	12.653721	1.816727	2.282077
42	6	0	11.304416	2.084320	2.588450
43	6	0	10.262333	1.477423	1.880624
44	6	0	-11.959559	0.302052	-0.536897
45	6	0	-12.987193	0.923768	-1.260261
46	6	0	-12.654131	1.817548	-2.280809
47	6	0	-11.304887	2.085383	-2.587211
48	6	0	-10.262667	1.478256	-1.879779
49	6	0	-10.231776	-1.817369	1.882541
50	6	0	-11.262429	-2.442821	2.590955
51	6	0	-12.616489	-2.198626	2.286042
52	6	0	-12.966275	-1.310645	1.266030
53	6	0	-11.950466	-0.670938	0.541641
54	1	0	5.687441	-2.283001	0.100063

55	1	0	8.161796	-2.300225	0.128847
56	1	0	8.200091	1.997907	-0.130559
57	1	0	5.725253	2.024391	-0.101172
58	1	0	-5.687369	-2.282851	-0.100129
59	1	0	-8.161668	-2.300175	-0.128721
60	1	0	-8.200085	1.998027	0.130100
61	1	0	-5.725305	2.024563	0.100431
62	1	0	9.195585	-2.004690	-2.135707
63	1	0	11.011040	-3.126254	-3.395185
64	1	0	13.392630	-2.700287	-2.854287
65	1	0	14.010059	-1.113700	-1.041112
66	1	0	14.026812	0.708929	1.035331
67	1	0	13.438706	2.305718	2.849283
68	1	0	11.065321	2.773064	3.392268
69	1	0	9.229562	1.683729	2.134109
70	1	0	-14.026976	0.709010	-1.034446
71	1	0	-13.439221	2.306703	-2.847727
72	1	0	-11.065927	2.774476	-3.390771
73	1	0	-9.229955	1.684720	-2.133369
74	1	0	-9.195323	-2.005614	2.135017
75	1	0	-11.010600	-3.127742	3.394150
76	1	0	-13.392268	-2.701572	2.853712
77	1	0	-14.009896	-1.114141	1.041334

Table S18. Computational result of optimized structure of **3k**.

Center number	Atomic number	Atomic type	Coordinates (Angstroms)		
			X	Y	Z
1	6	0	-0.707914	-1.214469	0.000201
2	6	0	0.707941	-1.214436	-0.000520
3	6	0	1.474254	-0.060575	-0.000373
4	6	0	0.725342	1.172407	0.000075
5	6	0	-0.725424	1.172373	-0.000011
6	6	0	-1.474281	-0.060644	0.000230
7	7	0	1.258862	2.394011	0.000158
8	16	0	-0.000094	3.455474	0.000214
9	7	0	-1.259003	2.393952	0.000117
10	6	0	-2.882413	-0.091556	0.000751
11	9	0	-1.305205	-2.414515	0.000620
12	9	0	1.305288	-2.414455	-0.001089
13	6	0	2.882389	-0.091424	-0.000902
14	6	0	-4.101325	-0.107294	0.001084
15	6	0	4.101301	-0.107137	-0.001253
16	6	0	-5.519008	-0.122488	0.001336
17	6	0	5.518985	-0.122364	-0.001531
18	6	0	-6.234311	-1.339209	0.031568
19	6	0	-7.620075	-1.352906	0.027299
20	6	0	-8.353915	-0.148881	0.001419
21	6	0	-7.642619	1.068637	-0.024420
22	6	0	-6.256955	1.080731	-0.028762
23	6	0	6.256964	1.080828	0.028786
24	6	0	7.642628	1.068707	0.024423
25	6	0	8.353904	-0.148823	-0.001661
26	6	0	7.620024	-1.352825	-0.027787

27	6	0	6.234263	-1.339095	-0.032024
28	7	0	-9.760590	-0.161773	0.001253
29	6	0	-10.497757	0.862141	-0.666364
30	6	0	-10.479390	-1.198344	0.669410
31	7	0	9.760560	-0.161721	-0.001451
32	6	0	10.479495	-1.198387	-0.669285
33	6	0	10.497656	0.862243	0.666240
34	6	0	-11.549048	-1.840024	0.027635
35	6	0	-12.263988	-2.838518	0.687686
36	6	0	-11.914452	-3.220448	1.985000
37	6	0	-10.845982	-2.585828	2.623165
38	6	0	-10.136615	-1.574421	1.977129
39	6	0	-11.578808	1.484299	-0.024459
40	6	0	-12.310956	2.470737	-0.683793
41	6	0	-11.967725	2.860010	-1.980603
42	6	0	-10.888062	2.244784	-2.618952
43	6	0	-10.161260	1.245392	-1.973636
44	6	0	11.549448	-1.839512	-0.027441
45	6	0	12.264540	-2.838087	-0.687205
46	6	0	11.914882	-3.220663	-1.984292
47	6	0	10.846123	-2.586598	-2.622527
48	6	0	10.136595	-1.575115	-1.976789
49	6	0	11.578116	1.485089	0.024028
50	6	0	12.310197	2.471555	0.683397
51	6	0	11.967456	2.860134	1.980546
52	6	0	10.888373	2.244211	2.619204
53	6	0	10.161651	1.244790	1.973834
54	1	0	-5.688175	-2.276772	0.043702
55	1	0	-8.146098	-2.300453	0.036568

56	1	0	-8.186221	2.006204	-0.033833
57	1	0	-5.727750	2.027891	-0.040881
58	1	0	5.727785	2.028000	0.041097
59	1	0	8.186232	2.006271	0.033979
60	1	0	8.146033	-2.300375	-0.037306
61	1	0	5.688109	-2.276645	-0.044346
62	1	0	-11.814336	-1.553029	-0.984502
63	1	0	-13.089727	-3.327567	0.179365
64	1	0	-12.469338	-4.002611	2.493618
65	1	0	-10.570515	-2.867050	3.635287
66	1	0	-9.317718	-1.071813	2.481105
67	1	0	-11.839249	1.191867	0.987380
68	1	0	-13.145308	2.944690	-0.175239
69	1	0	-12.536007	3.632854	-2.488672
70	1	0	-10.617183	2.531778	-3.630695
71	1	0	-9.333417	0.757885	-2.477821
72	1	0	11.814848	-1.552039	0.984530
73	1	0	13.090507	-3.326689	-0.178822
74	1	0	12.469891	-4.002888	-2.492682
75	1	0	10.570550	-2.868310	-3.634484
76	1	0	9.317487	-1.072939	-2.480850
77	1	0	11.838153	1.193148	-0.988059
78	1	0	13.144099	2.946068	0.174630
79	1	0	12.535681	3.632999	2.488647
80	1	0	10.617899	2.530683	3.631203
81	1	0	9.334244	0.756730	2.478203

Table S19. Computational result of optimized structure of **3I**.

Center number	Atomic number	Atomic type	Coordinates (Angstroms)		
			X	Y	Z
1	6	0	0.707483	1.153690	0.001480
2	6	0	-0.707552	1.153661	-0.002076
3	6	0	-1.475326	0.000076	-0.004724
4	6	0	-0.725654	-1.232669	-0.002785
5	6	0	0.725680	-1.232640	0.002468
6	6	0	1.475301	0.000134	0.004273
7	7	0	-1.259004	-2.454339	-0.004450
8	16	0	0.000058	-3.516196	-0.000021
9	7	0	1.259078	-2.454289	0.004291
10	6	0	2.882886	0.031928	0.007276
11	9	0	1.305205	2.354394	0.002422
12	9	0	-1.305321	2.354342	-0.003120
13	6	0	-2.882911	0.031810	-0.007710
14	6	0	4.102339	0.051501	0.009461
15	6	0	-4.102365	0.051363	-0.009795
16	6	0	5.518833	0.073823	0.010957
17	6	0	-5.518855	0.073733	-0.011199
18	6	0	6.230112	1.290292	-0.082137
19	6	0	7.614847	1.312947	-0.085981
20	6	0	8.360916	0.116769	0.011161
21	6	0	7.651280	-1.101373	0.108956
22	6	0	6.266558	-1.120610	0.104813
23	6	0	-6.266627	-1.120677	-0.104989
24	6	0	-7.651350	-1.101397	-0.109018
25	6	0	-8.360940	0.116766	-0.011169

26	6	0	-7.614824	1.312923	0.085895
27	6	0	-6.230092	1.290225	0.081938
28	7	0	9.760222	0.137771	0.010415
29	6	0	10.517850	-0.999989	-0.411446
30	6	0	10.483337	1.299881	0.426741
31	7	0	-9.760244	0.137808	-0.010252
32	6	0	-10.483405	1.299891	-0.426553
33	6	0	-10.517820	-0.999996	0.411602
34	6	0	11.484156	1.841758	-0.395713
35	6	0	12.210227	2.951996	0.012641
36	6	0	11.942253	3.560365	1.249131
37	6	0	10.942367	3.030216	2.074294
38	6	0	10.231282	1.900595	1.664258
39	6	0	11.542895	-1.507728	0.402924
40	6	0	12.302651	-2.593053	-0.011273
41	6	0	12.045410	-3.210466	-1.245545
42	6	0	11.021696	-2.714374	-2.062579
43	6	0	10.276290	-1.609255	-1.646895
44	6	0	-11.484417	1.841556	0.395807
45	6	0	-12.210534	2.951775	-0.012517
46	6	0	-11.942418	3.560347	-1.248876
47	6	0	-10.942345	3.030408	-2.073944
48	6	0	-10.231215	1.900801	-1.663948
49	6	0	-11.542693	-1.507929	-0.402860
50	6	0	-12.302372	-2.593308	0.011339
51	6	0	-12.045216	-3.210572	1.245703
52	6	0	-11.021674	-2.714282	2.062832
53	6	0	-10.276347	-1.609113	1.647139
54	8	0	12.840383	-4.275147	-1.555196

55	6	0	12.622629	-4.939578	-2.796613
56	8	0	12.703581	4.651097	1.552405
57	6	0	12.474092	5.308016	2.795715
58	8	0	-12.703802	4.651049	-1.552123
59	6	0	-12.474178	5.308151	-2.795310
60	8	0	-12.840100	-4.275316	1.555352
61	6	0	-12.622417	-4.939601	2.796861
62	1	0	5.679647	2.221823	-0.166234
63	1	0	8.132113	2.260912	-0.173255
64	1	0	8.197073	-2.033227	0.196066
65	1	0	5.743913	-2.067992	0.188653
66	1	0	-5.744019	-2.068076	-0.188863
67	1	0	-8.197176	-2.033236	-0.196080
68	1	0	-8.132063	2.260901	0.173184
69	1	0	-5.679591	2.221740	0.165979
70	1	0	11.691686	1.383551	-1.357212
71	1	0	12.985257	3.373809	-0.618883
72	1	0	10.718616	3.472655	3.037282
73	1	0	9.468479	1.485488	2.315099
74	1	0	11.742686	-1.042531	1.362705
75	1	0	13.096464	-2.988348	0.614057
76	1	0	10.805187	-3.164079	-3.023849
77	1	0	9.494909	-1.220315	-2.291798
78	1	0	-11.692062	1.383203	1.357211
79	1	0	-12.985713	3.373420	0.618938
80	1	0	-10.718478	3.472993	-3.036838
81	1	0	-9.468273	1.485862	-2.314732
82	1	0	-11.742409	-1.042842	-1.362710
83	1	0	-13.096055	-2.988761	-0.614056

84	1	0	-10.805240	-3.163870	3.024173
85	1	0	-9.495093	-1.220014	2.292101
86	1	0	13.352357	-5.748769	-2.835742
87	1	0	11.611895	-5.360256	-2.855048
88	1	0	12.783315	-4.266105	-3.646649
89	1	0	13.176549	6.141246	2.828852
90	1	0	11.450318	5.694511	2.862727
91	1	0	12.664409	4.640379	3.644232
92	1	0	-13.176729	6.141301	-2.828463
93	1	0	-11.450439	5.694779	-2.862096
94	1	0	-12.664266	4.640601	-3.643947
95	1	0	-13.352053	-5.748873	2.835980
96	1	0	-11.611639	-5.360150	2.855459
97	1	0	-12.783287	-4.266062	3.646811

Table S20. Computational result of optimized structure of **3m**.

Center number	Atomic number	Atomic type	Coordinates (Angstroms)		
			X	Y	Z
1	6	0	-0.707305	-1.256044	-0.000586
2	6	0	0.707279	-1.256049	-0.000532
3	6	0	1.476488	-0.103118	-0.000458
4	6	0	0.725983	1.129244	-0.000450
5	6	0	-0.725977	1.129250	-0.000525
6	6	0	-1.476508	-0.103108	-0.000553
7	7	0	1.259163	2.351066	-0.000401
8	16	0	0.000009	3.413147	-0.000503
9	7	0	-1.259149	2.351073	-0.000532
10	6	0	-2.883796	-0.136912	-0.000593
11	9	0	-1.305042	-2.457590	-0.000673
12	9	0	1.305005	-2.457600	-0.000563
13	6	0	2.883792	-0.136963	-0.000386
14	6	0	-4.103566	-0.165546	-0.000459
15	6	0	4.103559	-0.165609	-0.000390
16	6	0	-5.518960	-0.204704	-0.000346
17	6	0	5.518973	-0.204725	-0.000368
18	6	0	-6.216099	-1.432942	-0.000074
19	6	0	-7.599258	-1.478375	0.000141
20	6	0	-8.372977	-0.287230	-0.000056
21	6	0	-7.669387	0.946671	-0.000138
22	6	0	-6.285741	0.981217	-0.000343
23	6	0	6.285727	0.981203	0.000415
24	6	0	7.669382	0.946677	0.000466
25	6	0	8.372984	-0.287208	-0.000502
26	6	0	7.599286	-1.478362	-0.000951

27	6	0	6.216122	-1.432953	-0.000980
28	7	0	-9.745429	-0.327510	-0.000159
29	6	0	-10.515684	0.908452	0.001598
30	6	0	-10.441162	-1.606835	0.002035
31	7	0	9.745447	-0.327491	-0.001140
32	6	0	10.441126	-1.606833	0.001790
33	6	0	10.515712	0.908448	0.002811
34	1	0	-5.653105	-2.361031	0.000046
35	1	0	-8.086436	-2.445026	0.000471
36	1	0	-8.211995	1.883384	0.000014
37	1	0	-5.776859	1.939988	-0.000444
38	1	0	5.776847	1.939974	0.001107
39	1	0	8.211964	1.883403	0.001295
40	1	0	8.086485	-2.445005	-0.001267
41	1	0	5.653155	-2.361057	-0.001408
42	1	0	-10.307331	1.516723	0.891063
43	1	0	-10.305952	1.519653	-0.885457
44	1	0	-11.578040	0.667282	0.000261
45	1	0	-10.195870	-2.205031	-0.884838
46	1	0	-10.197042	-2.201772	0.891490
47	1	0	-11.515866	-1.428890	0.000891
48	1	0	10.195361	-2.205616	-0.884538
49	1	0	11.515839	-1.428940	-0.000095
50	1	0	10.197406	-2.201163	0.891782
51	1	0	10.307948	1.514955	0.893643
52	1	0	11.578070	0.667273	0.000257
53	1	0	10.305413	1.521405	-0.882871

Table S21. Computational result of optimized structure of **3n**.

Center number	Atomic number	Atomic type	Coordinates (Angstroms)		
			X	Y	Z
1	6	0	0.706411	-1.526621	0.005076
2	6	0	-0.706395	-1.526634	0.005128
3	6	0	-1.465071	-0.359132	0.004111
4	6	0	-0.725523	0.878784	0.003335
5	6	0	0.725502	0.878796	0.003302
6	6	0	1.465067	-0.359107	0.004008
7	7	0	-1.259474	2.103353	0.002524
8	16	0	-0.000030	3.163413	0.001763
9	7	0	1.259431	2.103376	0.002445
10	6	0	2.877383	-0.366077	0.003135
11	6	0	-2.877383	-0.366120	0.003455
12	6	0	4.097823	-0.380380	0.001712
13	6	0	-4.097825	-0.380435	0.002475
14	6	0	5.515113	-0.393299	-0.000729
15	6	0	-5.515112	-0.393349	0.000805
16	6	0	6.238456	-1.605871	-0.001538
17	6	0	7.622945	-1.623074	-0.004513
18	6	0	8.371897	-0.416825	-0.008247
19	6	0	7.642835	0.801597	-0.004851
20	6	0	6.258306	0.807348	-0.001894
21	6	0	-6.258285	0.807319	-0.002178
22	6	0	-7.642810	0.801593	-0.004253
23	6	0	-8.371885	-0.416836	-0.003850
24	6	0	-7.622960	-1.623104	0.000030
25	6	0	-6.238470	-1.605913	0.002051
26	7	0	9.746026	-0.428287	-0.015766

27	6	0	10.489365	0.823452	0.003557
28	6	0	10.468091	-1.692310	0.003708
29	7	0	-9.745982	-0.428274	-0.007364
30	6	0	-10.468105	-1.692378	-0.000123
31	6	0	-10.489312	0.823597	-0.004078
32	1	0	1.223323	-2.480361	0.005676
33	1	0	-1.223290	-2.480383	0.005776
34	1	0	5.695534	-2.545985	0.000802
35	1	0	8.130006	-2.579554	-0.003782
36	1	0	8.165664	1.749558	-0.004368
37	1	0	5.729872	1.755520	0.000162
38	1	0	-5.729821	1.755476	-0.002736
39	1	0	-8.165652	1.749547	-0.006201
40	1	0	-8.130059	-2.579566	0.001516
41	1	0	-5.695557	-2.546031	0.004828
42	1	0	10.258043	1.445925	-0.870047
43	1	0	10.277122	1.412017	0.905783
44	1	0	11.556669	0.605490	-0.013148
45	1	0	10.245718	-2.277360	0.905831
46	1	0	10.226623	-2.310868	-0.869983
47	1	0	11.538905	-1.492410	-0.012626
48	1	0	-10.240275	-2.287667	0.893657
49	1	0	-11.538971	-1.492230	-0.006894
50	1	0	-10.232077	-2.300993	-0.882499
51	1	0	-10.264083	1.432919	-0.888744
52	1	0	-11.556682	0.605414	-0.009381
53	1	0	-10.270893	1.425620	0.887481

Table S22. Computational result of optimized structure of **3o**.

Center number	Atomic number	Atomic type	Coordinates (Angstroms)		
			X	Y	Z
1	6	0	-0.709626	-1.450745	-0.013057
2	6	0	0.709669	-1.450731	0.012576
3	6	0	1.480844	-0.301677	0.016289
4	6	0	0.730647	0.928833	0.007743
5	6	0	-0.730664	0.928818	-0.007914
6	6	0	-1.480829	-0.301709	-0.016599
7	7	0	1.255747	2.160579	0.003418
8	16	0	-0.000033	3.220301	0.000038
9	7	0	-1.255791	2.160552	-0.003449
10	6	0	-2.956261	-0.351886	-0.010492
11	6	0	2.956274	-0.351809	0.010246
12	6	0	-3.635049	-1.384196	0.664190
13	6	0	-5.019288	-1.487475	0.660179
14	6	0	-5.819531	-0.552804	-0.041258
15	6	0	-5.140850	0.497333	-0.706027
16	6	0	-3.755324	0.588386	-0.687388
17	6	0	3.755265	0.588387	0.687343
18	6	0	5.140786	0.497354	0.706089
19	6	0	5.819539	-0.552666	0.041192
20	6	0	5.019373	-1.487272	-0.660427
21	6	0	3.635133	-1.384015	-0.664524
22	7	0	-7.197296	-0.662497	-0.078118
23	6	0	-7.991868	0.424962	-0.630316
24	6	0	-7.862843	-1.652768	0.755174
25	7	0	7.197276	-0.662224	0.078105

26	6	0	7.862978	-1.653369	-0.753990
27	6	0	7.991751	0.425278	0.630350
28	1	0	-1.209168	-2.413991	-0.041455
29	1	0	1.209234	-2.413969	0.040856
30	1	0	-3.066577	-2.111141	1.237008
31	1	0	-5.479460	-2.292477	1.219406
32	1	0	-5.698626	1.250213	-1.248792
33	1	0	-3.282481	1.407376	-1.216062
34	1	0	3.282358	1.407265	1.216134
35	1	0	5.698523	1.250097	1.249086
36	1	0	5.479614	-2.292159	-1.219767
37	1	0	3.066715	-2.110886	-1.237491
38	1	0	-7.858817	1.368574	-0.080834
39	1	0	-7.738320	0.606608	-1.680654
40	1	0	-9.046452	0.151882	-0.588680
41	1	0	-7.515015	-2.664245	0.518386
42	1	0	-7.702104	-1.481490	1.830086
43	1	0	-8.935113	-1.619299	0.561151
44	1	0	7.514608	-2.664528	-0.516639
45	1	0	7.702990	-1.482878	-1.829141
46	1	0	8.935139	-1.620157	-0.559322
47	1	0	7.857797	1.369078	0.081441
48	1	0	7.738929	0.606312	1.680991
49	1	0	9.046435	0.152762	0.587717

Table S23. Computational result of optimized structure of **3p**.

Center number	Atomic number	Atomic type	Coordinates (Angstroms)		
			X	Y	Z
1	6	0	3.022235	-1.485129	0.000045
2	6	0	1.599910	-1.444524	0.000042
3	6	0	0.870686	-0.270125	-0.000001
4	6	0	1.656516	0.941067	-0.000015
5	6	0	3.109507	0.903149	0.000006
6	6	0	3.789543	-0.349250	0.000023
7	7	0	1.159494	2.177261	-0.000073
8	16	0	2.445643	3.203023	-0.000075
9	7	0	3.676353	2.110506	-0.000006
10	35	0	5.671025	-0.446818	0.000036
11	9	0	3.583887	-2.698304	0.000064
12	9	0	0.973179	-2.628928	0.000053
13	6	0	-0.537243	-0.252913	0.000009
14	6	0	-1.756523	-0.218999	-0.000091
15	6	0	-3.170927	-0.171471	-0.000099
16	6	0	-3.857760	1.062828	-0.000020
17	6	0	-5.239955	1.118943	0.000000
18	6	0	-6.022934	-0.066758	-0.000065
19	6	0	-5.329095	-1.306689	-0.000190
20	6	0	-3.946181	-1.351967	-0.000196
21	7	0	-7.393910	-0.015668	-0.000063
22	6	0	-8.174527	-1.245599	0.000000
23	6	0	-8.080004	1.269349	0.000366
24	1	0	-3.286690	1.985863	0.000022
25	1	0	-5.719771	2.089179	0.000052

26	1	0	-5.879120	-2.238980	-0.000285
27	1	0	-3.445023	-2.314817	-0.000280
28	1	0	-7.970090	-1.856588	0.888292
29	1	0	-9.234757	-0.995588	0.000228
30	1	0	-7.970415	-1.856437	-0.888466
31	1	0	-7.830730	1.863695	-0.887850
32	1	0	-9.155941	1.099497	0.000603
33	1	0	-7.830264	1.863366	0.888665

14. Supplementary material reference

- [1] S.-H. Chen, S.-H. Luo, L.-J. Xing, K. Jiang, Y.-P. Huo, Q. Chen and Z.-Y. Wang, Rational design and facile synthesis of dual-state emission fluorophores: expanding functionality for the sensitive detection of nitroaromatic compounds, *Chem. Eur. J.*, 2022, **28**, e202103478.
- [2] A. Casey, Y. Han, E. Gann, J. P. Green, C. R. McNeill, T. D. Anthopoulos and M. Heeney, Vinylene-linked oligothiophene-difluorobenzothiadiazole copolymer for transistor applications, *ACS Appl. Mater. Interfaces*, 2016, **8**, 31154.
- [3] S. Hamer, F. Rohricht, M. Jakoby, I. A. Howard, X. H. Zhang, C. Nather and R. Herges, Synthesis of dipolar molecular rotors as linkers for metal-organic frameworks, *Beilstein J. Org. Chem.*, 2019, **15**, 1331.
- [4] S. H. Chen, Y. J. Li, C. Liu, W. L. Yang and Y. L. Li, Strong charge-transfer chromophores from [2+2] cycloadditions of TCNE and TCNQ to peripheral donor-substituted alkynes, *Eur. J. Org. Chem.*, 2011, **2011**, 6445.
- [5] J. Wang, H. Y. Cui, H. P. Ruan, Y. Zhao, Y. Zhao, L. Zhang and X. P. Wang, The lewis acid induced formation of a stable diradical with an intramolecular ion pairing state, *J. Am. Chem. Soc.* **2022**, *144*, 7978.
- [6] J. X. Zhang, T. C. Parker, W. Chen, L. Williams, V. N. Khrustalev, E. V. Jucov, S. Barlow, T. V. Timofeeva and S. R. Marder, C-H-activated direct arylation of strong benzothiadiazole and quinoxaline-based electron acceptors, *J. Org. Chem.*, 2016, **81**, 360.
- [7] I. S. Park, S. Y. Lee, C. Adachi and T. Yasuda, Full-color delayed fluorescence materials based on wedge-shaped phthalonitriles and dicyanopyrazines: systematic design, tunable photophysical properties, and OLED performance, *Adv. Funct. Mater.*, 2016, **26**, 1813.
- [8] H. T. Ding, Y. T. Sun, M. Tang, J. Y. Wen, S. W. Yue, Y. Peng, F. Li, L. Y. Zheng, S. N. Wang, Y. G. Shi and Q. Cao, Time-dependent photo-activated aminoborane room-temperature phosphorescence materials with unprecedented properties: simple, versatile, multicolor-tunable, water resistance, optical information writing/erasing, and multilevel data encryption, *Chem. Sci.*, 2023, **14**, 4633.
- [9] C. C. Liu, H. T. Bai, B. Z. He, X. W. He, J. Y. Zhang, C. Chen, Y. P. Qiu, R. Hu, F. X. Zhao, Y. X.

Zhang, W. He, J. H. C. Chau, S. J. Chen, J. W. Y. Lam and B. Z. Tang, Functionalization of silk by AIEgens through facile bioconjugation: Full-color fluorescence and long-term bioimaging, *Angew. Chem. Int. Ed.*, 2021, **60**, 12424.

[10] L. Wang, Y. Y. Ma, J. L. Yin, L. L. Zhu, S. F. Li and W. Y. Lin, A deep-red emission fluorescent probe for visualization of fluoride anion accumulation in a murine model of acute fluoride toxicity and the roots of *Arabidopsis thaliana*, *Sens. Actuators B Chem.*, 2022, **358**, 131508.